UNIVERSITÀ DEGLI STUDI DI PADOVA

DIPARTIMENTO DI BIOLOGIA

Corso di Laurea magistale in Biologia Sanitaria

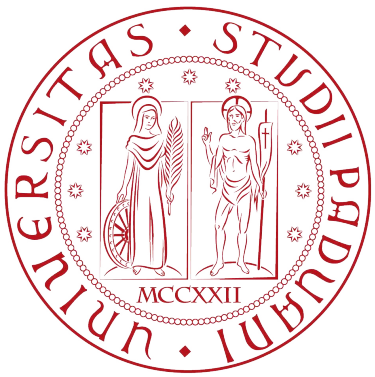

TESI DI LAUREA

Development of armed oncolytic agents based on the herpes simplex virus type I for the treatment of glioblastoma

Relatore:
Prof.ssa Arianna Calistri

Laureanda:
Alessia Zago

Correlatore:
Dott. Alberto Reale

ANNO ACCADEMICO 2022/2023

Summary

Riassunto

Il glioblastoma multiplo (GBM) rappresenta ancora oggi uno dei tumori più aggressivi che interessano il sistema nervoso centrale (CNS) e viene classificato come incurabile. I pazienti affetti da GBM non manifestano sintomi, se non a stadi avanzati della patologia, manifestano metastasi e hanno una breve aspettativa di vita dopo la diagnosi, solitamente di qualche mese. La terapia usata contro il GBM prevede la rimozione chirurgica della massa tumorale, seguita da radioterapia e chemioterapia con Temozolomide (TMZ). Tuttavia, spesso questo approccio non è efficace e i pazienti manifestano recidive.
Tra le caratteristiche che contraddistinguono il GBM e che concorrono alla manifestazione tipica di questo tipo di tumore, si evidenzia l'elevata eterogeneità genetica tra le cellule tumorali. Spesso le cellule tumorali presentano perdita di eterozigosi del cromosoma 10, che porta alla delezione del fattore di inibizione della fosfatasi ed omologo della tensina (PTEN) e a mutazioni a carico della proteina 53 (p53), due fattori correlati con la tumorigenesi. Inoltre, sono presenti alterazioni al recettore per il fattore di crescita epidermico (EGFR) e una sovra-produzione di citochine pro-infiammatorie, come IL-6, che contribuiscono in toto ad una sovra-attivazione della cascata di segnale JAK/STAT. Questa cascata di segnale è coinvolta nella regolazione della proliferazione cellulare, oltre che nella regolazione del ciclo cellulare e dell'apoptosi. Una sua deregolazione la si può ritrovare frequentemente in vari tipi di tumore, compreso il GBM. In aggiunta alla deregolazione della cascata JAK/STAT, anche il silenziamento dei geni codificanti proteine inibitrici del segnale delle citochine, ovvero le proteine SOCS, che inibiscono la cascata di JAK/STAT, contribuisce alla deregolazione della cascata stessa.
Oltre alle sopraccitate caratteristiche genetiche e molecolari, le cellule tumorali di GBM sono in grado di reclutare tutta una serie di cellule del sistema immunitario, tra cui i macrofagi associati al tumore (TAMs), che contribuiscono al mantenimento di un microambiente tumorale immunosoppressivo (TME).
In sostituzione alla terapia classica, dimostratasi poco efficace, nuove promettenti alternative stanno emergendo. Tra queste, l'immunoterapia sembra aver dato incoraggianti risultati preliminari, da ampliare e migliorare. Un esempio di immunoterapia è l'utilizzo di inibitori dei checkpoint cellulari o lo sviluppo di vaccini che inducano una risposta immunitaria contro le cellule tumorali. Altra strada promettente è quella che utilizza i virus oncolitici con l'obiettivo di eliminare le cellule tumorali. I virus oncolitici sono virus in grado di riconoscere, infettare e lisare in modo specifico le cellule tumorali, grazie a delle loro caratteristiche naturali o acquisite mediante l'impiego di tecniche di ingegneria genetica. Oltre a questa abilità peculiare, i virus oncolitici possiedono anche la capacità di innescare una risposta immunitaria in quei tumori che di base vengono classificati come "freddi", ovvero che sono contraddistinti da un TME altamente immunosoppressivo e sono, quindi, in grado di "nascondersi" dalle difese immunitarie dell'organismo. I virus oncolitici, inoltre, possono essere armati con geni terapeutici, che possono contribuire all'eliminazione delle cellule tumorali. Molti sono i virus oncolitici testati contro il GBM, e tra questi gli adenovirus e l'Herpes simplex virus di tipo I (HSV-1) sono i più analizzati.

Nel presente studio sperimentale, redatto durante il periodo di internato presso il gruppo di ricerca della Professoressa Calistri e del Dottor Reale, viene analizzato l'utilizzo di HSV-1 oncolitico (oHSV-1) come terapia contro il GBM. In particolare, la strategia analizzata è duplice: i) armare oHSV-1 con il gene terapeutico mSOCS3, ovvero la forma murina del gene codificante la proteina inibitrice delle citochine 3 e ii) migliorare il delivery dei virus oncolitici verso la sede tumorale, costruendo un virus oncolitico basato su Herpes simplex di tipo I che possieda un promotore specifico per monociti e macrofagi con lo scopo finale quello di usare i suddetti tipi cellulari come carrier cellulari del virus verso la sede tumorale e far esprimere in modo tessuto-specifico a queste cellule il recettore C-C per le chemochine di tipo 5 (CCR5) coinvolto nel reclutamento dei linfociti T, sfruttando i TAMs.
Per generare un oHSV armato con mSOCS3 è stata utilizzata la tecnica della BAC mutagenesi, con cui viene introdotto, grazie al meccanismo di ricombinazione omologa, un transgene all'interno di un cromosoma batterico artificiale (BAC) rappresentante il genoma di HSV. In questo caso specifico, l'oHSV generato possedeva nel genoma anche un gene reporter, codificante la green fluorescence protein (EGFP), in modo da poter analizzare l'infezione da parte di oHSV-mSOCS3-EGFP con l'impiego della microscopia a fluorescenza. Il suddetto virus oncolitico è stato utilizzato per infettare cellule di GBM umano e murino (rispettivamente GL261 e LN229), in modo da poter analizzare la permissività di queste due linee cellulari all'infezione e da valutare l'effetto citopatico che causa il virus oncolitico. Successivamente, le cellule di GBM murino sono state utilizzare per estrarre le proteine e valutare l'eventuale produzione di SOCS3 in seguito all'infezione di oHSV armato con mSOCS3.
Nella seconda parte del lavoro sono stati generati due oHSV contenenti il gene per una proteina reporter fluorescente rossa (mCherry) sotto il controllo trascrizionale di due promotori diversi: il promotore di Citomegalovirus umano (hCMV), un promotore forte e che garantisce un'espressione quasi ubiquitaria, e il promotore monociti/macrofagi-specifico CD68 umano, che limita l'espressione solo a monociti e macrofagi umani. Per generare i due virus oncolitici è stata impiegata nuovamente la tecnica della BAC mutagenesi. oHSV-hCMV-mCherry possiede nel backbone del suo genoma anche la sequenza target per il mir124, un trascritto solitamente sovraespresso nei neuroni e che porta a neuro-attenuazione del virus oncolitico. Per analizzare la capacità di killing delle cellule tumorali da parte del virus neuro-attenuato, oHSV-hCMV-mCherry è stato utilizzato per infettare le cellule GL261 e LN229 in modo da poter valutare la differenza in vitalità cellulare tra cellule non infettate e infettate. Successivamente, entrambi i virus oHSV-hCMV-mCherry ed oHSV-CD68-mCherry, sono stati usati per infettare due linee di GBM, una murina e una umana (sempre GL261 e LN229), e due linee di monociti, una umana (CD14+) e una murina (WEHI), in modo da poter valutare, grazie alla microscopia in fluorescenza, l'espressione di mCherry in modo differenziale tra le varie linee cellulari. Oltre a ciò, i surnatanti prelevati dalle cellule infettate sono stati titolati per valutare la capacità di replicazione virale anche in eventuale assenza di fluorescenza.

1 Abstract

Glioblastoma (GBM) is one of the most common and aggressive malignant brain tumors in adults. Patients affected by glioblastoma show poor prognosis and low survival rate after the diagnosis. Indeed, nowadays, glioblastoma is mostly untreatable and intervention procedures rely on classic, no-specific treatments, such as surgical resection followed by radiotherapy and chemotherapy. Part of the difficulties in the treatment of glioblastoma arises from the complex molecular background of the cancerous cells and from the high heterogeneity in the genetic processes that lead to the development of the tumor. New approaches are under evaluation, including new prediction techniques and innovative therapies, like immunotherapy. Among the novel therapeutic strategies, oncolytic viruses that specifically replicate in and kill tumor cells are emerging as interesting alternatives. Furthermore, oncolytic viruses can be engineered for targeting particular signal pathways. Herpes simplex virus type I (HSV-1) is the focus of the present study, in which the virus, used in its oncolytic form, was armed with different therapeutic genes or modified in order to improve its delivery and killing activity toward the tumor cells.

2 Introduction

2.1 Glioblastoma: a general overview

Glioblastoma (GBM) is the most common primary malignant brain tumor, with an incidence rate of 3.2 per 100,000 in the population [1]. The median age of occurrence of glioblastoma is around 64 years, but it can develop at any age, also in childhood. Incidence is a bit higher in men than women and in Caucasian people than people of other ethnicities [2].
GBM usually occurs in the brain, but it can also affect the brain stem, cerebellum and the spinal cord. It can arise from a multitude of cell types, but all of them have neural stem cell-like properties. These cells stop at different stages of differentiation, that can range from stem cell to glia, with a diversity of alterations in the molecular signaling pathway, which justifies the wide heterogeneity present it the tumor mass [2].
GBMs can be classified as primary tumor, when the precursors prior the onset of the tumor are unknown, or secondary tumor, when a low-grade cancer progresses, over time, into GBM. Thanks to genetic and epigenetic analysis, GBMs can also be classified in four subtypes, i.e. classical, pro-neural, neural, and mesenchymal. Primary GBM is the most common among the patients affected and, usually, the symptoms appear only at an advanced stage of the disease [3]. Despite the treatments, the average survival of GBM patients is 14.5 months, and 70% of the patient affected by GBM will undergo disease progression in about one year, and only a small part of the patients, less than 5%, can survive over 5 years after the diagnosis. Therapy to tackle is still difficult, due to the physiologic characteristics of this type of tumor, its molecular and genetic heterogeneity and the poor prognosis [2].

2.2 Glioblastoma genetic features

In terms of the genetic mechanisms beyond the development of GBM, it is important to underline the differences between primary GBM and secondary GBM. There are some common genetic alterations, shared by both types of GBM, but some genetic alterations are more frequent in primary GBM than secondary GBM and vice versa. The most recurrent alterations are loss of heterozygosity (LOH), alterations of EGFR/PTEN/Akt/mTOR pathway and mutations in TP53 gene [4].
As far as LOH is concerned, this is the most common alteration occurring in both primary and secondary GBM, roughly at the same frequency (60-80%). Often this LOH is caused by the deletions or mutations in the 10q region of the chromosome 10, for both the types of GBM. Typically, the loss of the entire chromosome 10 is a more frequent in primary GBM and partial or complete loss of the 10q with no alteration of 10p is more common in secondary GBM [5]. Since various tumor suppressor genes map within the 10q region, the loss or mutation of this part of the chromosome can be associated with the pathogenesis of both types of GBM.
One of the genes present in the 10q region is *PTEN* (10q23.3), a gene mutated almost exclusively in primary GBM. *PTEN* is classified as a tumor suppressor

gene and encodes the homonymous protein PTEN, which stands for phosphatase and tensin homolog [4]. This protein has a phosphatase activity and it is involved in cell proliferation. Thus, the mutation of *PTEN* gene can cause uncontrolled cell dividing. More specifically, PTEN has a tensin-like domain and a catalytic domain similar to the catalytic domain of the dual specificity protein tyrosine phosphatase enzymes family. However, unlike most of the protein tyrosine phosphatases, this protein preferentially dephosphorylates phosphoinositide substrates, such as PIP3 in EGFR/PTEN/Akt/mTOR pathway [6]. In this pathway, EGFR (Epidermal Growth Factor Receptor) is an extracellular receptor, activated by the binding with its ligands, i.e. Epidermal Growth Factor (EGFR) and Transforming Growth Factor- (TGF-). Once activated, EGFR recruits the PhosphatidylInositol 3-Kinase (PI3K) to cell membrane, which phosphorylates phosphatidynositol-4,5-bisphosphate to PhosphatidylInositol (3,4,5)-trisPhosphate (PIP3). PIP3 activates downstream effector molecules such as Akt (protein kinase B) and mTOR (mammalian Target of Rapamycin), both kinases involved in cell proliferation and increasing cell survival, by blocking apoptosis. PTEN inhibits the PIP3 signal with its phosphatase activity, thus inhibiting cell proliferation. In primary GBM, typically, there is amplification of EGFR and more frequently overexpression of this gene. *EGFR* is often mutated. The most common variant is variant 3 (*EGFRvIII*), characterized by the deletion of exons 2 and 7. The receptor encoded by this variant is constitutively active, resulting in enhanced cell proliferation [4].

Another gene frequently mutated in glioblastoma, more specifically in secondary GBM, is *TP53*. This gene encodes the protein p53, a transcriptional activator involved in the regulation of cell cycle, in the response of cells to DNA damage, cell death, cell differentiation and neovascularization. p53 regulates the transcription also of its negative regulator factors, causing a negative feedback loop [4]. Usually, the mutations in *TP53* are missense mutations and occurs in highly conserved domains of the encoded protein, which are fundamental for DNA binding. The mutations of *TP53* or the amplification and overexpression of the negative regulator of p53 genes results in blocking p53 activity and potentially lead to uncontrolled cell proliferation [7].

In addition to these genetic alterations in glioblastoma, there are also variations in the epigenetic pattern of the DNA in glioblastoma cells. These alterations in the epigenetic pattern lead to changes in the normal gene expression of the cell, without modification of the DNA sequence. The main variations are focused on the methylation pattern, where there is i) hypermethylation of CpG island, often in regions corresponding to tumor suppressor genes, ii) gene-specific hypomethylation, resulting in activation of oncogenes, and iii) genome-wide hypomethylation, potentially causing chromosomal instability and uncontrolled cell proliferation [7]. One gene affected by these alterations is *MGMT*.

MGMT encodes the homonymous protein MGMT (O^6-methylguanine-DNA methyltransferase) which is an enzyme involved in the DNA repair after the DNA has been damaged by alkylating agents, causing mutations in the DNA sequence during replication. More specifically, this enzyme removes the methyl group present in the O6 position of guanine, preventing G:C $\longrightarrow$ A:T genetic

alterations. Patients affected by glioblastoma that present hypermethylation of *MGMT* gene show a better response to chemotherapy with Temozolomide (TMZ), which is an alkylating agent [6].
IDH1 and *IDH2* are two genes that encode the two respective isoforms of the enzyme isocitrate dehydrogenase, which catalyzes the oxidative carboxylation of isocitrate to produce ∝-ketoglutarate. When these two genes present mutations, a-ketoglutarate is converted in 2-hydroxyglutarate, which is an oncometabolite that causes the hypermethylation of DNA, in particular, where there are promoters and CpG islands [6], [7].

2.2.1 A focus on JAK/STAT pathway

EGFR is involved in a plethora of signal pathways, and one of these is JAK/STAT cascade of signal, which is often deregulated in many types of tumors, including glioblastoma. STAT signal is involved in many processes, such as cell differentiation, growth and apoptosis [8].
Under physiological conditions, when JAK/STAT pathway is not deregulated, EGFR bind its ligand with the extracellular portion of the receptor. EGFR has an intrinsic tyrosine kinase activity, and it autophosphorylates the cytoplasmic tail of the receptor. Tyrosine-phosphorylated EGFR receptors can dock cytoplasmatic monomeric STAT proteins, thank to theirs SH2 domains, and after this interaction, STAT proteins can dimerize and establish a classical JAK/STAT signaling cascade. Another way to activate the pathway is by cytokines receptors. After binding the cytokine, the receptors dimerize and recruit receptor-associated tyrosine kinases, like JAKs proteins, that phosphorylate the cytoplasmatic tails of the receptors. The phosphorylated receptors can bind STAT proteins. There are seven types of STAT proteins (STATs 1, 2, 3, 4, 5a, 5b, 6), and they can dimerize as homodimers or heterodimers. A prerequisite to form a dimer between two STAT proteins is SH2 domain phosphorylation, which is induce by EGFR receptors. The dimers translocate to the nucleus, interact with other transcriptional modulators, and induce gene expression (Figure 1).

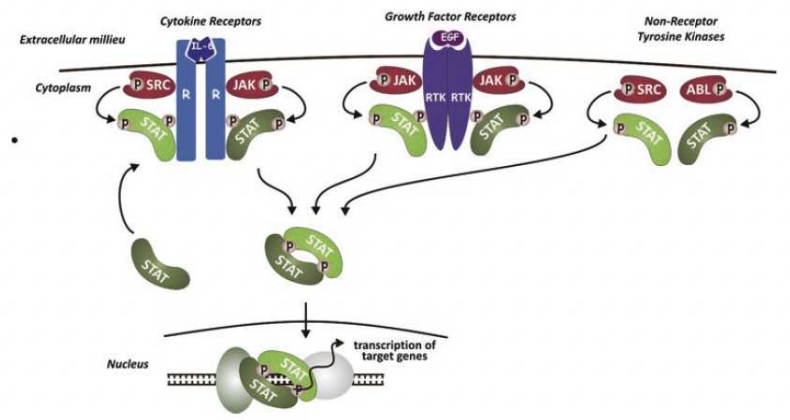

Figure 1. *Schematic representation of JAK/STAT pathway [9].*

To turn-off the signal, phosphorylated STAT proteins are dephosphorylated by

nuclear tyrosine phosphatase or they are degraded through proteolytic degradation. There are also modulators of STAT signaling pathway, such as SOCS (suppressor of cytokine signaling) protein family, that can bind and inhibit JAK kinases. SOCS proteins family counts seven proteins (SOCS1-7) and the expression of some of them, like SOCS1 and SOCS3, is induced by cytokines and growth factor stimulation or by STATs proteins, in a negative feedback loop [9].
Under physiological conditions, the activation and duration of the JAK/STAT signal is strictly controlled and can last from few minutes to several hours [9], [10].
It has been demonstrated that STATs expression is modified in gliomas, with relevance of STAT3 expression. STAT3 is constitutively active in malignant gliomas tumors, and pSTAT3 (the phosphorylated and activated form of STAT3) level increase with malignancy, being the highest in glioblastomas. Has been demonstrated that the activation of STAT3 can be connected to clinically more aggressive behavior in glioblastomas, and tumors with high level of pSTAT3-positive cells are linked to lower survival rate. This alteration in the expression of STAT can be linked to mutations in the gene encoding EGFR receptor. Usually, mutations of cytokine receptors and JAKs are infrequent, while mutations in growth factor receptors are quite common in tumors. Variant III of EGFR is a ligand-independent receptor, which means that EGFRvIII is constitutively active [9].
Also altered expression of negative modulators of STATs can contribute to constitutive activation of the signal pathway. It has been seen that SOCS3 is often silenced by hypermethylation in cancerous cells and, specifically, in glioblastoma [11].
STAT3 is consider as an oncogene because STAT3 protein has effects on cell cycle and is linked to cell proliferation and suppression of apoptosis. STAT3 is important also for cell invasion of tumor cells, because it up-regulates the expression of metalloproteinases, and it is a direct transcriptional activator of VEGF, which acts as one of the main signals for angiogenesis. Finally, STAT3 seems to promote an immunosuppressive tumor microenvironment, by promoting a T regulatory profile of immune cells [8].
Since STAT3 and its regulation play important roles in glioblastoma they both can be used as targets in therapy for this type of tumor.

2.3 Standard therapies and novel approaches adopted against glioblastoma

GBM is currently almost untreatable and the only therapies commonly adopted are classic standard treatments, that do not improve the survival rate of patients in a significant way. Moreover, the probability of recurrence of the malignancy after treatments is quite high, which lowers the overall survival rate after 5 years from the treatment (an important parameter to estimate the efficacy of the therapy in tumors) of affected patients [12].
The difficulties in the treatment of this type of tumor rely on the high genetic heterogeneity of GBM and on its complex molecular background. Also, the

blood-brain barrier (BBB) is an obstacle for the delivery of therapeutic agents. For this reason, there is the need to find new therapies that are effective and specific for some pathways within the cancerous cells or that can target the tumor mass without damaging the healthy tissue of the brain.
Standard therapies for glioblastoma include surgery to remove the main tumor mass, followed by radiation with adjuvant Temozolomide (TMZ) chemotherapy to target residual tumor cells. However, because of the presence of GBM stem cells (GSCs), that contribute to the invasiveness of GBM and are usually refractive to therapies, the infiltrating nature of GBM and some genetic and molecular features of tumor cells, that can lend therapy resistance, this approach of treatment often lead to fatal recurrence [13]. Maximal surgical resection consists in the removal of most of the tumor mass, in order not to damage the surrounding healthy tissue. However, usually, it is not enough to completely remove the tumor, because tumor cells infiltrate non-tumor tissues and are not surgically accessible. Furthermore, the location of the tumor must be taken into account, as it can affect very specialized areas of the brain. As a consequence, surgical resection would compromise basic functionalities of the brain, like speech, motor function and senses [13].
Surgical resection is usually combined with radiotherapy, which is also the primary treatment modality for unresectable GBM. Radiotherapy is typically joint with TMZ chemotherapy, and it was demonstrated that the combination of these two treatments is more effective than the single treatment performed alone. Nevertheless, TMZ can present some toxicity, and not all GBM patients benefits from its administration. TMZ is a second-generation DNA alkylating agent and it is an oral medication that can cross BBB and accumulates in high concentrations in the brain and in high angiogenic tumors like GBM. Its acts by methylating adenine e guanine residues to form the corresponding methylated bases, which are source of DNA mutation or can lead to apoptosis and are repair by DNA repair mechanisms to prevent cell death. One of the enzymes involved in DNA repair is MGMT and studies show that those patients with methylated *MGMT* promoter, resulting in lower level of the enzyme, has a better response to TMZ chemotherapy. Yet, patients with unmethylated *MGMT* promoter show a worse response to TMZ treatment and there are emerging cases of resistance [12].
New approaches in the treatment of GBM count use of nanoparticles, photodynamic therapy, CAR T therapy, focused ultrasound therapy, immunotherapy e oncolytic virotherapy.
Nanoparticles are used to help antitumoral drugs, that cannot cross BBB, to be delivered to the brain, or to improve GBM diagnosis by imaging, to impact certain cell pathways or a specific population of tumor cells. One example are liposomes loaded with drugs, antibodies o peptides to help these molecules to cross the BBB [13].
In the photodynamic therapy, photosensitizers are used. These molecules are selectively introduced in tumor cells and photoirradiation can activate them, leading the sensitizers to an excited energy state. Oxygen is required to accept the energy from the sensitizer. Excited atoms of energy can cause ROS production within cells, resulting in organelles and macromolecules damage and

cell death [14].
CAR T therapy is based on engineering immune system cells, in particular lymphocytes T, to express chimeric antigen receptors (CARs), which are designed to target specifically tumor antigens to trigger the immune response in patients [15].
Another approach to improve the drugs delivery to the brain is focused ultrasound therapy which is an emerging technology for targeted delivery to CNS. Some new studies show that low-intensity pulsed ultrasound increase the concentrations of systemically administered drug therapies in the brain parenchyma in animal models [15].
Immunotherapy is one of the most promising strategies for GBM treatment. It is based on harnessing the body's immune system against cancerous cells.
In the end, oncolytic virotherapy take advantage of the ability of some virus to naturally detect, infect and kill tumor cells. This characteristic can also be artificially acquired by genetic engineering and viral genome can also be edited to arm the virus with therapeutic genes, useful in tumor treatment [13].
Some of these strategies can be combined to maximize the effect of the therapy or to overcome some obstacles of one approach, such as the difficulties in the delivery.

2.3.1 Immunotherapy of GBM

As mentioned above, immunotherapy takes advantage of the host's immune system to trigger an immune response against tumor cells. CNS is thought to be an immune-privileged site, with strict access to the profound brain by immune system cells, but there is a classic lymphatic system that carries fluids and immune cells from cerebrospinal fluid to CNS. In addition, microglia, usually quiescent in healthy brain, can be activated upon inflammation and orchestrate and immune response. All these characteristics show that there is a chance to develop an effective immunotherapy against tumors [15]. However, one of main difficulties in using immunotherapy with glioblastoma is the strong immunosuppressive microenvironment all around the tumor, the prevent the immune system to recognize and target cancerous cells. GBM is define as a "cold tumor" because it presents a low grade of somatic mutations and lack T-cell inflammation compared to other types of tumors. Also, tumor cells produce cytokines and molecules that turn-off the immune response and can "hide" the tumor from immune cells or recruit immunosuppressive cells, such as Treg. For this reason, three different strategies of immunotherapy are being studied: immune modulating cytokine therapy, passive therapy and active immune therapy, with cancers vaccines [15].
Cytokines therapy uses mediators of immune activation and proliferation to induce an anti-tumor immune response. A variety of cytokines are considered, such as IL-2, IL-7 and IL-12. Cytokines immune therapy is effective in activating the immune response, but the immune effects are non-specific and often lead to extensive toxicities, limiting their use. Moreover, because of the multitude of immune evasion mechanisms played by the tumor, cytokines therapy showed disappointing results during clinical tests and it must be refined to be more effective [12].

Passive therapy is mostly based on immune checkpoints blockade. Immune checkpoints are used by the immune system to prevent autoimmunity, where immune checkpoints receptors, after interacting with their ligand, modulate immune activity toward targeted cell. Some tumors, like glioblastoma, can hijack the immune response by expressing immune checkpoint receptors ligands and turning off the T cells-mediated immune response. One of the main mediators of this mechanisms is programmed death-1 (PD-1) and its ligand (PD-L1), which is a negative regulator of T cells activity. It has been seen that PD-L1 is expressed by glioma cells and that the expression level is higher at the tumor edges than in the tumor core, forming a sort of "molecular shield" between tumor cells and cytotoxic T cells. Clinical trials showed that immune checkpoint blockade has limited efficacity and it must be improved [12].
Cancers vaccines, as a form of active immunotherapy, can have both therapeutical and preventing qualities. Cancers vaccines are designed on tumor-associated antigens that can trigger a primary and acquired immune response. As far as is GBM concerned, one of the main targets used to develop vaccines is EGFRvIII. Nevertheless, the results for cancers vaccines are not very promising, due to lack of GBM-specific antigens and the high heterogeneity of the tumor. Recent progresses in next generation sequencing and bioinformatic analysis helped develop synthetic antigens that can be used in vaccines. Further developments are needed and there are other obstacles to overcome, such as the tumor immunosuppressive microenvironment [12].

2.3.2 Oncolytic virotherapy

Oncolytic virotherapy is a type of immunotherapy which takes advantage of the natural or acquired capability of some viruses to identify, infect and kill cancerous cells [16]. Oncolytic viruses (OVs) can use tumor-specific mutations or signaling pathways that are constitutively active in tumor cells and can also be armed with genes that increase toxicity or cell death in tumor cells or are engineered to improve the delivery of the virus toward the tumor. GBM is particularly suitable to oncolytic virotherapy because of lack of distant metastases and the confinement of the tumor within the brain, surrounded by terminally differentiated cells, that do not replicate, like those of the tumor mass (replicating cells is one of the requisites for viral replication). Oncolytic virotherapy uses oncolytic viruses that can normally replicate and selectively infect tumor cells or replication-deficient viral vectors employed as vehicles for therapeutic genes [15].
Oncolytic viruses are not used only for their cell-lysis capability but they can also stimulate an immune response in the organism, which is useful particularly in those tumors that have an immunosuppressive TME. The mechanisms in which OVs are involved are direct tumor lysis, modulation of the TME, priming of immune responses mediated by CD8+ T cells and innate immune cells and vascular modifications. OVs usually trigger immunogenic cell death and in situ inflammation, by causing the release of danger-associated molecular patterns (DAMPs) and tumor-associated antigens (TAAs), which attract innate immune system cells to the tumor and leading to the recruitment and maturation of tumor specific T cells in the TME. TAAs can act as neoanti-

gens and be patient-specific since they can originate from mutations within tumor cells. Also, viruses trigger innate immune response, thanks to their pathogens-associated molecular patters (PAMPs). In this prospective, OVs can be used to disrupt an immunologically cold tumor TME. In some clinical trials with GBM, the therapeutic benefit of OVs seems to be more related to the immunostimulatory role of the oncolytic virus that to its cell lysis ability [17]. Pseudoprogression of the tumor is another feature of the use of OVs. Analyzing the tumor by imaging, it looks like the tumor is growing, but it is just an artifact caused by the recruitment of inflammation-associated cells after the OV infection. Moreover, oncolytic virotherapy does not show toxicity associated with the administration of the OV, but usually, the only toxicity can arise from the inflammation process elicited by lysed cells [18].
Many viruses can be employed in oncolytic virotherapy. In GBM one of the most studied OVs is Herpes simplex virus type I (HSV-1). However, the selection of the right virus to use in therapy is not simple and there are many parameters to consider. First, the viral genome is important to choose the right virus. Both RNA and DNA viruses can be used, single-stranded and double-stranded. DNA viruses have some advantages. DNA genomes are typically larger than RNA genomes and they can be easily manipulated and engineered to accommodate quite big transgenes. Also, some viral genes are not essential and can be eliminated or modified to modulate viral capability to infect non-cancerous cells and viral replication and to add genes of interest to the viral genome. DNA genomes are more stable and have greater integrity than RNA genomes [19].
Besides the choice about the viral genome, the virus must have the right balance between lytic power and the ability to stimulate an adaptive antitumor immune response to ensure that the tumor cells are not lysed before producing immunomodulatory molecules. Highly lytic viruses can be more immunogenic and trigger an antiviral adaptive immune response, which leads to rapid clearance of the virus before it can activate an immune response toward infected cancerous cells. In addition, highly lytic viruses can lyse targeted cells before the expression of therapeutic genes introduced in their genomes can begin. On the other hand, less lytic virus can be not sufficiently powerful to generate the desired immune response [19].
Oncolytic virotherapy can be used in combination with other types of therapies. Combination of OVs with traditional treatments, such as radiation and chemotherapy, is feasible. For example, in glioblastoma, the combined use of radiation or chemotherapy with TMZ and OVs was shown to have a synergic effect [17].
Frequently, OVs are associated with immune checkpoint inhibitors (CPIs). Tumors with low T cells infiltration, like GBM, do not get significant benefit from CPIs treatment, because checkpoint inhibitors work by blocking the negative regulators of T cells function and sustaining T cells activity. Since the use of oncolytic viruses increase the infiltration of T cells into tumor site, they can also increase the beneficial power of CPIs therapy [17]. OVs can be armed with genes encoding proteins capable of remodeling the extracellular matrix (ECM) of the tumor. The ECM can be fibrous-like thanks to cancer-associated

fibroblasts, that make the ECM restrictive to the migration of immune cells into the cancer site. ECM remodelling proteins encoded by armed OVs genes can ease the migration of immune cells [19].
Two main problems about oncolytic virotherapy are the pre-existent immunologic memory of the organism toward the virus used and the delivery of the virus in the tumor site. The presence of an immunologic memory against the virus, originated from a previous infection of the virus, is a problem for those viruses that are diffused in the population. In this case, the use of this therapy can cause an immune response against the therapeutic virus consequently leading to a more rapid clearance of the virus from the organism. The OV eliminated does not have enough time to elicit its therapeutic effect. A solution to this problem could be the development of engineered OVs that are not recognized by the host immune system. As about the delivery of OVs, there is the possibility of limiting the quantity of virus that can reach the tumor site, making the virus dose insufficient to produce its therapeutic effect. On the other hand, direct administration of OVs into the tumor cannot help with metastases or tumors in other sites [19].

2.4 Herpes simplex virus type I

Herpes simplex virus type I (HSV-1) belongs to the *Herpesviridae* family. The *Herpesviridae* family accounts for many different viruses, sharing common features. Indeed, all of them are characterized by icosahedral capsids enwrapped in a lipidic envelope. Between the capsid and the envelope there is an amorphous layer of proteins useful for efficient infection, called tegument. The herpesviruses' genome is double-stranded DNA. The envelope originates from cellular membranes and displays many viral glycoproteins, some of which are used for receptor recognition and internalization of the virus into the target cell.
Herpesviruses are divided into three subfamilies, alpha, beta and gamma, based on their biological characteristics, DNA sequence relatedness and the cell types or tissue they infect. HSV-1 is an alpha herpesvirus, along with HSV-2 and varicella zoster virus. These herpesviruses have the ability to establish latent infections in neurons.
HSV-1 is carried by 45-90% of the population [21]. Primary infections usually result in the establishment of latent infections in sensory neurons, and the primary infection site is typically the oral mucosa and, less frequently, the genital mucosa. During the primary infection, viral particles enter the neuronal axons and travel to the neuronal nuclei, in the cell body in the ganglion, where the viral genome is assembled into a repressed extrachromosomal chromatin structure. In this form, HSV-1 initiates a latent infection. In one single neuron there can be from tens to hundreds of viral genomes. Because neurons are terminally differentiated cells, they do not divide and the viral genomes are maintained. Also, viral protein expression is almost absent and latently infected neurons are not susceptible to immunological surveillance. HSV-1 can exist its latent status and reactivate, beginning with its lytic cycle. When this happens, the clinical signs of HSV-1 infection appear. The reactivated virus

in neurons is transported down the axon to the peripheral site of the primary infection, in a retrograde way. Here, it originates the typical lesions. However, if HSV-1 enters the central nervous system, it can cause more serious diseases, such as herpes encephalitis.
There is not a vaccine for HSV-1, but there are effective antiviral drugs. One of the most used drugs is acycloguanosine (acyclovir), which is a nucleoside analogue that cannot be phosphorylated by the cellular replication enzyme and act as a chain terminator, inhibiting DNA replication when incorporated in replicating DNA in virus-infected cells. Drugs as acyclovir limit the lytic cycle of the virus but they have no power against the latent form of HSV.
HSV-1 is an excellent model to study viral replication and for other research purposes, because it replicates rapidly and efficiently in a wide range of cell types [20].

2.4.1 HSV-1 genome and biologic cycle

HSV-1 has a double-stranded DNA genome of around 152 kbp. The genome can be divided into segments: a long segment called UL and a short segment called US. Both these segments have two inverted repeated sequences at their ends, respectively IR_L and TR_L and IR_S and TR_S. Externally to these repeated regions there are shorter repeated segments, called 'a' sequence, that are used to invert the orientation of the UL and US segments, thus creating four genomic isomers in equal ratios and with the same functionality. 80 genes have been identified from the analysis of HSV-1 genome.

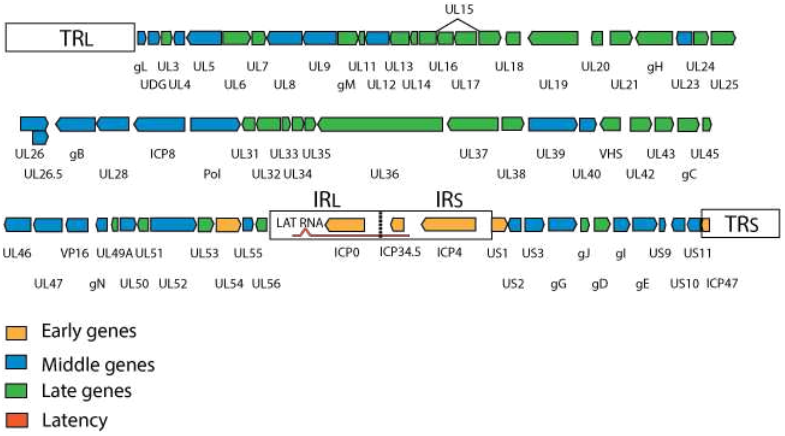

Figure 2. *Schematic representation of HSV-1 genome [20].*

To entry into target cell, HSV-1 uses a multistage process, that requires both cellular receptors on the surface of the cell and viral glycoproteins of the virus envelope. The first interaction is between cellular heparin sulphate and glycoprotein gC, followed by the interaction between cellular receptors, such as herpes virus entry mediator (HVEM) and nectin-1, and glycoprotein gD. Glycoprotein gB is required for the fusion of the envelope with the cellular membrane, with the assistance of gH/gL complex. Once released in the cytoplasm, the capsid is carried along the microtubules to the microtubule-organizing center (MTOC) and then transported to the nuclear envelope. Here, the capsid

associate with nuclear pores, the viral genome is uncoated and enter the nucleoplasm through the nuclear pore, in a poorly understood mechanism. The proteins of the tegument are present from the earliest stages of infection and they can regulate the initial events of infection, guarantying an efficient infection. VP1/2, produced from UL36, is essential for viral genome release from the capsid into the nucleus and for tegumentation and capsid envelopment.

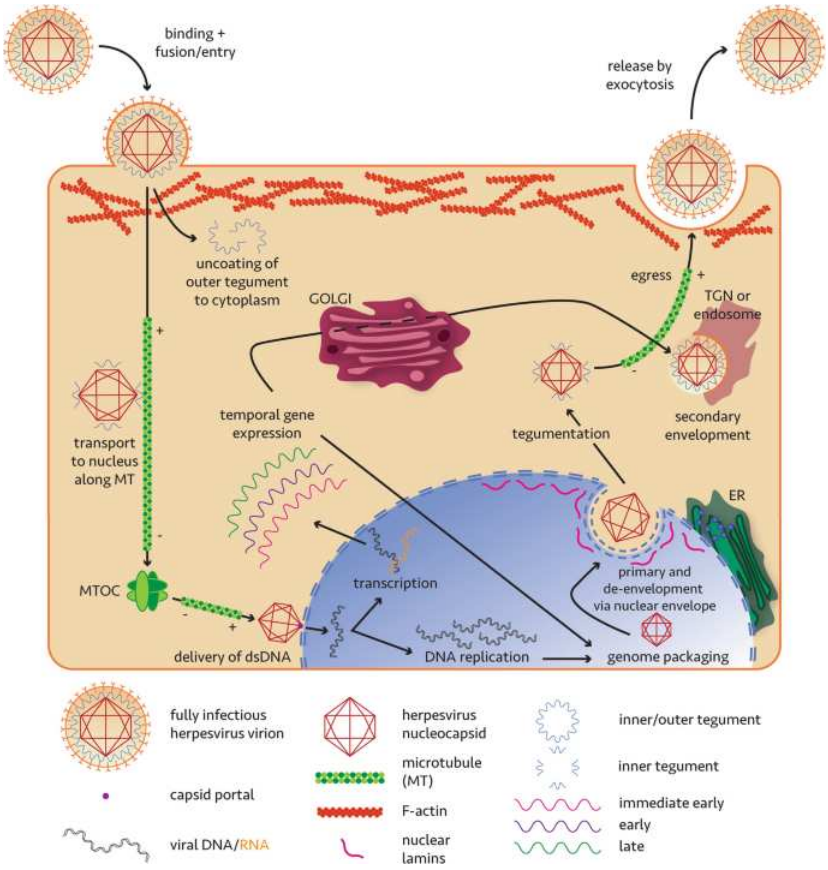

Figure 3. *Schematic representation of HSV-1 infection cycle [20].*

Viral gene expression is divided into three groups: immediate-early genes (IE or α), early genes (or β) and late genes (or γ), divided in leaky-late (γ_1) and true-late (γ_2). Immediate-early genes are the first to be transcribed using the host transcriptional apparatus stimulated by the tegument protein VP16 and the process does not require de novo viral gene expression. Early genes are transcribed once IE proteins have been synthesized and the transcription is independent of viral DNA replication. Late genes are transcribed once viral DNA replication has started. The difference between leaky-late and true-late genes depends on the strictness of requirement for DNA replication for their transcription. Usually, after DNA replication has begun, all three groups of genes can be expressed simultaneously. Also the promoter of the three groups of genes are different: IE genes have the most complex promoters, with a TATA box and transcription factor-binding sites, early genes have simpler promoter, with a TATA box and an upstream transcription factor-binding element, while late genes promoters are the simplest, with only a TATA box and an initiation region.

DNA replication takes place in the cell nucleus and begins after early gene expression has started. HSV-1 has three origins of DNA replication, one in each of the two repeated sequences at the US ends and one in the middle of UL. HSV-1 genome encodes all the proteins required for its DNA replication, like a viral DNA polymerase. DNA replication is very efficient, producing hundreds to thousands copies of viral genome and it produces long concatemers of viral DNA which are then processed into unit length molecules during the DNA packaging process into new capsids.
Mature HSV-1 capsids are icosahedral structures formed by 162 capsomers, each including six (hexons) or five (pentons) molecules of the major capsid protein called VP5 (UL19). One vertex of the structure is different from the others because it represents the portal for packaging of viral DNA into the maturing capsids. Immature capsids accumulate in the nucleus. DNA is then packaged through the portal in new capsids, forming mature capsids. Mature capsids bud through the inner nuclear membrane into the perinuclear space. These particles then bud again through the outer nuclear membrane via membrane fusion, releasing the capsids in the cytoplasm. The capsids associate with the membranes of Golgi vesicles, where the tegument and the envelope mature, acquiring the envelope glycoproteins. After the fusion of the Golgi vesicles containing the viral particles with the cytoplasmatic membrane, mature viral particles are released from the cell [20].
Latency of the virus is associated with latency-associated transcripts (LATs), which are non-coding RNAs. Once the viral genome enters the nucleus of the neuron, it is assembled into a chromatin structure resembling heterochromatin and it becomes transcriptionally repressed. LATs RNAs are produced by the activity of ICP0, a viral protein that can also reactivate HSV-1 from latency. Thus, ICP0 seems to be crucial to keep the balance between laten infection and lytic activity of HSV-1. Reactivation of the virus can be caused by hormonal fluctuations, trauma, UV light and immunosuppression [20], [21].

2.4.2 HSV-1 oncolytic virus and genomic modifications

Among OVs, Herpes Simplex Virus I (HSV-1) is one of the most tested viruses and investigated in numerous pre-clinical studies. Oncolytic HSV-1 (oHSV-1) is often engineered to reduce its neurovirulence and enhance its anti-tumor lytic activity and immunogenicity [22]. The first oHSV-1 were mutated or multimutated conditionally replicating recombinants, obtained by the deletion or inactivation of one or more viral genes for nucleotide metabolism, necessary for the virus replication in non-dividing cells [23]. This strategy was then refined, adding transgenes in HSV-1 genome to improve its tumor-specific targeting activity. HSV-1 has a relatively large genome that facilitates modifications that can enhance anti-tumorigenic features and reduce neurovirulence. Engineering strategies aim at preventing of nervous system, enhancing tumor selectivity and increasing immunogenicity [24]. However, some strategies to make the virus safe for use caused in multimutated oHSVs an attenuation, in terms of replication efficiency in tumor cells, as compared to wildtype HSV. A strategy to overcome this problem is to arm multimutated backbones of attenuated oHSVs with transgenes to restore their oncolytic efficacity [23].

Among the most frequently modified HSV genes there is *γ34.5* which encode a factor required for neurovirulence. *γ34.5* is present in two copies in HSV genome, within the inverted repeat regions. Both copies of *γ34.5* o just one can be deleted and numerous studies have demonstrated the safety of both these variants with limited side effects [24]. Another commonly modified gene is *US12*, that encodes ICP47, an immune evasion protein blocking viral antigens presentation by infected cells. Deletion of this gene makes infected cells more immunostimulatory than infected cells with wildtype HSV [23].
Tropism retargeting is an alternative approach to use oHSV respecting safeness and exploiting cancer specificity and its full oncolytic power without resorting to attenuation. This strategy relies on the expression of cancer-specific antigens exposed on tumor cell plasma membranes combined with a profound knowledge of receptor binding and entry mechanism of HSV. HSV uses envelope glycoproteins to bind target cells receptors and enter. This is an advantage because viral glycoproteins in the envelope are more flexible and motile that proteins of the capsid, which allows more steric and spatial space to play with while engineering glycoproteins. Thus, the most successful retargeting strategies are based on HSV envelope glycoproteins (i.e. gD, gB, gH/gL complex), with good result in terms of high titer viral replication and tumor specificity [23].
The first HSV-1 oncolytic virus approved by Food and Drugs Administration (FDA) in 2015 was called Talimogene laherparevec (T-VEC). T-VEC is a JS1 strain HSV-1, selected for its ability to specifically replicate in and kill human tumor cells. T-VEC has function deletion of UL34.5 and US12 genes and is armed with the human transgene coding for a cytokine granulocyte macrophage-colony stimulating factor (*GM-CSF*). As previously said, UL34.5 encodes ICP34.5, a multifactorial virulence factor and its deletion convey tumor-specificity. ICP34.5 can complex with protein phosphatase 1 alpha (PP1α) to dephosphorylates the alpha subunit of eukaryotic initiation factor 2 (eIF2), thus blocking the action of ds-RNA- dependent protein kinase R (PKR) and inhibiting protein production. The deletion of UL34.5 block T-VEC replication in non-tumor cells but maintaining replication capacity in tumor cells due to the absence of PKR activity in most tumor cells. Also, HSV-1 infected cells activate autophagy thanks to PKR signal pathway in response to infection, and ICP34.5 is able to block this response. Moreover, ICP34.5 can impede dendritic cells maturation and presentation of viral antigens, thus inhibiting the activation of adaptive immune response. ICP47, encoded by US12, interfere with viral antigen presentation by acting as a high affinity competitor for the peptide-binding site on a host cell's transporter-associated protein (TAP), which loads the peptide in MHC I complex for antigen presentation to cytolytic T lymphocytes (CTL). This result in immune response attenuation against infected cells and US12 lead to robust CTL activation and recruitment against infected cells. In addition, US12 deletion shift US11 gene under the US12 promoter. US11 gene is a late gene that inhibit antiviral response mediators and enhancing viral expansion. Under US12 promoter US11 become an early gene. In the end, the expression of *GM-CSF* leads to the recruitment of an array of immune cells to the infection site and promotes

maturation of dendritic cells, macrophages, and granulocytes. Therefore, all T-VEC genome mutations allows the virus to replicate successfully in tumor cells by suppressing cellular antiviral response, while simultaneously promoting immune response to infection, resulting in tumor-specific killing properties of this OV [21].
Similar to T-VEC, G207 has deletion of both UL34.5 copies of the gene. G207 come from HSV-1 strain F and deletion of UL34.5 leads to alteration of LAT genes expression, resulting in the inability of the virus to establish latency. G207 also has lacZ insertion in UL39, the gene encoding ICP6, a large subunit of the viral ribonucleotide reductase, that is inactivated as a result of *lacZ* insertion. ICP6 is necessary for efficient growth of the virus in non-dividing cells, which do not produce a functionally equivalent enzyme like that produced by proliferating host cells. Inactivation of ICP6 prevent G207 from replicating in quiescent cells like those surrounding GBM tumor and improve its safety. Also, *lacZ* expression is useful for viral replication and viral spread detection in treated tumors.
G47Δ originates from G207 and has an additional US12 gene deletion, the same of T-VEC. The modifications to the G47Δ genome have given it a higher replication capacity than T-VEC and higher antitumor activity than its G207 parent virus. Thus, G47Δ can be a good candidate for future antitumoral therapies [21].
In rQNestin34.5 UL34.5 has been reintroduced. The gene is under the regulation of *nestin* promoter, a GBM-specific gene, which is expressed only during embryogenesis, is shut down in adult brain cells but active in glioblastoma cells. Thus, this promoter should give rQNestin34.5 glioblastoma specificity [21].

2.5 Delivery strategies and biosafety of oncolytic viruses

The guidelines for the administration of oncolytic viruses are still unclear. Indeed, the route of administrations varies based on tumor site, tumor type and other parameters that can depend on the ongoing study. When choosing the most appropriate way of administration, the effect of the immune system on the virus and the presence of physical barriers in the organism, such as the blood-brain barrier, are two of the main constraints that must be considered [25]. OVs delivery is primarily based on intratumoral injection and intravenous injection. However, there are other less used ways of delivery and some new approaches are being analyzed.
Intratumoral injection is usually the recommended delivery method for superficial tumors, like melanoma, that are easily accessible [26]. This method provides accuracy and control over the concentration of OV administrated and side effects caused by virus being mistargeted to other organs can be prevented. The main advantage in using this way of administration is the maintenance of stable OV concentration in the tumor site, which leads to define therapeutic effects and reproducible results from in vivo and in vitro analysis. However, there are some limitations. Intratumoral injection cannot be used for deep-localized tumor or not directly accessible, like glioblastoma. It has low power

against metastases, that cannot be reached from the site of administration and there can be some restrictions given by the ECM of some organs that prevent the virus transmission. The latter problem can be solved arming the oncolytic virus with genes encoding enzymes that can remodel ECM [25].
Intravenous administration of OV is a systematic delivery method in which OV is injected into peripheral veins to migrate to the tumor site via the circulatory system. This method is the chosen way of administration of OV for those tumors that are not easily accessible and it is a useful way to deliver the therapy in secondary sites of development of the tumor or in case of metastasis. Intravenous therapy also facilitates the administration of combinatory therapy, such as the injection of oncolytic viruses with an antibody. However, there are some limitations. For the administration of OVs that originates from viruses with a high seroprevalence in the population, like HSV-1, the immune response of the organism must be considered. Indeed, in these cases, the clearance of the virus can be remarkable and the virus is not able to reach the tumor site in sufficient quantity to elicit its effect. Also, the dilution of the virus in the bloodstream must be considered. For this reason, high quantities of virus must be injected, because only viral doses beyond a certain threshold can be detected. This can be a risk for safety of using oncolytic viruses because it can lead to toxicity [26]. Also, the presence of physical barriers, like the blood-brain barrier, can limit the access of the virus toward the tumor site [25].
Some strategies can be implemented to overcome the immune system clearance of the virus. OVs can be injected in combination with natural immune pathway inhibitors. Carrier cells can be exploited to "hide" the virus from the immune system and deliver it in the tumor site. Candidate cells used as carriers must have a tropism towards tumor, must be susceptible to OV infection or allow virions to stably attach to their cell membrane and must maintain viability for a sufficient time to deliver the virus to the tumor bed. A variety of cells are being consider for this purpose, such as mesenchymal stem cells (MSCs) or T lymphocytes [27].
Among the less used ways of administration, there is thoracoabdominal injection. This method involves the injection of OV directly into the cavity, that can be thoracic or intraperitoneal cavity. Here, the virus is absorbed by the local veins and it can elicit its effect on local tumors or be delivered to other tumor sites using the bloodstream. This way of administration is used mainly for tumors in the injected cavity and has some restrictions, like the need of higher doses of OV for injection. Moreover, thoracic injection requires a pre-buried tube into the pleural cavity, which can be cause of infections. Intraperitoneal injected viruses can be absorbed by the portal vein and taken to the liver, where the virus can cause severe damages [26].
Other experimental ways of administration are aerosol delivery, recommended for lung tumors, and ultrasound cavitation. Nevertheless, aerosol delivery is not powerful, because of low systemic exposure, unpredictable dose delivery and formulation challenges, while ultrasound cavity seems to increase tumor penetrance for OVs [19].
Regarding oncolytic virotherapy biosafety, oncolytic viruses usually cause mild flulike adverse symptoms, like fever, chills, nausea, headache, etc. These symp-

toms can disappear spontaneously or with a symptomatic therapy based on non-steroidal anti-inflammatory drugs. Other more severe symptoms, such as anemia, liver dysfunction and hematological abnormalities are caused only by some viruses, like HSV or adenovirus. The most severe adverse symptoms, that harm patients' health, are rare and limited to few viruses, and usually are manageable. Long-term adverse effects are still unclear and must be investigated whether oncolytic virotherapy can be cause of adverse symptoms after several years from treatment [26].

3 Aim of the study

The aim of this study is to evaluate oncolytic virotherapy as a possible treatment for glioblastoma (GBM). Since GBM does not have an effective therapy and it is characterized by poor prognosis with frequent metastasis and recurrence, it represents a good candidate for oncolytic virotherapy.
Oncolytic virotherapy is based on the employment of oncolytic viruses, i.e. attenuated forms of the original virus that specifically replicate in tumor cells. Indeed, oncolytic viruses upon infection lead to a selective lysis of tumor cells, thus they are promising agents for the development of tumor-specific therapies. HSV-1 is one of the most studied oncolytic viruses and it can be useful for GBM therapy thanks to its natural tropism for neuronal cells.
This project presents a dual strategy to improve oncolytic virotherapy based on HSV-1: i) arming oncolytic HSV (oHSV) with therapeutic genes that may cause tumor regression and ii) improving the delivery of oncolytic viruses by using monocytes as carriers. As for the first aim, this research work focuses on SOCS3 which is one of the main inhibitors of STAT3, a protein involved in JAK/STAT3 cascade of signal, typically deregulated in GBM.
On the other hand, our group has recently reported the first evidence in the literature that monocytes can represent suitable carrier for the delivery of oHSV to cancer cells [28]. Building on these results, here we investigated whether a monocyte specific promoter could drive the expression of a reporter gene in these type of cells. The final aim is to exploit this promoter to regulate the production of specific factors in the carrier cells, while shutting down their expression within the tumor bed.
Overall, the achieved results are promising and pave the way to further studies on the adoption of oHSV and monocytes in an innovative strategy for the treatment of GBM.

4 Materials and methods

4.1 Materials

4.1.1 Plasmids

pZeoH-SOCS3 is a plasmid containing the murine form of the therapeutic gene SOCS3 (called mSOCS3 for this reason). SOCS3 gene is under the control of the P1 promoter and has a flag sequence at its 3' end, which encode for eight amino acids and can be used for protein detection and purification. Kanamycin resistance gene is also present in the plasmid, and it acts as a selection factor for bacteria that has acquired the plasmid. The gene cassette with SOCS3 is flanked by the two zeocin homology sequences, used for homology recombination in BAC mutagenesis process (see paragraph 3.2.4 below). The structure of the entire plasmid is displayed in Figure 4.

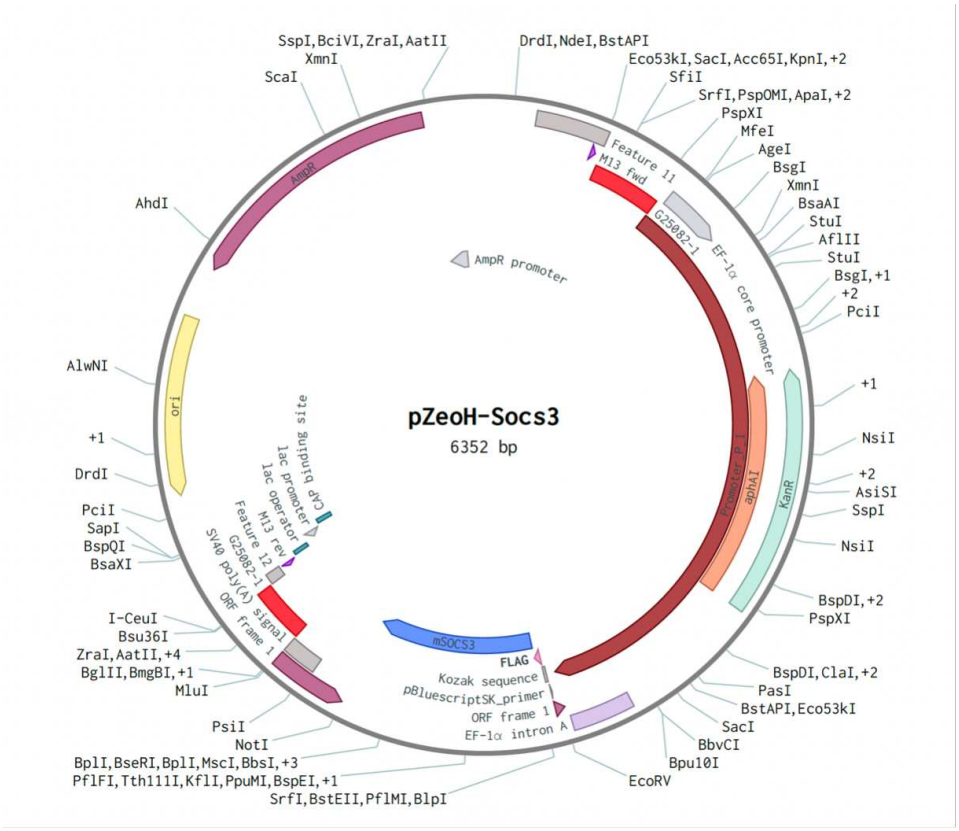

Figure 4. *Schematic representation of pZeoH-SOCS3 plasmid.*

pCeu-mCherry is a plasmid provided with mCherry gene, that encodes the homonymous red fluorescence protein, useful for visual detection of transfected cells via fluorescence microscopy. mCherry gene is under the control of the human Cytomegalovirus (hCMV) promoter, which ensures an almost ubiquitous expression of mCherry. Moreover, the plasmid has a kanamycin resistance gene, used as a selection factor, and the ICeuI restriction sites for ICeuI restriction enzyme, that can be used to cut the gene cassette from the plasmid and clone the gene of interest in another construct. The structure of the plasmid is shown in Figure 5.

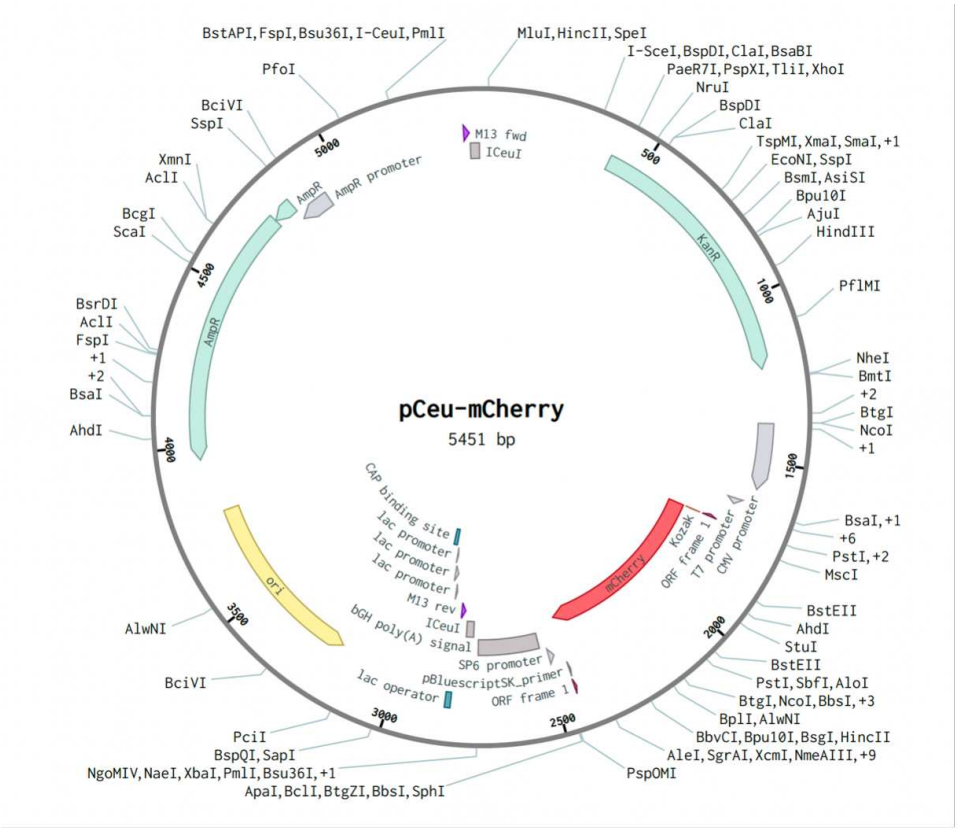

Figure 5. *Schematic representation of pCeu-mCherry plasmid.*

pZeo-CD68-mCherry is a plasmid provided with mCherry red fluorescence protein gene under the control of CD68 promoter, which is a human monocyte specific promoter. As the aforementioned plasmids, pZeo-CD68-mCherry has the kanamycin resistance gene and it has also the zeocin homology sequences useful for homology recombination (Figure 6).

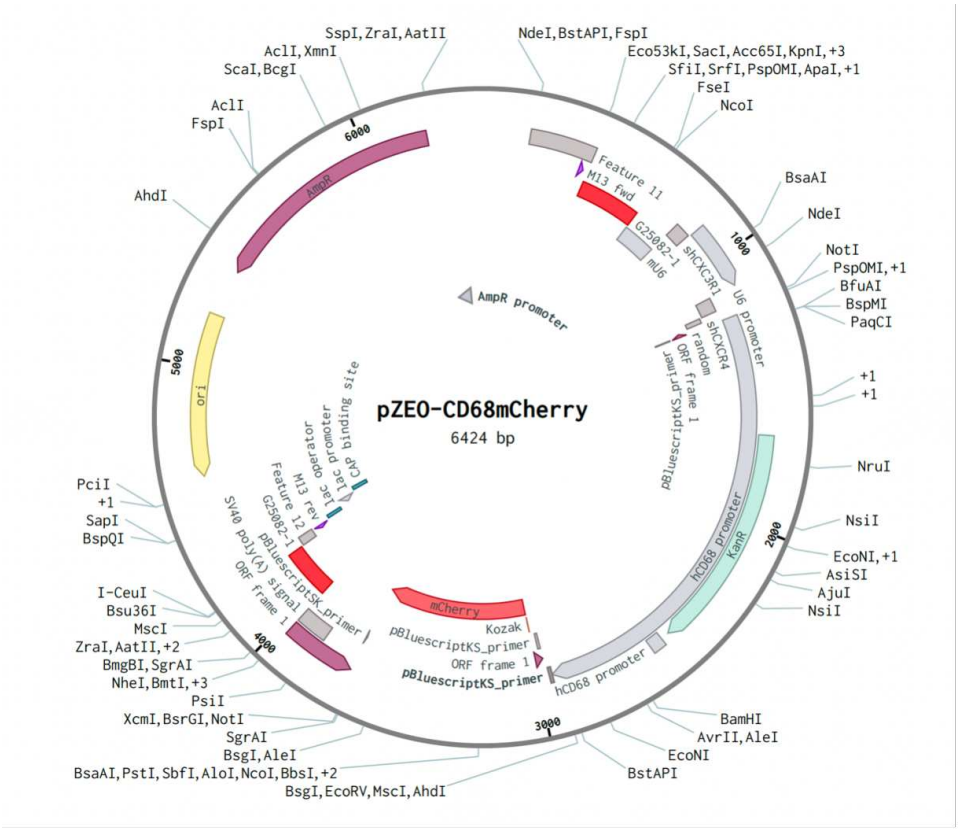

Figure 6. *Schematic representation of pZeo-CD68mCherry plasmid.*

4.1.2 Bacterial artificial chromosomes (BAC) containing recombinant HSV-1 genome, adopted in this research work as starting point for further manipulation

pHSV1(17+)Lox-EGFP-Δγ34.5-Zeo-ΔUs12 is a bacterial artificial chromosome containing the HSV-1(17+) genome, modified in some of his parts, previously generated in the laboratory [27]. Both copies of *γ34.5*, encoding the viral protein ICP34.5, has been deleted. Zeocin resistance gene was introduced instead of *γ34.5* gene and it is useful to integrate transgenes with zeocin homology tails via recombination. *US12* gene was deleted. This gene is an immediate early gene encoding the viral protein ICP47. Its deletion shift *US11* gene under US12 promoter, thus *US11* become an immediate early gene. In UL55-UL56 region, the gene encoding EGFP was introduced under the control of hCMV promoter. The remaining part of the BAC DNA contains chloramphenicol resistance gene and Cre recombinase gene under an eucaryotic promoter. This region is flanked by LoxP sites that allow the excision of the cassette to re-form HSV genome after transfection in eucaryotic cells. All the features of the BAC are shown in Figure 7.

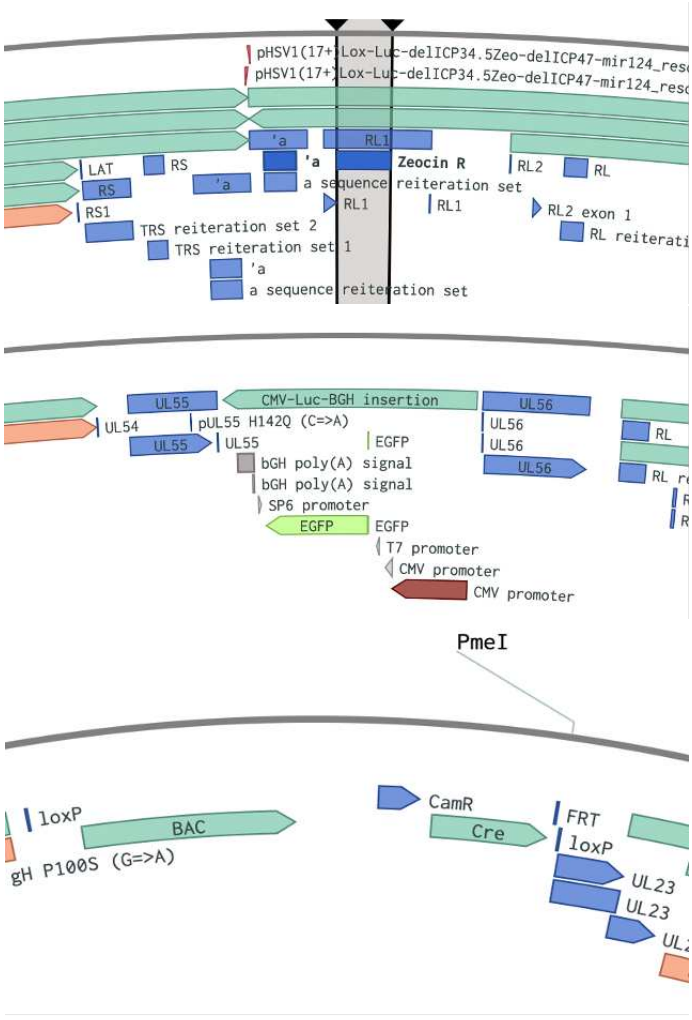

Figure 7. Schematic representation of pHSV1(17+)Lox-EGFP-Δγ34.5-Zeo-ΔUS12 characteristics. ***1)*** *Zeocin resistance gene.* ***2)*** *EGFP gene.* ***3)*** *BAC DNA with Cre recombinase gene, loxP sites and Chloramphenicol resistance gene.*

pHSV1(17+)Lox-Luc-Δγ34.5-Zeo-ΔUs12-UL29mir124 is similar to the bacterial artificial chromosome aforementioned and was previously developed in the laboratory. It has the deletion of both copies of *γ34.5* gene, replaced with zeocin resistance gene, and the deletion of *Us12* gene. In UL55-UL56 intergenic region, the luciferase gene is present under the control of hCMV promoter. At 3' end of *UL29* gene has been introduced a 3p+5p target sequence for two isoforms of mir124 to neuro-attenuate the resulting HSV virus. Chloramphenicol resistance gene and Cre recombinase gene are present in the BAC DNA region not connected with HSV genome. LoxP sites are present at both ends of this cassette to remove the cassette after eucaryotic cells transfection of the BAC DNA to reform HSV genome.
All the additional characteristics of this BAC DNA are shown in the Figure 8.

1.

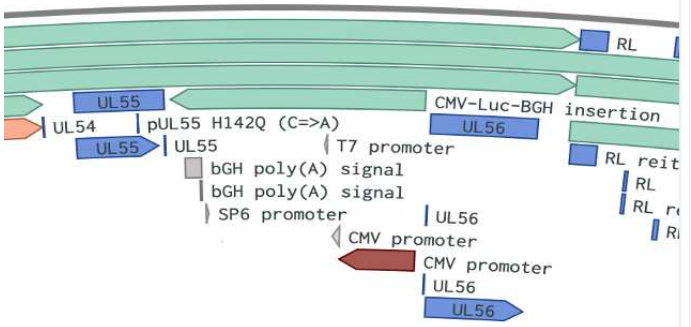

2.

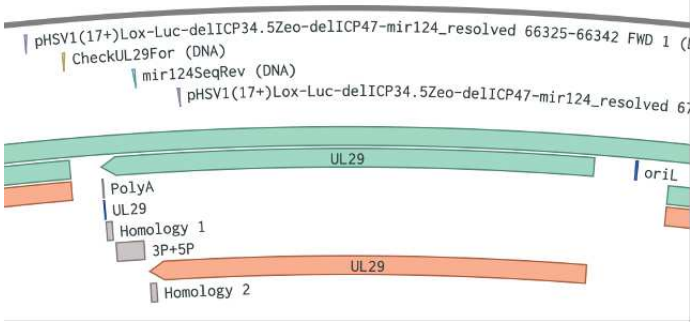

Figure 8. Schematic representation of pHSV1(17+)Lox-Luc-Δγ34.5-Zeo-ΔUs12-UL29mir124 characteristics. ***1)*** *Luciferase gene under the control of hCMV promoter.* ***2)*** *UL29 region with 3p+5p target sequence for mir124.*

4.1.3 Bacterial strains

GS1783 (genotype: DH10B l cI857 Δ(cro-bioA)<>araC-PBADIsceI) is a E. coli strain originated from DH10B strain of E. coli and used for the mutagenesis process with Lambda Red technique (paragraph 4.2.4). In their genome GS1783 bacteria have Lamba Red recombinase and I-SceI restriction enzyme genes permanently inserted. The expression of Lamba Red gene is controlled by c1857 repressor, which is active at a temperature lower than 42°C. Thus, bacteria are incubated at 42°C to inactivate the repressor and allow the expression of the recombinase. I-SceI is an endonuclease whose gene is under the control of an arabinose inducible promoter and the expression of the enzyme is achieved by adding arabinose to the culturing medium. I-SceI originates from Saccharomyces cerevisiae and it has a 18 bp restriction site which is not frequently present in bacterial sequences. This characteristic makes the I-SceI enzyme more efficient and less prone to aspecific restrictions. GS1783 bacteria are cultivated in Luria Bertani (LB) liquid or solid medium or in LB Low Salt.

4.1.4 Media for bacterial growth

Luria Bertani (LB) is a bacteria medium composed by 10 g/L of NaCl 10 g/L (Carloerba), 10 g/l di BactoTM Triptone (BD Biosciences), 5 g/L of BactoTM yeast extract (BD Biosciences) and 0,1 mM NaOH to have a final pH of 7. LB can be used both liquid and solid (LBA), by adding 15 g/L of agarose (BactoTM agar – BD Bioscience) and used to create Petri plates.

LB is autoclaved and antibiotics are added to the medium, in sterile conditions (Bunsen). The antibiotics added can be Chloramphenicol 100 µg/mL, Kanamycin 50 µg/mL and/or Ampicillin 100 µg/mL, based on the resistance gene present in the bacteria to select.

Luria Bertani Agar low salt (LBA LS) is a variant of LB/LBA characterized by a low concentration of salts, used with Zeocin antibiotic, which is sensitive to ions concentration and pH. It is composed by 5 g/L of NaCl 10 g/L (Carloerba), 10 g/l di BactoTM Triptone (BD Biosciences), 5 g/L of BactoTM yeast extract (BD Biosciences) and it has a pH of 7.5.

4.1.5 Oligonucleotides

In this experimental work, the following oligonucleotides were adopted:

Name	5'-3' sequence	Application
Zeo Short Forward	tgcacgcagttgccg	Mutagenesis verification
Zeo Short Reverse	cggagcggtcgagttct	
BAC EF1	cgtgaggctccggtgc	Kan resistance gene excision verification
BACSV40	taagatacattgatgagtttggacaaacca	
UL55	gcggcagagcatcgacg	mCherry mutagenesis verification
UL56	ggtatgctgtgaggggttg	

4.1.6 Cell lines and primary cells

HEK-293T (ATCC® CRL-3216™) is a cell line originated from human embryonic kidney cells. HEK-293T cells grow in adhesion in DMEM (Dulbecco's modification of Eagle Medium, high glucose) (Gibco) medium with 10% v/v fetal bovine serum (FBS) and 1% v/v penicillin/streptomycin (P/S). This cell line allow the replication of plasmids provided with SV40 replication site, since HEK-293T cells constitutively express T antigen of SV40.

GL261 (DSMZ: ACC-802) is a mouse glioblastoma cell line. It was induced by intracranial injection of methylcholanthrene followed by subcutaneous transplantations of tumor fragments into syngeneic C57BL/6 mice. GL261 cells has TP53 and KRAS mutations. They grow in adhesion, in DMEM 10% v/v FBS with 1% v/v of penicillin/streptomycin.

LN229 (ATCC® CRL-2611™) is a human glioblastoma cell line with an epithelial-like morphology. They grow in adhesion, in DMEM 10% v/v FBS with 1% v/v of penicillin/streptomycin.

Vero CCL81 (ATCC® CCL-81™) is a continuous cell line originated from kidney epithelial cell of a green African monkey, Cercopithecus aethiops. They are employed in various application, like infection assays, titration and viral amplifications since the lack of the interferon response and are highly permissive towards viral infections. Vero CCL81 grow in adhesion, in DMEM 10% v/v FBS with 1% v/v of penicillin/streptomycin.

WEHI-3 (ATCC® TIB-68™) is a mouse cell line isolated from the peripheral blood of a mouse with leukemia. They grow in suspension, in DMEM 10% v/v FBS with 1% v/v of penicillin/streptomycin.

CD14+ human monocytes obtained from the buffy coats of healthy donors (blood bags from Padua Hospital) via the procedure explained in paragraph 3.2.16.1.

4.1.7 Cell culture media

DMEM (Dulbecco's Modified Eagle Medium, Gibco™) is a cell culture medium widely used with mammalian cell, like fibroblasts, glia cells and cell lines such as Vero, 293T and HeLa. The original formulation is characterized by a concentration of glucose of 1 g/L and contains sodium pyruvate. There are also other formulations, some of which broadly used, with high concentration of glucose and without sodium pyruvate. DMEM is proteins, lipids and grow factors free, thus fetal bovine serum is added in a concentration of 10% v/v. To preserve the medium pH, the medium is kept in an environment with 5-10% of CO_2 and the medium contains a sodium bicarbonate buffer solution.

Opti-MEM (Gibco™) is an improved Minimal Essential Medium (MEM), that allows for a reduction of FBS supplementation by at least 50% with no change in growth rate or morphology. Opti-MEM medium is also recommended for use with cationic lipid transfection reagents, such as Lipofectamine™ reagent. To preserve the medium pH, the medium is kept in an environment with 5-10% of CO_2 and the medium contains a sodium bicarbonate buffer solution.

RPMI (Roswell Park Memorial Institute 1640 Medium, Gibco™) is a cell culture medium originally developed to culture human leukemic cells in suspension and as a monolayer, but it proved to be suitable for a variety of mammalian cells, like HeLa, PBMC and astrocytes. It contains the reducing agent glutathione and high concentrations of vitamins, as biotin, vitamin B12, and PABA. Vitamins inositol and choline are present in very high concentrations. RPMI does not contain proteins, lipids and grow factors, therefore it requires supplementation with 10% v/v Fetal Bovine Serum (FBS). To preserve the medium pH, the medium is kept in an environment with 5-10% of CO_2 and the medium contains a sodium bicarbonate buffer solution.

4.2 Methods

4.2.1 Bacterial cultures

Both mini-inoculums and maxi-inoculums have been done for bacteria.
Mini-inoculi have been executed by picking the selected colony from a bacteria plate and putting it in ventilated 15 mL tubes with 3 mL of LB medium (paragraph 3.1.4) and the desired antibiotic (can be kanamycin or chloramphenicol based on the use of the inoculum). In alternative, 100 µl of a previous inoculum were added in 3 mL of LB with antibiotic. Bacteria were then incubated at the wanted temperature (32°C or 37°C) overnight in shaking. This strategy

allows bacteria to have the right amount of air inside the tube and all the bacteria can have access to the air thanks to the shaking.
Maxi-inoculi followed the same protocol of mini-inoculums, but in flask with 100 mL of LB medium with antibiotic.
Bacteria were cultivated also on LB agar plates. 100 µl of inoculum or bacteria glycerol stock were spread on LB agar plates with a loop and then the plate was incubated overnight at the desired temperature.
Glycerol stocks were made by mixing 700 µl of bacteria mini-inoculum with 700 µl of LB with 60% v/v of glycerol. The final concentration of glycerol was 30% v/v. Vials of 1,4 mL were made and placed in ice for 30 minutes then moved at -80°C.
All the aforementioned procedures were carried out near a Bunsen to reduce the possibility of environmental contaminations.

4.2.2 Electrocompetent bacteria

Electrocompetent bacteria are bacteria capable of internalizing exogenous DNA. E.coli GS1783 bacteria were used for this purpose since the expression of Lamba Red recombinase and I-SceI restriction enzyme can be induced in these bacteria.
Mini-inoculum has been done from the glycerol stock of the bacteria and incubated at 32°C overnight. All the mini-inoculum was used to do a maxi-inoculum in LB medium with 100 µl of chloramphenicol and incubated at 32°C for as long as the optical density (OD, measured at the spectrophotometer) of the inoculums reached a value between 0.5 and 0.7. Chloramphenicol resistance gene is present in BAC DNA in the bacteria and it is independent from the exogenous DNA (in this study HSV DNA) to insert in the BAC DNA. When the OD reached the right value, the bacteria were moved in two 50 mL falcon and put in a thermostatic bath set at 42°C for 15 minutes in shaking. This temperature is useful to induce the expression of the recombinase enzymes. After the 15 minutes, the bacteria were placed in ice for 20 minutes, to stop the expression of the recombinase enzymes and to avoid enzyme degradation. Bacteria were then centrifuged at 5000 rpm, 4°C for 10 minutes. LB medium was discarded and bacteria were washed three times with sterile milliQ water by suspending them with water and centrifuge them at 5000 rpm, 4°C for 5 minutes. After the third centrifuge, water was discarded and bacteria were suspended in 600 µl of 10% v/v glycerol. They were then divided in previously cooled Eppendorf, 50 µl per vial, and electrocompetent bacteria were stocked at -80°C.

4.2.3 Polymerase chain reaction (PCR)

Polymerase chain reaction (PCR) was employed as a verification method or for amplification of a template. Different polymerases were used, based on the requirement.
AmpliTaq Gold® DNA polymerase (ThermoFisher) was usually employed for most of the verifications PCRs. The reaction mix for a single sample had a total volume of 50 µl (comprehensive of the template or water for negative

control) and was made by 5 µl of 10X PCR Buffer I, 1 µl of 10 mM dNTPs solution, 1 µl for each of the 10 mM primer solutions, 0.5 µl of DNA polymerase (i.e. 2.5 functional units), around 10 ng of DNA and water to 50 µl volume.
Q5® High-Fidelity DNA Polymerase (New England BioLabs) was tipically used for amplification of difficult templates, prone to aspecific products. The PCR mix had a final volume of 50 µl per sample and was made by 10 µl of 5X Reaction Buffer, 1 µl of 10 mM dNTPs solution, 10 µl of GC enhancer, 1 µl for each of the 10 mM primer solutions, 0.5 µl of DNA polymerase, around 10 ng of template and water to the final volume.
The cycling parameters (table below) were set according to the productor directions. The elongation time was fixed based on the enzyme specific polymerisation speed and the annealing temperature for each primers pair was determined using NEB Tm Calculator online tool and then optimized to reduce aspecific products. 35 amplification cycles were carried out for each PCR, as reported below.

Polymerase	Initial denaturation	Denaturation	Annealing	Elongation	Final elongation
AmpliTaq Gold®	10' 95°C	15" 95°C	30" Primer Tm	60"/kb 72°C	5' 72°C
Q5®	30" 98°C	10" 98°C	30" Primer Tm	25"/kb 72°C	2' 72°C

4.2.4 Bacterial artificial chromosome (BAC) based mutagenesis of HSV-1 genome

4.2.4.1 Electroporation

Electroporation is a procedure used to internalize the constructs with mSOCS3, mCherry and CD68-mCherry genes into GS1783 bacteria provided with $pHSV1(17+)Lox-EGFP-Dg34.5-Zeo-DUs12 or pHSV1(17+)Lox-Luc-Dg34.5-Zeo-DUs12-mir124BAC$.
An amount of 500 ng of construct were added to a vial of electrocompetent bacteria (paragraph 3.2.2) defrosted in ice. The sample was placed in a pre-cooled cuvette for electroporation (it has a gap of 2 mm and electrodes at each side of the gap). The electroporation was carried out with the following parameters, to have a 4-5 ms time constant: 10 µF as capacitance value, 200 Ω as resistance value and 2.5 kV as voltage value.
After the electroporation, 1 mL of SOC medium was added to the sample, the sample was moved in an Eppendorf and incubate at 32°C for 1 hour in shaking. After the incubation, bacteria were centrifuged, the excess medium was discarded and the bacteria were suspended in the remaining medium. Bacteria were plated on LBA-Kan-Chl plate and incubated overnight at 32°C. The day after, mini-inoculi were made from some selected colonies. They were incubated at 32°C, overnight in shaking. BAC DNA was extracted from the bacteria following the home-made protocol (paragraph 3.2.5) and used as a template for PCR, to evaluate the efficiency of the mutagenesis. Two PCR were carried out: one with transgene-specific primers to verify the presence of the transgene and another PCR with primers the allowed the amplification of the entire region interested in the mutagenesis, to verify the presence of the

transgene and the insertion site. Bacteria in which the transgene should be integrated in the zeocin resistance gene were also plated in LBA-LS plates with zeocin as an additional prove of the right integration. Since zeocin resistance gene should be interrupted by the transgene, bacteria in which the integration was successful should not grow.
The constructs were also controlled by sequencing performed by BMR Genomics. Samples were prepared according the BMR Genomics directions.

4.2.4.2 Resolution of bacteria colonies with integrated gene

The resolution process involves the removal of kanamycin resistance gene present in the integrated construct in the BAC DNA representing HSV genome.
The Bacteria in which the integration was proved to be successful by PCR and sequencing were refreshed and incubated at 32°C overnight. 100 µl were then added to 1 mL of LB+Chl and incubated for 1-2 hours at 32°C in shaking. After the incubation, 1 mL of LB with 2% of arabinose was added to the bacteria and they were incubated for 1 hour at 32°C. Arabinose is used to induce the expression of I-SceI restriction enzyme, whose promoter is arabinose-inducible. After the latter incubation, bacteria were placed at 42°C for 20 minutes to induce the expression of Lambda Red recombinase and, after that, they were incubated again at 32°C for 2-3 hours in shaking. After 2-3 hours, optical density was measured and bacteria plated on LBA+Arabinose 1%+Chl at different dilutions based on the value of the OD: $OD_{600} < 0.5$ dilution 1:100, $OD_{600} > 0.5$ dilution 1:1000, taking a volume of bacteria between 5 and 25 µl. Plates were incubated at 32°C for 1-2 days.
Both solved and unsolved bacteria can grow on LBA+Arabinose 1%+Chl, thus 20 well-spaced colonies were selected and they were plated on both LBA+Kan+Chl and LBA+Arabinose 1%+Chl plates using the replica picking method and incubated at 32°C overnight. Colonies that grew only in LBA+Arabinose 1%+Chl were selected, since those colonies derived from bacteria in which the kanamycin resistance gene was removed and could not grow in LBA+Kan+Chl. Mini-inoculums were made from the selected colonies and BAC DNA was extracted using the home-made protocol. The absence of kanamycin resistance gene was additionally evaluated by PCR. All positive clones were also controlled by sequencing performed by BMR Genomics. One solved colony was selected for BAC DNA extraction with ZM BAC DNA Miniprep Kit (see paragraph 3.2.6) that provides constructs of a quality suitable for transfection in HEK-293T cells for viral reconstitution (paragraph 3.2.8).

4.2.5 Home-made DNA extraction

Home-made DNA extraction is used to extract BAC DNA from bacteria. BAC DNA is a quite large construct and cannot be extracted with plasmid extraction kits. This approach is suitable for the extraction of large constructs, however it is a low efficiency method, that produce a DNA extraction with a high level of impurities, usually used for verification via PCR and electrophoresis. For higher purity BAC DNA extractions, ZM BAC DNA Miniprep Kit was adopted (paragraph 3.2.6).

Home-made extraction protocol relies on the use of home-made solutions that are able to lyse the bacteria and isolate DNA from cell debris. Three home-made solutions were made before DNA extraction. The first solution was the glucose-Tris-EDTA (GTE) solution, made with glucose 50 mM, Tris-HCl pH 8.0 25 mM and EDTA pH 8.0 10 mM. The lysis solution was made of SDS 1% and NaOH 0.2 M diluted in water. The third solution was used to separate cell debris from the liquid phase containing DNA and was made with potassium acetate 5 M and glacial acetic acid diluted in water.From a 3 mL bacteria inoculum, 1.5 mL of bacteria suspension was transferred in 1,5 eppendorfs and centrifuged at maximum velocity for 1 minute. After the centrifuge, the medium was discarded and the bacteria pellet was dried putting the eppendorfs upside-down on a piece of paper towel. Pellet was suspended with 100 µl of GTE solution, then 200 µl of lysis solution were added and mixed by inversion. 150 µl of the third solution were added and mixed by inversion. A white floc started to form inside the Eppendorf. Samples were centrifuged at 14000 rpm for 10 minutes in a previously set centrifuge at 4°C. After the centrifuge, the samples were kept in ice and supernatants were collected and transferred in new eppendorfs, avoiding the white pellet in the sample. 1 mL of ethanol 95% was added to the sample and mixed by inversion to make the DNA precipitate. Samples were centrifuged at 14000 rpm for 20 minutes at 4°C. After the centrifuge, supernatants were discarded and 200 µl of ethanol 70% was used to wash the DNA pellet, paying attention not to touch the pellet and suspend it. DNA pellet was let air dry and 30 µl of elution buffer with 10% v/v of RNase was added onto the pellet once it was dry. Samples were put at 37°C in a thermostatic bath for at least 30 minutes to make the pellet suspend.

4.2.6 ZM BAC DNA Miniprep Kit (Zymo Research)

ZM BAC DAN Miniprep Kit is used to extract BAC DNA from bacteria with high efficiency and a low amount of impurities. DNA minipreps obtained with this kit are suitable for transfection in eucaryotic cells.
According to the producer protocol, all 3 mL of inoculum were used and centrifuged at 13000 rpm for 1 minutes. Medium was then discarded and the bacteria pellet was suspended in 200 µl of P1 buffer. 200 µl of P2 buffer were added and the sample was mixed 4-6 times by inversion. The solution should turn purple and be transparent and viscous, as the cells lysis was accomplished. After 1-3 minutes, 400 µl of P3 buffer were added and gently mixed. P3 buffer neutralized the action of the enzyme previously added and the solution should turn yellow. The sample was centrifuged at 13000 rpm for 1 minutes and the supernatants were collected and transferred in a Zymo-Spin™ IC-XL column with a collecting tube underneath. The column was centrifuged for 1 minute at 13000 rpm and the eluate was discarded. The membrane in the column was washed with 200 ul of Endo-Wash Buffer and centrifuged. 400 µl of Plasmid Wash-Buffer were added and centrifuged again for 1 minute at 13000 rpm. After the centrifuge, the column was moved on a new eppendorf, 50 µl of Elution buffer were added to elute the DNA and the sample was centrifuged for 1 minute at 13000 rpm. The DNA was quantified with NanoDrop One/OneC

Spectrophotometer (ThermoFisher).

4.2.7 Cell cultures

Cells were generally cultured in T75 flasks, with an adhesion area of 75 cm^2, at 37°C. Cells were diluted twice a week (at 1:10 or 1:5), based on their confluence level. To detach the cells and dilute them, trypsin was used. Exhausted medium was collected and cells were washed with DPBS (Dulbecco's phosphate-buffered saline) to remove all the medium residues. 3 mL of trypsin were added to the cells and the flask was placed at 37°C to minimize cell stress. After 5-10 minutes, trypsin was inactivated with 7 mL of DMEM with 10% v/v FBS. 8 or 9 mL were collected, based on the dilution ratio, and discarded and the same volume of DMEM 10% v/v FBS was added.
Cells in excess could be stocked at -80°C. A mix with 50% of dymethil sulfoxide (DMSO) and 50% of DMEM 10% v/v FBS was used and cells were transferred in cryovials. Before shelving them at -80°C, cryovials were placed in ice. DMSO is a cryo-protective agent that prevents the formation of ice crystals that can damage the cells inside the vial. DMSO is toxic for cells, thus, while thawing, cells were centrifuged to form a pellet and discard the medium with DMSO. Cells were then washed and suspended in 2 or 5 mL of DMEM 10% v/v FBS, based on the number of cells present, and transferred in a 6-well plate or in a T25 flask respectively. When cells reached the right level of confluence, they were moved in a T75 flask. For cell infection or other experiments, cells were counted and cultured in multi-well plates. For a 6-wells plate, usually 500,000 cells/well were cultured in 2 mL of cell medium; in a 12-wells plate, 250,000 cells/well were cultured in 1 mL of cell medium. In a 24-wells plate, 100,000 cells/well were cultured in 500 µl of cell medium; in a 48-wells plate, 50,000 cells/well were cultured in 250 µl of cell medium. In a 96-wells plate 10,000 cells/well were cultured in 100 µl of cell medium.
All the procedures involving cells were carried out in BL2 biohazard hood to guarantee sterility and avoid environmental contaminations.

4.2.7.1 Cell counting by trypan blue exclusion

Cells were counted using trypan blue and a counting chamber. Cells were taken from the cell suspension and diluted in DPBS. Usually, the dilution ratio was 1:100, Ten µl of cells suspension was diluted in 990 µl of DPBS. 10 µl of the dilution were mixed with 10 µl of trypan blue and the mix was poured in the counting chamber. After counting the cells in the four outer quadrants delimited by three lines, the obtained numbers were: i) summed up and the mean between the four quadrants was calculated; ii) the mean was multiplied for the dilution factor used at the beginning while mixing the cell suspension with DPBS (usually 1:100 or 1:10) and for the dilution factors used while mixing the cell suspension in DPBS with trypan blue (it is a dilution 1:2); iii) the result was multiplied for the counting area of the counting chamber (10,000 in the counting chamber used). The resulting number is expressed in cell/mL.

4.2.8 Viral reconstitution via cell transfection with lipofectamine

Viral reconstitution is the process that allows the reconstitution of virions stating from the viral genome transfected in eucaryotic cells. For this process, HEK-293T cells were used for transfection, since they have high efficiency in transfections. Lipofectamine 2000 (Termofisher) is a positively charged solvent and it was used to create complexes with DNA, which is negatively charged, in order to make the DNA to enter 293T cells.
A T25 flask with HEK 293T cells was produced, using DMEM 10% v/v FBS as a medium. Cells were let grow till 80% of confluence. Next, lipofectamine solution and DNA solution were prepared. Twenty µl of lipofectamine were mixed with 480 µl of Opti-MEM in one eppendorf and the volume of BAC DNA extraction (paragraph 3.2.8) corresponding to 1 ug of DNA (based on DNA quantification) was mixed with Opti-MEM to have 500 µl of DNA solution. The solutions were mixed together and incubated for 10 minutes at room temperature. The resulting solution was mixed with 4 mL of Opti-MEM and the mix was used to replace the medium in which HEK 293T cells grew (DMEM 10% v/v FBS). 293T cells were incubated overnight and the day after the Opti-MEM solution was replaced with DMEM 10% v/v FBS. HEK-293T were monitored for the following days (generally 3 days) to evaluate the cytopathic effect of viral production and choose the right timepoint in which cells supernatant has a good amount of virions and can be collected. At the chosen timepoint, 293T cells were detached from the flask and transferred in a 15 mL falcon. The falcon was vortexed and centrifuged to cause the release of intracellular virions and remove all the cellular debris. Supernatant was collected and used for viral stock amplification.

4.2.9 Viral stock amplification in Vero CCL81 cells

To increase the viral titer after viral reconstitution, the viral stock is amplified in Vero CCL81 cells.
Vero CCL81 cells ($3 * 10^6$) were cultured in a T75 flask and infected with the HEK-293T supernatant containing virions. To infect the cells, DMEM 10% v/v FBS was discarded from the T75 flask with Vero cells and cells were washed with DPBS. Vero CCL81 were incubated for 1 hour with a mix of 5 mL of HEK-293T supernatant and 5 mL of DMEM without FBS. After the incubation, the mix was replaced with DMEM 2% v/v FBS and Vero cells were incubated at 37°C. The day after the cytopathic effect was evaluated and the cell medium was collected and used to infect 4 T75 of Vero CCL81, with 3 millions of cells per flask, previously cultured. The cell medium was removed from every flask, cells were washed with DPBS and a mix of 2.5 mL of Vero supernatant with virions from the previous flask and 7.5 mL of DMEM without serum was add in each of the 4 flasks. The 4 flasks were incubated for 1 hour at 37°C and, at the end of the incubation, medium with virions was discarded and 10 mL DMEM 2% FBS was added in each flask. Cytopathic effect was monitored to evaluate the correct timepoint in which 90% of the cell layer was wiped out (typically in 72 hours). At this point, cells were detached with a cell scraper from each flask and the cell suspensions were collect in falcons. Cells

were centrifuged at 1500 rpm for 4 minutes at 4°C and the supernatants were discarded. The cell pellet was suspended in 300 µl of DMEM 10% v/v FBS and the cell suspensions were moved in two 1.5 mL eppendorfs. Cells underwent 4 cycles of freezing in dry ice and defrosting at 37°C and vortex to lyse cell membranes and release the intracellular virions in the medium. To complete the cell lysis, cells were sonicated in ice for 3 minutes. The eppendorfs were centrifuged at 11000 rpm for 15 minutes at 4°C, to eliminate all the cellular debris. Supernatants were split in vials and stocked at -80°C. One vial was used for viral titer determination.

4.2.10 Viral titer determination via plaque assay

Plaque assay is used for viral titer determination and return as a result the number of plaque-forming units (PFU) per mL (PFU/mL) is present for the viral stock or the supernatant containing virions.
This assay was performed in a 48-wells plates in which Vero CCL81 cells, 50,000 cells/well, were cultured (paragraph 4.2.7). Serial dilutions of the viral stock or supernatant with virions were made. For viral stock titer determination, the dilution range is 10-2-10-7, while for supernatants the dilution range is generally 10-1-10-5. Dilutions are made by mixing 100 µl of supernatant or the previous dilution with 900 µl of DMEM without serum. For viral stock titer determination, the first dilution was made by mixing 10 µl of viral stock with 990 µl of DMEM without serum. For each viral stock or supernatant the infections for titer determination were made in duplicates, thus for each 48-wells plate maximum 4 viral stocks or supernatants can be titrated. The first row of the plate was usually designated for negative controls, in which cells were not infected with the viral stock or the supernatant. All the cell medium was discarded from the wells of the plate and, starting with the controls, cells were washed with DPBS. In the negative control wells, 125 µl of DMEM without serum were added while in the wells for the infection 125 µl of dilution were used, starting from the bottom of the plate with the more diluted mix. The plate was incubated for 1 hour at 37°C and after the incubation, DMEM without serum and medium with virus was discarded. The cells were washed with DPBS and in each well 250 µl of carboxymethyl cellulose were added. Plates were incubate for 48 hours at 37°C. Next, the medium was discarded and cells washed with DPBS. Cells were fixed with 5% v/v paraformaldehyde, 200 µl per well, and incubated for 10 minutes at room temperature. Then, paraformaldehyde was discarded and cells were stained with 200 µl of crystal violet 0,1% v/v (BBL™), left to act for 5 minutes. After that, crystal violet was removed and the plates were washed with water. Plaques were counted at the microscope, in those wells where there were between 10 to 100 plaques. For each supernatant or viral stock, the mean number of plaques between the replicates was calculated and the result was multiplied for the dilution factor. To obtain the titer as plaque forming units (PFU) per mL, this number is divided for the volume of infection expressed in ml.

4.2.11 GL261 and LN229 infection assay with oHSV-mSOCS3-EGFP

For GL261 and LN229 infection assay, both cell lines were cultured in a 6-wells plates. For each cell line, 4 wells of one plate were used for cells seeding, counting 500.000 cells per well. The day after, cells were infected with oHSV-mSOCS3-EGFP. GL261 were infected with MOI 10 PFU/cell and LN229 were infected with MOI 1 PFU/cell. The volume of viral stock needed for the infection was calculated based on the chosen MOI. oHSV-mSOCS3-EGFP stock had a titer of 4 * 10^7 PFU/mL. Cells were infected (500,000 cells/well) at a MOI of 10 PFU/cell for GL261 cells line, and of 1 PFU/cell in the case of LN229 cells. The plates were incubated for 1 hour at 37°C and, after that, the medium with virus was discarded, cells were washed with DPBS, and the medium was replaced with 2 mL of DMEM 2% v/v FBS. LN229 were monitored for 24 hours and GL261 for 48 hours and used for protein extraction at this timepoint.

4.2.12 Protein extraction

Protein extraction was carried out for GL261 cells infected with oHSV-mSOCS3-EGFP. Cells were detached from a 6-well plate, where 2 wells contained non-infected cells and other two wells had infected cells. The cells suspensions were put in two 15 mL falcon and centrifuged at 1500 rpm for 4 minutes. Cell medium was discard and the cell pellet was washed with 500 µl of PBS by resuspension. Cells were centrifuged again at 1500 rpm for 4 minutes and cell pellets were suspended in Radioimmunoprecipitation lysis (RIPA) buffer 1X (10mM Tris-HCl, pH 8.0, 1mM EDTA, 0.5mM EGTA, 1% Triton X-100, 0.1% Sodium Deoxycholate, 0.1% SDS, 140mM NaCl) containing protease inhibitors 1X (Protease inhibitor cocktail cOmplete™, Roche) and phosphatase inhibitors 1X (PhosSTOP™, Roche). The mix was kept in ice till use. Samples were kept in ice for 30 minutes. Next, the eppendorfs were centrifuged at maximum velocity for 30 minutes at 4°C. Finally, supernatants were collected and conserved at -20 °C until use.

4.2.13 Bicinchoninic acid assay for protein quantification

Bicinchoninic acid assay (BCA) was performed to quantify proteins in cells supernatants with Protein Assay Kits (Thermo Scientific™), following the manufacturer's instructions. This assay exploits the ability of proteins to reduce Cu^{2+} present in the solution for quantification to Cu^{+}. The amount of reduced copper formed is proportional to the quantity of proteins present in the stock to quantify. Bicinchoninic acid then reacts with the reduced copper to form a colored product that highly absorb at 562 nm. A 96-well plate was used for the assay. 3 wells were used for blank triplicate, putting 97 µl of water and 3 µl of RIPA buffer. Two rows of 10 wells each were used for the two standard quantification with BSA protein, used to interpolate the absorbance values of the unknown sample and quantify them. A solution of 0.2 mg/mL BSA was used for one row and a 2 mg/mL BSA solution was put in the other one. Starting from the left of the plate, decreasing amounts of water were added in

each well (from 96 µl to 87 µl) for both the rows and 3 µl of RIPA buffer were added in each well. Increasing amounts of BSA solutions were added (from 1 µl to 10 µl). 3 wells for each sample were used to have replicates for the quantification: 97 µl of water and 3 µl of sample were put in each well. The scheme of a typical 96-well for this assay is shown below.

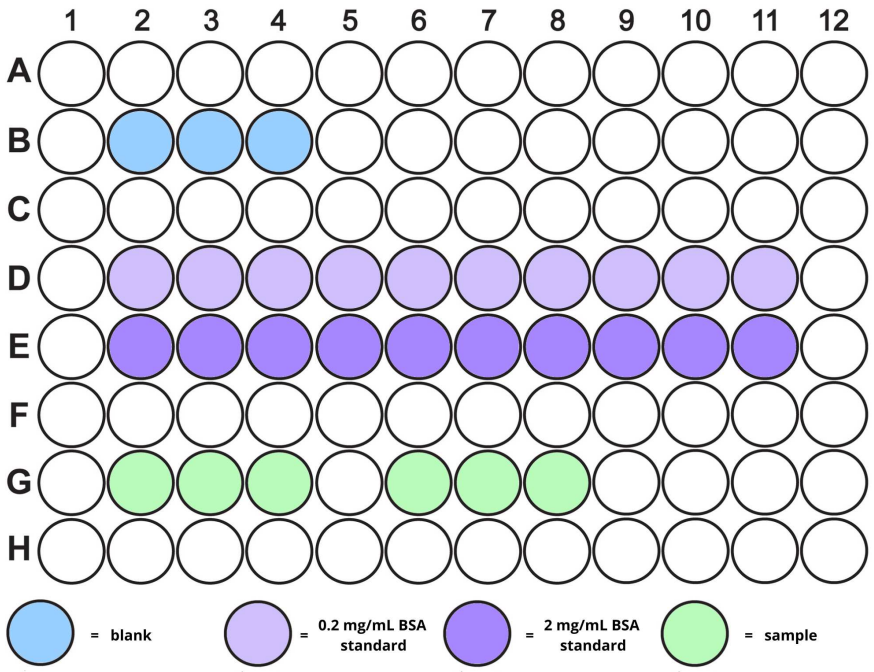

In each well 100 µl of revealing solution was added. The revealing solution was made by mixing reagent A and reagent B at 50:1 ratio, according to producer protocol. The plate was incubated at 37°C for 30 minutes, wrapped in tin foil to avoid light exposure. After 30 minutes, absorbance was detected at 562 nm using a spectrophotometer. The values were plotted to find the equation of the standard curve with BSA and used to interpolate the values of the sample to determine the concentration of the proteins.

4.2.14 Western Blot

Western blot was performed to analyze the expression of SOCS3 protein in infected cells compared to non-infected cells.

4.2.14.1 Solutions and polyacrylamide gel

All the solutions useful for the procedure were prepared in advance. A solution 1.5 M Tris-HCl, pH 8.8 was made by dissolving 18.15 g of Tris base in 80 mL of distillated water. The pH was adjusted by adding 6N HCl and the solution was brought to the final volume of 100 mL by adding distillated water. 0.5 M Tris-HCl, pH 6.8 solution was made by dissolving 6 g of Tris base in 80 mL of distillated water. pH was adjusted to 6.8 with 6N HCl and 100 mL of solution were made by adding distillated water to the final volume. Running Buffer 10X was made with 30.2 g of Tris and 144 g of glycine dissolved in 1L of deionized water (final volume of 1L) and stored at room temperature. Running

buffer for the SDS-page was made with 100 mL of running buffer 10X (1X is the final concentration), 10 mL of SDS 10X (final concentration 0,1X) and deionized water to the final volume of 1L of solution. This buffer was stored at 4°C till use. A small amount of running buffer for SDS-page (about 200 mL) was made every time before gel running and it was used inside the watertight cassette created by the support and the gel. This prevented the alteration of the components of the running buffer and the assured an efficient run of the proteins inside the polyacrylamide gel. Transfer buffer was made under fume hood with 100 mL of running buffer 10X, 200 mL of methanol and deionized water to 1L volume. It was stored at 4°C till use. Ammonium persulfate (APS) 10% was made by dissolving 1 g of APS powder in 10 mL of deionized water, under fume hood. Vials of 500 µl were created and stored at 4°C. Loading buffer 2X for proteins was made by mixing 3.125 mL of Tris-HCl 0.5 M, pH 6.8, 1.125 mL of glycerol, 2.5 mL of SDS 10%, 0.125 mL of bromophenol blue 1% and 0.61 mL of β-mercaptoethanol with 5.01 mL of deionized water, with a final volume of 12.5 mL. Vials of 1 mL were made and stored at -20°C.
The polyacrylamide gel was made in two parts: first the running gel and then the stacking gel. The running gel was made to have a 10% final concentration of acrylamide, which was the right concentration to separate proteins between 15 and 100 kDa, the range in which is SOCS3 (∼30 kDa). Under chemical hood, running gel was made by mixing 4 mL of deionized water with 2.5 mL of 1.5 M Tris-HCl, pH 8.8, 100 µl of SDS 10%, 3.3 mL of acrylamide, 100 µl of APS and 40 µl of TEMED (10 mL as final volume). All the components were kept in iced till use and they were mixed in a previously cooled beaker to prevent advance-time gel polymerization. The solution was poured in the gap between the two glasses used to create the gel assembled on a support and 1 mL of isopropanol was pour above to level the gel. A small amount of acrylamide solution was left in the beaker to see when the gel polymerized. When the gel polymerized, isopropanol was discarded and the gel was washed with deionized water. Tissue paper was used to wipe excess water between the two glasses. The stacking gel was poured above the running gel and was made by mixing 4.7 mL of water with 2 mL of 0.5 M Tris-HCl, pH 6.8, 80 µl of SDS 10% v/v, 1.2 mL acrylamide, 80 µl of APS and 20 µl TEMED. All the components were kept in ice and mixed under chemical hood. The stacking gel solution was poured in the gap between the glasses till the edge of the smaller glass. The comb to create the wells was inserted between the glasses and the gel was let to polymerize. Polyacrylamide gel was wrapped in wet paper towel and tin foil, stored at 4°C and used in maximum 2 days.

4.2.14.2 Protein preparation and gel running

The volume of proteins to be loaded was chosen based on BCA quantification (paragraph 4.2.13). Since proteins extracted from the infected cells were diluted, the maximum volume of proteins that can be loaded in gel well was taken, i.e. 35 µl of proteins (a gel well can contain 70 µl maximum of protein and loading buffer). The volume of proteins extracted from the control non-infected cells was calculated based on the BCA quantification in order to have the same amount of proteins in ng for both sample. The same volume of load-

ing buffer 2X was added to the proteins, thus resulting in a dilution 1:1. The proteins with the loading buffer were heated at 99°C for 10 minutes to denature them. In the meantime, the watertight cassette with the gel was assemble, putting the smaller glass on the inside of the cassette. The cassette was placed inside the support cassette and the 200 mL of running buffer freshly made (paragraph 4.2.14.1) were used to fill up the space inside the watertight cassette. The comb can be removed from the gel and the support cassette can be filled with the other running buffer for SDS-page. 5 µl of marker (PageRuler™ Plus Prestained Protein Ladder, 10 to 250 kDa, Thermo Scientific™) and the sample were loaded, avoiding the outer wells in which the samples could run unevenly. The support cassette was closed and connected with the electrodes. The run was set at 75 V for 10 minutes to let the proteins to enter the gel from the wells, then 90 V for 10 minutes to let the proteins reach the border between stacking gel and running gel and at the end the power supplier was set at 100 V. The run was carried out until running front of the loading buffer exits the gel.

4.2.14.3 Proteins transfer

For protein transfer, the wet method was chosen. Two pieces of tissue paper and the blot membrane were cut. The tissue paper was cut 8x10 cm while the membrane was cut 8x6 cm. For SOCS3 protein, according to the antibody producer and the literature, Polyvinylidene Difluoride (PVDF) membrane was chosen since it has a superior protein-absorption capability than nitrocellulose membranes. The membrane cannot be touched with hands and must be activated before use by putting it in methanol for about 1 minute. After the activation, the membrane must be washed with transfer buffer. Gel with proteins was extracted from the cassette and the two glasses were opened with the help of a spatula. The stacking gel portion was eliminated and the gel was detached from the glass with the spatula and placed in the transfer sandwich. The transfer sandwich was assembled in a bowl with transfer buffer, placing one of the two sponges on the support, followed by one piece of tissue paper, the gel with proteins at the negative pole side of the support, the activated membrane, the other tissue paper piece and the other sponge. After the second piece of tissue paper the sandwich was flattened with a roller and after the second sponge was added, the sandwich support was closed without moving the components and press to drip the excess transfer buffer. The transfer cassette was assembled by putting the sandwich in the support and filling the cassette with transfer buffer. The cassette was closed and connected with the power supplier. The transfer was made at 50 V for 120 minutes, which is the right amount of time for most of the proteins (between 30 kDa and 160 kDa) transfer.

4.2.14.4 Antibody blotting and reveal

For antibody blotting iBind™ Flex Western Device (Invitrogen™) was used. The blot solution (1X iBind Flex Solution), used to block aspecific binding sites of the membrane and to dilute the antibodies was prepared according to the producer protocol. The sandwich was extracted from the cassette and

opened. The blotted membrane was cut to remove the excess in which there was not proteins and split in two parts by looking at the marker, one in which there should be the internal control protein and the other in which there should be the protein of interest. The gel was removed with a tweezer and the blotted membranes were placed in a bowl with 10 mL of blot solution, paying attention to leave the side with the proteins above. This step is required to block the non-specific binding sites of the membrane. In the meantime, dilutions of the antibodies were prepared according to the device producer protocol, following the recommendations for mini blot membranes. The primary antibody used for SOCS3 (SOCS3 Monoclonal Antibody (1B2), Invitrogen™, catalog #37-7200) was used at 1:500 dilution (4 µl in 2 mL of blot solution), the primary antibody used for α-tubulin (Monoclonal Anti-α-Tubulin antibody produced in mouse, T5168 - clone B-5-1-2, SIGMA) was diluted 1:1000 (2 µl in 2 mL of blot solution) and the secondary antibody, an anti-mouse antibody conjugated with horseradish peroxidase (HRP) (ECL Anti-mouse IgG peroxidase-linked whole, Amersham) antibody, was diluted at 1:1000 (4 µl in 4 mL of blot solution). The iBind device was assembled as explained in the producer protocol, the membranes were placed inside the device, with the side of the proteins face down, and the iBind Flex was loaded with the antibody solutions and the blot solution, used as a wash buffer. The incubation was carried out overnight.
After the incubation time, the detection was made with ECL Plus Western Blotting Detection Reagents kit (Amersham). Since the membranes are small, 300 µl of detection solution were enough for each membrane. The detection solution, containing HRP substrate, was made by mixing reagent 1 and 2 at 1:1 ratio (150 µl + 150 µl in this case). The membranes were taken out from the device and washed with deionized water. After that, the membrane was placed on a piece of transparent acetate sheet, incubate with the detection solution for 1 minute, cover with another piece of acetate sheet and the excess of detection solution was removed by flattening the acetate with a piece of paper towel. Detection was carried out using Uvitec Essential V6 device, taking a photo in visible light of the marker and detecting the chemiluminescence produced by the secondary antibody for proteins analysis.

4.2.15 GL261 and LN229 infection for cell viability assay

GL261 and LN229 cells were infected with oHSV-hCMV-mCherry for cell viability assay. For this assay a virus with mir124 in its backbone was required and oHSV-hCMV-mCherry was chosen because of the presence of the gene for mCherry red fluorescence protein that acts as a reporter factor of the infection. GL261 and LN229 were seeded in 4 different 24-wells plates, 2 plates for each cell line, 6 wells in every plate. 100.000 cells per well were seeded, choosing the wells in the middle of the plate to prevent adverse effects caused by medium evaporation. For each plate, 3 out of 6 wells were infected with the virus while the remaining 3 wells were used as negative controls. The day after cell seeding, cell medium was discarded, cells were washed with DPBS and GL261 were infected at MOI 1 PFU/cell and LN229 were infected with MOI 0.1 PFU/cell. In the 3 wells designated as negative controls, 250 µl of DMEM without serum per well was used. Cells were incubated for 1 hour at 37°C. After the incuba-

tion, all the medium was discarded, cells were washed and 500 µl of DMEM 2% v/v FBS were added in each well. Both cell lines were monitored at 48 hours and 72 hours post-infection at fluorescence microscopy to evaluate the cytopathic effect caused by the infection. To evaluate cell viability, cells were detached and counted at 48 hours and 72 hours post-infection, as described in paragraph 4.2.7.1. The mean number of cells out of the three wells, infected and non-infected, was calculated and the two numbers were compared.

4.2.16 GL261, LN229, CD14+ monocytes and WEHI infection assay with oHSV-hCMV-mCherry and oHSV-CD68-mCherry

4.2.16.1 CD14+ monocytes preparation from buffy coast

Human CD14+ monocytes were extracted from buffy coats of healthy donors. Twenty-five mL of Ficoll was poured in two 50 mL falcons each. Twenty-five mL of blood were gently added to each falcon and blood was centrifuged for 20 minutes at 2000 rpm at 4°C. After the centrifuge, a gradient was visible (Figure 9). Centrifuge was carried out without the rotor brake to prevent gradient disruption.

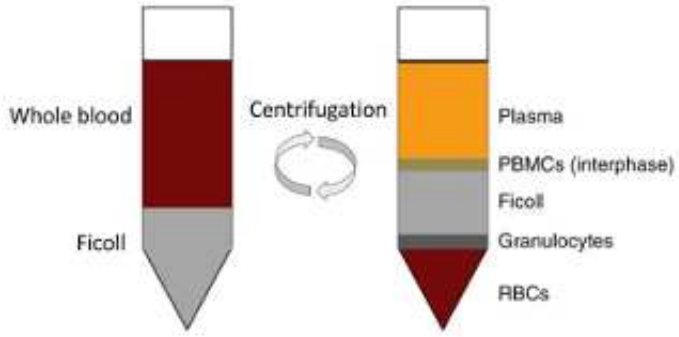

Figure 9. *Schematic representation of the blood gradient created by Ficoll followed by centrifuge.*

The aqueous phase, i.e. plasma, was removed, paying attention not to disturb the underlying phases. With the help of a pipette, PBMCs were taken from the buffy coat visible in the falcon and placed in a 15 mL falcons. PBMC were diluted 1:100 with DPBS 2% v/v FBS. A second dilution 1:10 with DPBS 2% v/v FBS was made and cell were counted with the trypan blue exclusion method (see paragraph 4.2.7.1). To isolate CD14+, 108 cell/mL are required, thus cells were centrifuged at 2000 rpm for 10 minutes at 4°C, supernatants was discarded and cell pellet was suspended with DPBS 2% v/v FBS to have the required concentration. CD14+ were purified from the PBMCs by using EasySep™ Human CD14 Positive Selection Kit II (StemCell Technologies). 2 mL of cell suspension was transferred in FACS tubes and 200 µl of anti-CD14+ antibody were added to cell suspension. The antibody was incubated for 10 minutes at room temperature. 200 µl of magnetic beads were added to the mix and incubated for 3 minutes at room temperature. FACS tube with cells was placed inside EasySep™ Magnet for 3 minutes. The supernatants was discarded by inversion, keeping the tube inside the magnet, and CD14 selected with the

magnet were washed with 2 mL of DPBS 2% v/v FBS. FACS tube was taken out of the magnet and cells were suspended with 1 mL of RPMI 10% v/v FBS. Isolated CD14+ were counted and seeded or stocked at -80°C. For seeding the desired number of cells were placed in a multi-well plate with RMPI 10% v/v FBS, while for cell storing, CD14+ were resuspend in a mix made by 50% of DMSO and 50% of RPMI 10% v/v FBS.

4.2.16.2 Infection of GL261/ LN229 cells and human primary CD14+ monocytes with oHSVs

GL261, LN229 and CD14+ monocytes infection assay was carried out according to the procedure of GL261 and LN229 infection assay with oHSV-mSOCS3-EGFP (paragraph 4.2.15), by calculating the number of PFU of the viral stock and the number of PFU required by the given MOI and calculating the dilution factor of the stock. All cell lines were seeded in two 24-wells plates, 4 wells per cell line and 100,000 cells per well.
The day after seeding, cell medium was discarded from every well of the plate, cells were washed with DPBS and 3 out of 4 wells for each cell line in both plates were infected with the appropriate infection mix for 1 hour at 37°C. GL261 were infected at MOI 1 PFU/cell, LN229 were infected at MOI 0.1 PFU/cell and CD14+ were infected at MOI 5 PFU/cell. oHSV-hCMV-mCherry viral stock titer was 1.2 * 10^7 PFU/mL, while oHSV-CD68-mCherry viral stock titer was 6.4 * 10^6 PFU/mL. For both CD14+ monocytes and WEHI infection (explained in the next paragraph) the chosen MOI was 5 PFU/cell. Two different infection mix were made for the two cells lines because CD14+ needed RPMI without serum as medium while WEHI cells required DMEM without serum. However, the calculations were the same for both cell lines mix. In the remaining well, used a negative control, cell medium was replaced with DMEM or RPMI without serum for 1 hour at 37°C. After the incubation, the medium was discarded from every well, cells were washed with DPBS for 3 times and 500 µl of DMEM 2% v/v FBS or RPMI 2% v/v FBS were added in each well. Cells were monitored by fluorescence microscope to evaluate the level of red fluorescence present in both plates for every cell line. Cell supernatants were also collected as described at the paragraph 3.2.16.4 to be titrated via plaque assay and evaluate the viral production at different time-points post infection.

4.2.16.3 Infection of WEHI cells with oHSV

Since WEHI cells grow in suspension, their infection was carried out with a different protocol. The day of the infection the required volume of cells suspension was harvested. Cells were counted, centrifuged and the medium was discarded. Cells were washed with DPBS, centrifuged again, and 300,000 cells were suspended in 750 µl of the infection mix, one containing oHSV-hCMV-mCherry and one oHSV-CD68-mCherry. Cells were incubated for 1 hour at 37°C and then centrifuged to remove the medium with virus, washed with DPBS 3 times and the final pellet suspended with DMEM 2% v/v FBS. Control cells were subjected to the same procedure, but without adding viral particles. 500 µl of cell suspension was put in each well of the two plates, one control well and 3 infected wells.

WEHI were monitored by fluorescence microscopy and supernatants were collected at selected time-points, as described below, for viral titration.

4.2.16.4 Collection of cell supernatant upon viral infection

Infected cells supernatants were collected at 24h, 48h and 72h for LN229, CD14+ monocytes and WEHI, while GL261 supernatants were collected at 24h, 6 days and 10 days post-infection.For adherent cells, supernatants were collected at each time-point. The triplicates supernatants were not mixed, but put in separate tubes and stored at -80°C until the titration. Fresh DMEM 2% v/v FBS or RPMI 2% v/v FBS was added in each well, control included, to replace the collected supernatants. For WEHI cells, all the well content was harvested, centrifuged,the supernatants collected at each time-point in eppendorfs and stored at -80°C. The cell pellet was suspended in DMEM 2% v/v FBS and cell suspension was placed in the plate well. The medium of the control cells was replaced by centrifuge of the cell suspension and resuspension with new DMEM 2% v/v FBS. Titration was performed as described at the paragraph 4.2.10.

5 Result

5.1 mSOCS3-armed oncolytic HSV-1 infects human and murine glioblastoma cells and leads to the expression of the transgene

The aim of the following experiments is to create an HSV-1 oncolytic virus armed with the SOCS3 expressing sequence and to analyze its ability to infect murine and human glioblastoma (GBM) cells. Since JAK/STAT3 is one of the main deregulated pathways in GBM, SOCS3 was chosen as a therapeutic gene because of its inhibitory action towards STAT3. Thus, the aim of using SOCS3 is to contrast STAT3 deregulation. The murine version of the protein was initially selected as the oncolytic HSV-1 (oHSV) expressing mSOCS3 will be adopted in experiments based on a mouse model of glioblastoma (GBM). However, the developed oHSV was tested also in human GBM cells as the transgene sequence is expected to minimally influence the viral replication ability in a cell type specific manner. Furthermore, the murine and human versions of SOCS3 differ only in some aminoacidic residues, thus the effect of murine SOCS3 in human GBM cells was expected to be similar to the effect of the human form of SOCS3.

5.1.1 mSOCS3-EGFP oHSV generation by bacterial artificial chromosome (BAC) based mutagenesis

The starting point for the generation of mSOCS3-EGFP oHSV is the plasmid pZeoH-SOCS3 that has SOCS3 gene integrated, in frame with a flag sequence that can be used for detection with antibodies. The transgene is under the transcriptional control of the P1 promoter, interrupted by kanamycin resistance gene. The gene cassette is flanked by homology sequences for zeocin resistance cassette. A schematic representation of this construct is reported in Figure 4. The homology regions are useful for BAC mutagenesis process that uses the recombination with Lambda Red recombinase.
BAC mutagenesis follows the protocol described in the paragraph 4.2.4. pZeoH-SOC3 plasmid was electroporated as described in paragraph 3.2.4.1 in previously prepared electrocompetent bacteria (paragraph 4.2.2) already transform with BAC pHSV1(17+)Lox-EGFP-$\Delta\gamma$34.5-Zeo-ΔUs12. Electroporated bacteria were plated on LB agar with chloramphenicol (Chl) and kanamycin (Kan) (LB + Chl + Kan). Chloramphenicol is the selection factor of BAC, not related to HSV genome, while kanamycin is the selection factor present in the gene cassette within the plasmid. In this way, only the bacteria containing the BAC DNA and that have been transformed by the plasmid can grow in the plate. Mini inoculums were made from grown colonies, in LB + Chl + Kan medium and inoculated overnight at 32°C. BAC DNA was then extracted following the home-made extraction protocol explained in paragraph 4.2.5. A PCR was carried out to verify the result of the recombination between the plasmid and the BAC DNA. The PCR was made using zeocin resistance-specific primers. The presence of the integrated transgene cassette would result in a band running

higher than the amplification product of the zeocin resistance alone (Figure 10). Furthermore, successful recombination was also controlled by negative selection in zeocin containing plates and by sequencing. Only the colonies, as the ones depicted in Figure 10, where the recombination was successful were chosen for the resolution of the integrated colonies.

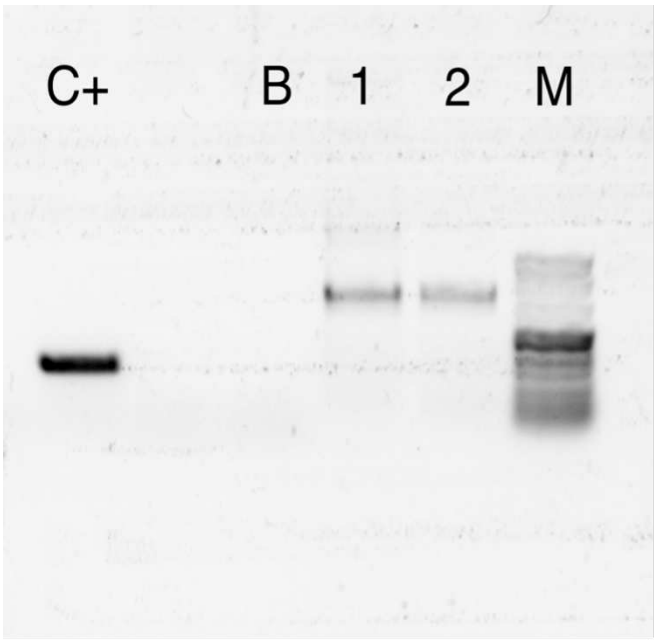

1.

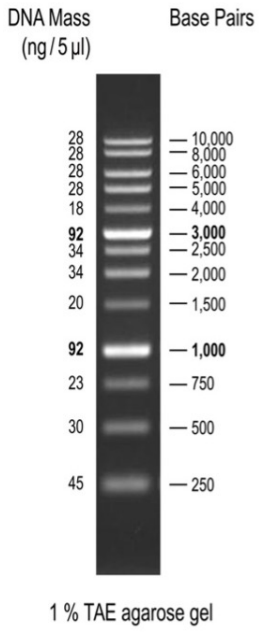

2.

Figure 10. Results of the PCR carried out to evaluate the integration of the transgene in the zeocin cassette. PCR was performed on DNA extracted by 2 colonies by adopting the primers amplifying the zeocin resistance gene. ***1)*** *PCR products were loaded on an agarose gel (agarose 1% w/v);* ***1, 2:*** *PCR products of the 2 colonies;* ***B:*** *negative control (water);* ***C+:*** *positive control represented by the amplification of the zeocin gene without the gene cassette integrated;* ***M:*** *DNA molecular weight marker 1kb (Invitrogen, ThermoFisher).* ***2)*** *DNA molecular weight 1kb ladder scheme with the related DNA fragments indicators.*

The resolution process of the integrated colonies is described in the paragraph 4.2.4.3. Bacteria were plated on LBA with addition of chloramphenicol and arabinose. Arabinose activate the transcription of I-SceI restriction enzyme. Around 10 colonies from the plate were selected and were plated on other two plates, one of LBA with chloramphenicol and kanamycin and the other of LBA with chloramphenicol and arabinose. Since kanamycin resistance gene should not be present in those colonies in which I-SceI enzyme was transcribed and was able to excide kanamycin resistance gene, only the colonies grown exclusively in LBA + Chl + Arabinose were selected. From these colonies, BAC DNA was extracted following the home-made extraction protocol. As an additional verification, the extracted BAC DNA was used as a template for PCR, to verify the actual excision of kanamycin resistance gene (Figure 11).

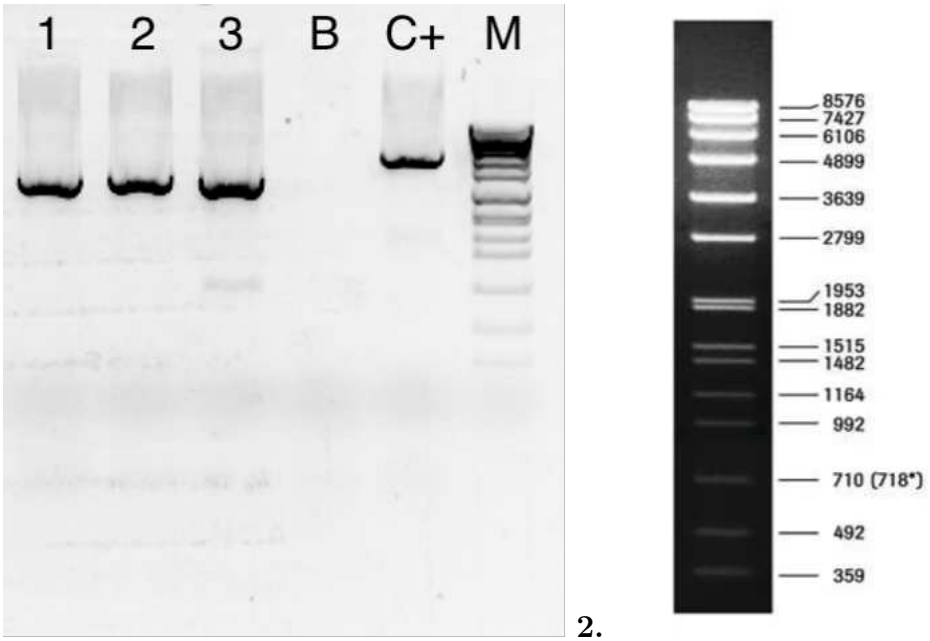

1. **2.**

Figure 11. Results of the PCR performed to evaluate the excision of kanamycin resistance gene. *DNA extracted from 3 colonies was subjected to amplification by adopting BAC EF1 and BAC SV40 primes (paragraph 4.1.4).* ***1)*** *PCR products were loaded on an agarose gel (agarose 1% w/v);* ***1, 2, 3:*** *PCR products of the 3 colonies;* ***B:*** *negative control (water);* ***C+:*** *positive control represented by BAC DNA with kanamycin gene still integrated;* ***M:*** *: DNA molecular weight marker VII (Roche).* ***2)*** *DNA molecular weight marker VII scheme with the related DNA fragments indicators.*

Bacteria of the correct colonies were refreshed by adding LB + Chl and from these BAC DNA was extracted with ZM BAC Miniprep kit (paragraph 4.2.6). HSV-1 $\Delta\gamma$34.5/ΔUs12/mSOCS3-EGFP oncolytic virus was then reconstituted by transfection of human embryonic HEK-293T cells with the purified BAC DNA, as explained in the paragraph 4.2.8. Recombinant virus was then amplified in Vero CCL81 cells (paragraph 4.2.9) and viral titer was determined by plaque assay (paragraph 4.2.10), resulting in a titer of $4 * 10^7$ plaque forming units per mL (PFU/mL).

5.1.2 LN229 and GL261 cells infection with oHSV-mSOCS3-EGFP

Following the production of oHSV-mSOCS3-EGFP viral stock, GL261 and LN229 cells were cultured and infected with the virus. According to paragraph 4.2.7, GL261 and LN229 were cultured in 4 wells of two 6-wells plate, 500,000 cell/well. The day after, two of the four wells were infected with the virus, with a multiplicity of infection (MOI) of 10 PFU/cell for GL216 and MOI 1 PFU/cell for LN229, following the procedure in paragraph 4.2.11. The uninfected wells were used as a negative control. Viral infection in both cell lines were monitored by fluorescence microscopy as the oHSV expresses the reporter green fluorescent protein (GFP) (see schematic representation in Figure 7). As shown in Figure 12, panel 1, at 24h post-infection LN229 infected cells were green. By looking with visible light, LN229 infected cells showed some signs of cytopathic effect, with round detached cells, caused by oHSV infection (Figure

12, panel 2). By contrast, control cells did not show green fluorescence (Figure 12, panel 3); they formed a uniform cell layer and they were not affected by the cytopathic effect since they were not infected by the virus (FIgure 12, panel 4).

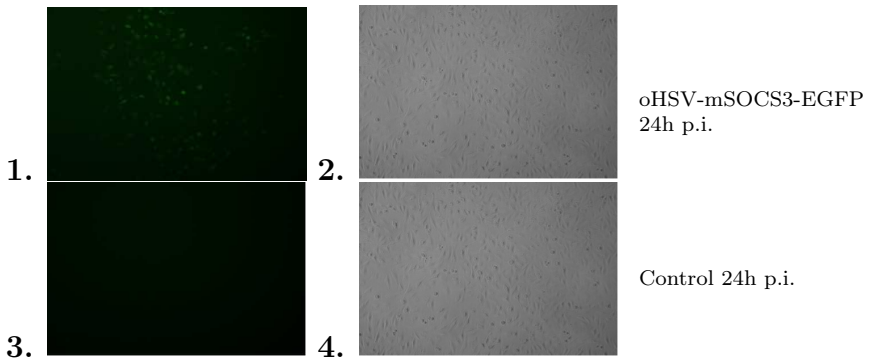

Figure 12. oHSV-mSOCS3-EGFP infects the human GBM cell lines LN299. *LN229 were infected with oHSV-mSOCS3-EGFP (1, 2) or were mock infected (3, 4). Twenty-four hours post infection, cells were observed with a fluorescence microscope (Leica DM4000) with green fluorescent filter (left) and in brightfield (right). Representative imagines at a magnification of 10x are displayed*

In the case of GL261 cell line, at 24h post infection, cells were green and show signs of cytopathic effect caused by the virus (Figure 13, panel 1 and 2). At 48h, GL261 show a higher level of green fluorescence, indicating that the virus was spreading in the cellular population (Figure 13, panel 5). By looking at the cells in brightfield, the changes in morphology were evident. Infected cells were clearly suffering, showing a round shape. Some cells were in suspension (Figure 13, panel 6). By contrast, at both times of observation, control cells were not green or interested by signs of cytopathic effect (Figure 13, panel 3, 4, 7 and 8).

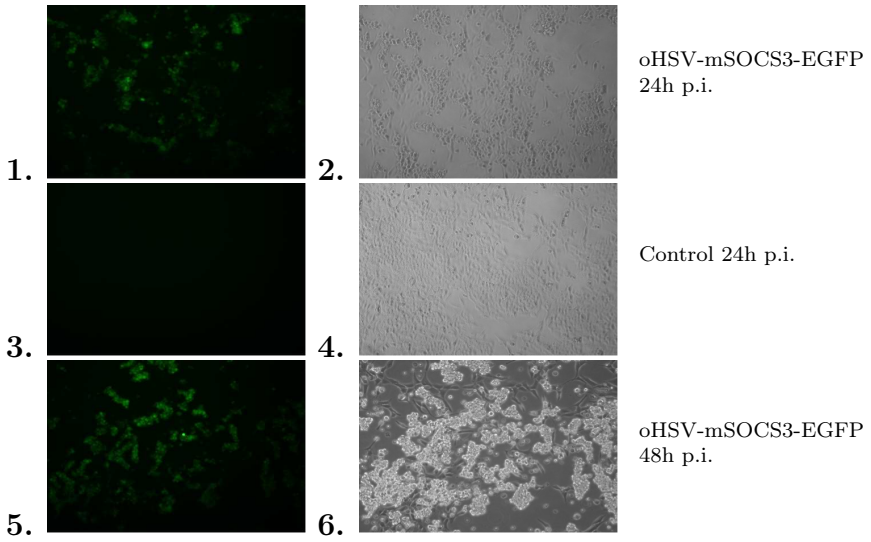

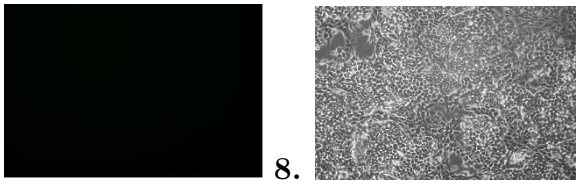

Figure 13. oHSV-mSOCS3-EGFP infects the murine GBM cell lines GL261. *GL261 were infected with oHSV-mSOCS3-EGFP (1, 2, 5, 6) or were mock infected (3, 4, 7, 8), as indicated. Twenty-four hours (1 to 4) and forty-eight hours (5 to 8) post infection, cells were observed with a fluorescence microscope (Leica DM4000) with green fluorescent filter (left) and in brightfield (right). Representative imagines at a magnification of 10x are displayed.*

After the visual analysis, at 48h post infection, GL261 were detached from the plate with a cell scraper and lysed as described in paragraph 4.2.12.
Supernatants from the cell lysis were stored to proceed with protein quantification.

5.1.3 Protein quantification and western blot

Protein quantification was carried out with BCA method, according to paragraph 4.2.13. After calculating the BSA standard curve expression, the mean of the absorbance of control cells proteins and infected cells proteins were used to find the concentration of the samples. By interpolation, control cells proteins had a concentration of 6.37 mg/mL while infected cells proteins were more diluted with a concentration of 2.99 mg/mL. Interpolation curve is shown in Figure 14.

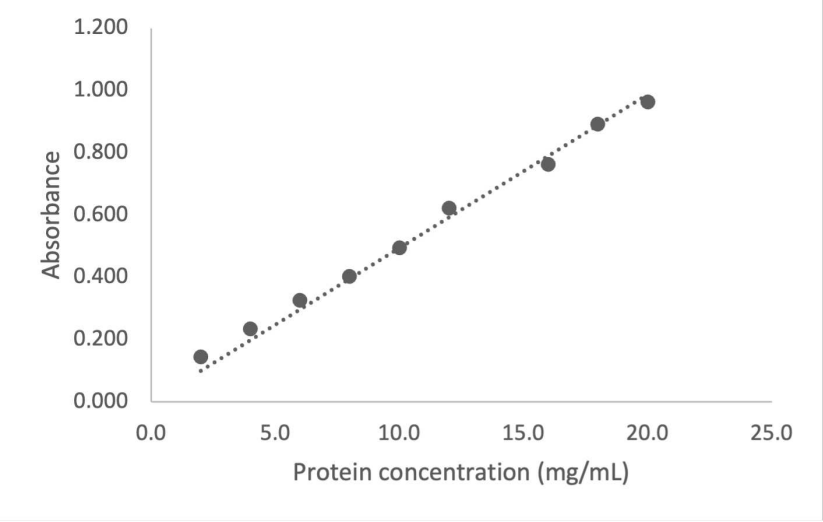

Figure 14. Graphic representation of BCA standard curve obtained with the BSA at a concentration of 2 mg/mL. *On the y-axis the absorbance is represented, while in the x-axis the protein concentration in mg/mL is represented. The formula of the standard curve is y = 0.0494x and the R2 of the linear regression model is 0.998.*

By using the concentrations found, the volume of cell lysates harvested from infected and control cells were adjusted to load the same amount of proteins

for both samples. Next a western blot (WB) was carried out according to the procedures described at paragraph 4.2.14. The membrane was cut in two pieces, by looking at the marker, between the band of 55 kDa and 35 kDa, as SOCS3 protein should run around 35 kDa, while α-tubulin, used as an internal loading control, should be around 55 kDa. Each piece of membrane was incubated with a specific antibody. Chemiluminescence emitted by the HRP conjugated with the secondary antibody was read at Uvitec Essential V6 device (Uvitec Ltd. Cambrige). The results are shown in Figure 15.

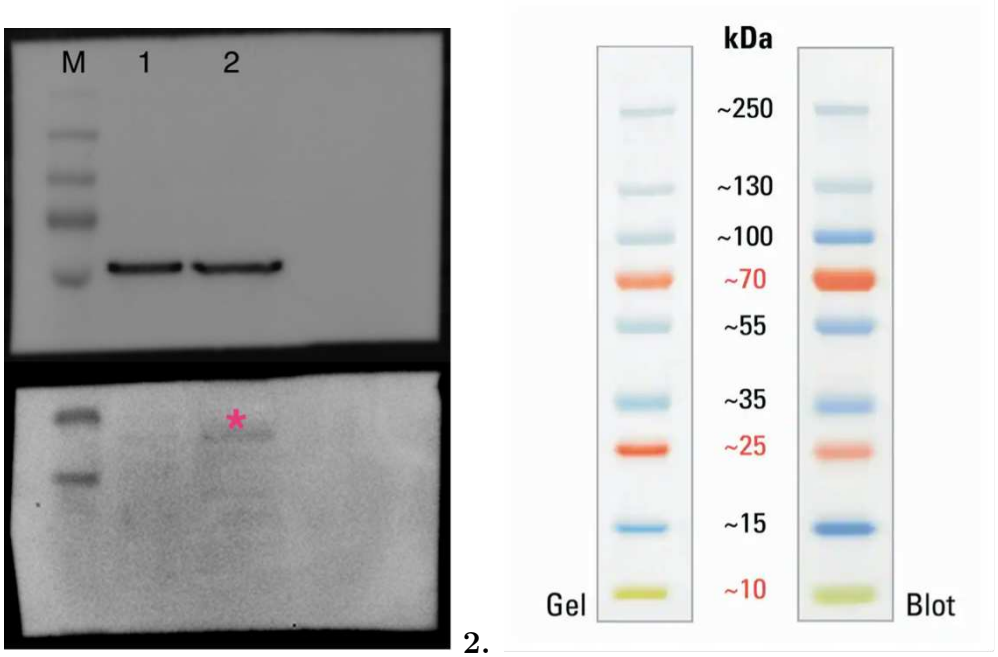

Figure 15. mSOCS3 is expressed in the murine GBM cells GL261. *GL261 cells were infected with oHSV-mSOCS3- EGFP at the MOI of 10. 48h post infection, uninfected and infected cells were lysed, proteins quantified and the same amount (90 µg) was loaded on an SDS PAGE gel. A WB was performed by adopting an anti-tubulin (1, upper panel) or and anti mSOCS3 (1, lower panel) antibody. The asterisk points to the mSOCS3 band;* ***M:*** *PageRulerTM Protein Ladder;* ***1:*** *proteins harvested from uninfected cells;* ***2:*** *proteins harvested from infected cells proteins harvested from infected cells.* ***2)*** *Schematic rappresentation of PageRuler™ Plus Prestained Protein Ladder, 10 to 250 kDa (Thermofisher).*

As shown in the WB image (Figure 15), the internal control (α-tubulin) was present in both samples analyzed, indicating that proteins were extracted correctly and were present in the cell extract. Moreover, the bands were similar in intensity, indicating that indeed the amount of proteins loaded for both samples were comparable. Regarding mSOCS3 protein, a slight band around 35 kDa could be seen in oHSV-mSOCS3-EGFP infected cell sample. This indicates that mSOCS3 is expressed in GL261 cells upon infection. Starting from this encouraging results, experiments are ongoing to optimize the WB results, by harvesting cells at different times post infection and by infecting cells with different MOIs. Furthermore, as HSV-1 infection per se can induce SOCS3 expression, at least in human cells [29], we plan to repeat the western blot by using an antibody recognizing the Flag tag present at the 3' end of mSOC3 (paragraph 4.1.1). Furthermore, we will infect human cells with

oHSV-mSOCS3-EGFP, to check mSOCS3 expression by adopting an antibody specific for the murine version of the protein.

5.2 CD68 promoter leads to a monocyte specific expression of the mCherry reporter gene cloned in the context of an oHSV improved in its neuroattenuation but still able to infect and kill human and murine GBM cells

Previous experiments carried on in the laboratory had shown that monocytes can be adopted as suitable carrier for the systemic delivery of oHSV1 [27]. In order to improve the homing of these cells towards tumors cells in vivo, oHSV will be armed with specific cytokine receptors (i.e. receptor for CCR5) known to have this function. However, these factors need to be expressed only by monocytes and not by cancer cells, once oHSV has reached the tumor bed. For this reason, those molecules will be cloned within the oHSV genome, but under the transcriptional control of a monocyte specific promoter. The second aim of this work was then to analyze the cell specific expression of the red fluorescent reporter protein mCherry cloned within the genome of two different oHSV in which the reported protein is under the transcriptional control either of the human (h) cytomegalovirus (CMV) ubiquitous and strong promoter, or of the monocyte specific CD68 promoter. The two promoter/mCherry cassettes were cloned into an oHSV backbone oHSV-mir124 that was previously developed in the laboratory. This oHSV has been described at the paragraph 4.1.2 and carries the target sequence of the mir124 following the sequence encoding one of the HSV-1 essential protein. The mir124 is over-expressed in normal neurons [4] and indeed oHSV-mir124 was proved to be attenuated in murine brain organoids more than a simple γ34.5 deleted HSV-1 (unpublished data from the laboratory).

5.2.1 oHSV-hCMV-mCherry viral stock generation

The generation of oHSV-hCMV-mCherry followed a procedure similar to the one described for oHSV-mSOCS3-EGFP (paragraph 5.1.1). The main difference relies on the site of insertion within the viral genome. Indeed, oHSV-hCMV-mCherry was generated starting from the plasmid pCeu-mCherry (see Figure 5), which contains the cassette encompassing the gene encoding for mCherry along with the sequence for the kanamycin resistance, that acts as a selection factor for the next steps. The plasmid was electroporated in electrocompetent bacteria already transformed with BAC pHSV1(17+)Lox-Luc-$\Delta\gamma$34.5-Zeo-ΔUs12-mir124 (paragraph 4.2.2 and 4.2.4). The gene cassette was integrated in UL55/UL56 of the aforementioned BAC by exploiting homologous recombination between hCMV promoter and bGH poly(A) signal sequences present in both the plasmid and the BAC (see Figure 5 and 8). Thus, the luciferase gene in UL55/UL56 region of the BAC DNA was substituted with mCherry gene cassette and mCherry gene was placed under the

control of hCMV promoter already present in the BAC DNA. After the electroporation, the generation of oHSV- hCMV-mCherry follows the same steps explained above in the case of oHSV-mSOCS3-EGFP. Upon reconstitution in 293T cells, amplification and titration in Vero cells (see paragraphs 4.2.9 and 4.2.10), the titer obtained for oHSV-hCMV-mCherry was 1.2 * 10^7 PFU/mL.

5.2.2 HSV-hCMV-mCherry infects and kills murine (GL261) and human (LN229) GBM cells

As it was previously demonstrated in the laboratory that oHSV-mir124 replicates less efficiently in murine brain organoids than a simple γ34.5 deleted virus (unpublished observations of the laboratory), first of all we tested the ability of oHSV-hCMV-mCherry to infect and kill murine and human GBM cells. To this end, GL261 and LN229 were seeded in four different 24-wells plates (paragraph 4.2.7). For each plate, 6 wells were used for cell seeding, 100,000 cell/well, choosing the wells in the middle of the plate to avoid adverse effects caused by medium evaporation. The day after, all four plates were infected with oHSV-hCMV-mCherry (paragraph 4.2.15). Three of the six wells for plate were not infected and were used as negative control. GL261 cells were infected at the MOI of 1 PFU/cell while LN229 cells were infected at the MOI of 0.1 PFU/cell. The plates were then monitored at 48h and 72h via fluorescence microscopy to evaluate the spreading of infection and the related cytopathic effect.

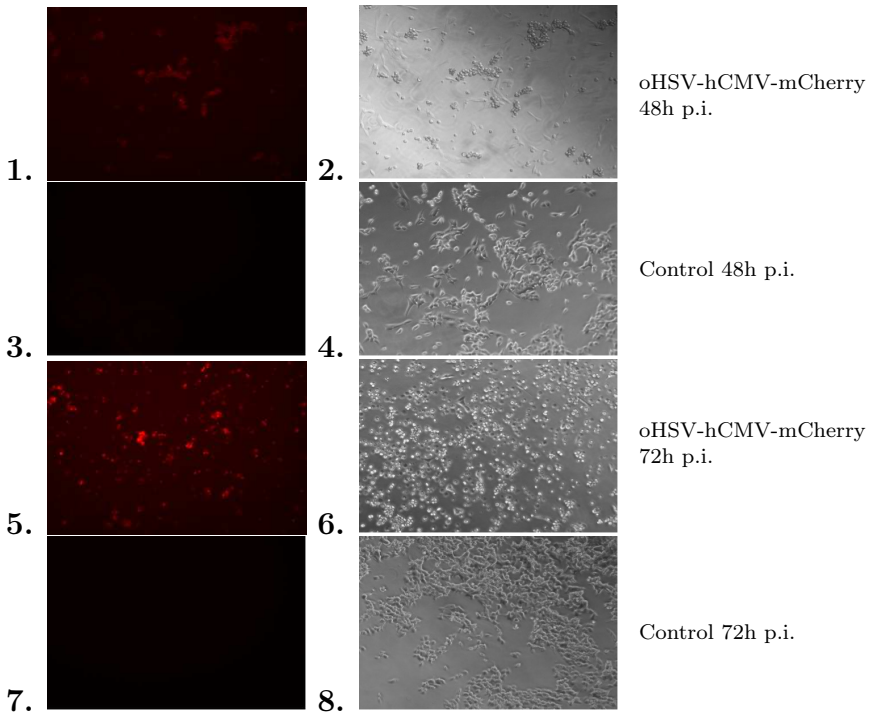

Figure 16. oHSV-hCMV-mCherry infects the murine GBM cell lines GL261. *GL261 were infected with oHSV-hCMV-mCherry (1, 2, 5, 6) or were mock infected (3, 4, 7, 8). Forty-eight hours (1 to 4) and seventy-two hours (5 to 8) post infection, cells were observed with a fluorescence microscope (Leica DM4000) with red fluorescent filter (left) and in brightfield (right). Representative imagines at a magnification of 10x are displayed.*

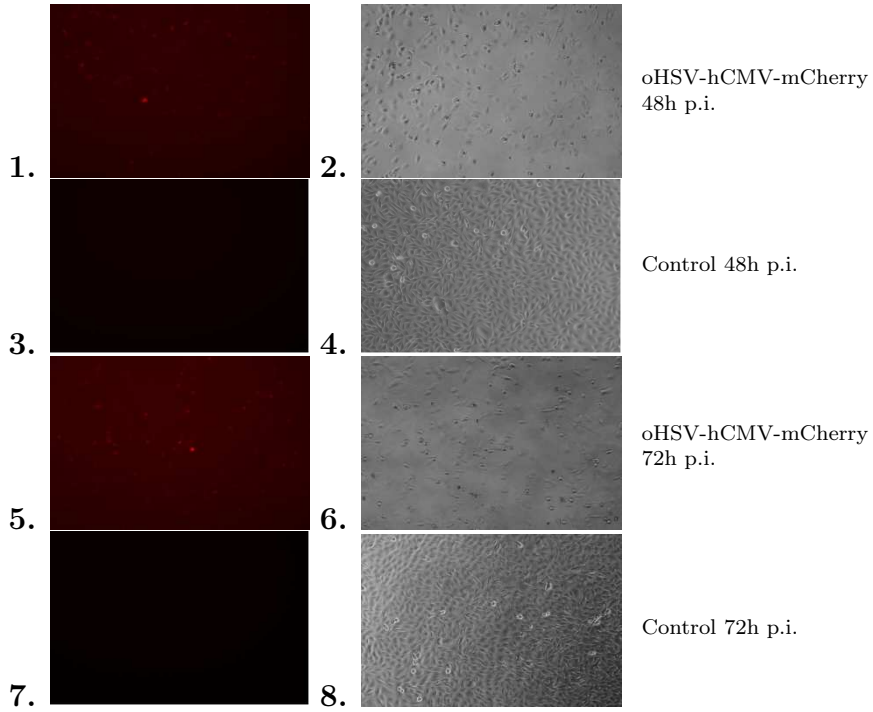

Figure 17. oHSV-hCMV-mCherry infects the human GBM cell lines LN229. *LN229 were infected with oHSV-hCMV-mCherry (1, 2, 5, 6) or were mock infected (3, 4, 7, 8). Forty-eight hours (1 to 4) and seventy-two hours (5 to 8) post infection, cells were observed with a fluorescence microscope (Leica DM4000) with red fluorescent filter (left) and in brightfield (right). Representative imagines at a magnification of 10x are displayed.*

At a visual analysis, both GL261 and LN229 cells showed red fluorescence at 48h (Figure 16, panel 1, and 17, panel 1), indicating that both these cell lines were permissive towards oHSV-hCMV-mCherry infection. Moreover, both cell lines showed signs of cytopathic effect, caused by the virus (Figure 16, panel 2, and 17, panel 2). At 72h, GL261 and LN229 cells displayed a higher level of red fluorescence, implying that more cells were infected at this timepoint (Figure 16, panel 5, and 17, panel 5). In agreement, a higher level of cytopathic effect could be observed (Figure 16, panel 6, and 17, panel 6).
In addition and to support this conclusion, at 48h and 72h post infection both GL261 and LN229 cells were detached from the plates and counted (paragraph 4.2.7.1) to compare the number of living cells between the control samples and the infected samples. The means of the cell numbers of the triplicates for each condition and cell line were calculated and plotted in the graphics below (Figure 18 and 19).
As shown in the graphics, a t-test was performed for control cells against infected cells, at each timepoint and for both cell lines. The null hypothesis to test was that the mean of the cell numbers of the controls was equal to the mean of the cell numbers of the infected cells, while the alternative hypothesis stated that the means were different. A significant level of $\alpha = 0.05$ was chosen. For GL261 at 48h the mean number of cells for the control was 463333 cell/mL while the mean number of cells for the infected cells was 70,000 cell/mL. The t-test between these two conditions returned 0.0019 as a result, indicating that the difference between the two conditions was statistically significant,

since the p-value calculated was inferior to 0.05. For GL261 at 72h the mean number of cells for the control was 206,640 cell/mL while the mean number of cells for the infected cells was 62,450 cell/mL. The t-test between these two conditions returned 0.0102 as a result, indicating that the difference between the two conditions was statistically significant, since the p-value calculated was inferior to 0.05. For LN229 at 48h the mean number of control cells was 151,327 cell/mL while the infected cells were 81,854 cell/mL on average. The t-test performed gave 0.0098 as a result, indicating that the difference between the two conditions was statistically significant, since the p-value calculated was inferior to 0.05. At 72h, the mean numbers of control cells and infected cells were respectively 90,185 cell/mL and 11,547 cell/mL. The t-test returned 0.0003 as a result, indicating that the difference between the two conditions was statistically significant, since the p-value calculated was inferior to 0.05.

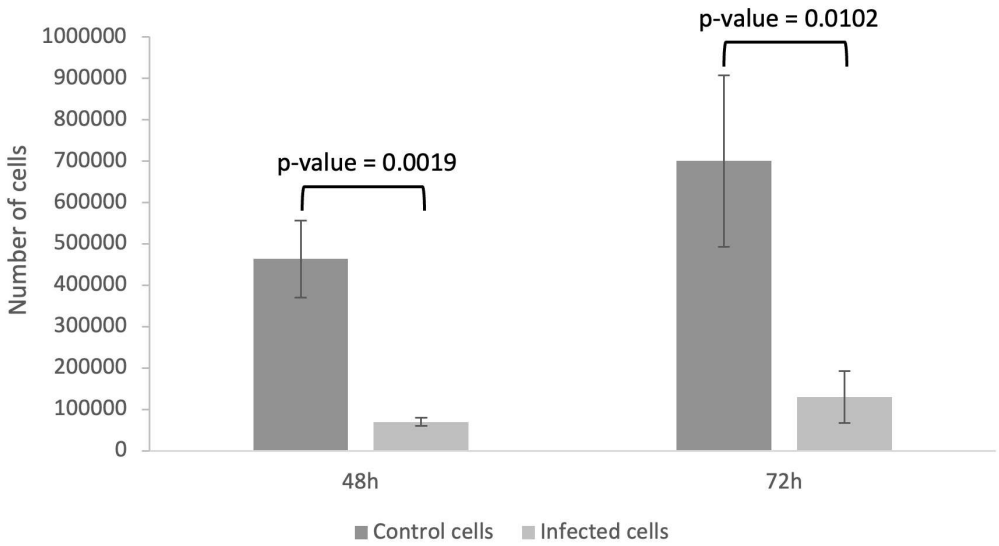

Figure 18. oHSV-hCMV-mCherry efficiently kills GL261 cells. *Cell were infected with oHSV-hCMV-mCherry at the MOI of 1 PFU/mL. Both un-infected and infected cells were detached and counted at 48h and 72h post-infection. The y-axis reports the means of the number of cells for each condition, the x-axis represents the two different timepoints. The error bars stand for the sample standard deviations. The p-values were calculated between the mean number of viable un-infected cells and the mean number of viable infected cells. Both p-values resulted below the significance level ($\alpha = 0.05$) indicating that the difference in viability between the two conditions was statistically significant for both time points.*

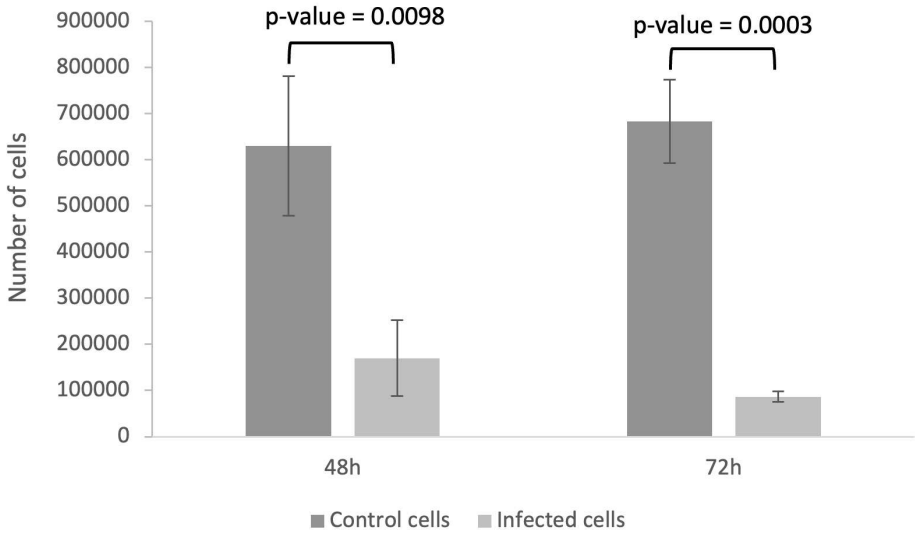

Figure 19. oHSV-hCMV-mCherry efficiently kills LN229 cells . *Cell were infected with oHSV-hCMV-mCherry at the MOI of 0.1 PFU/mL. Both un-infected and infected cells were detached and counted at 48h and 72h post-infection. The y-axis reports the means of the number of cells for each condition, the x-axis represents the two different timepoints. The error bars stand for the sample standard deviations. The p-values were calculated between the mean number of viable un-infected cells and the mean number of viable infected cells. Both p-values resulted below the significance level ($\alpha = 0.05$) indicating that the difference in viability between the two conditions was statistically significant for both time points.*

5.3 oHSV armed with monocyte-specific promoter CD68 production for oncolytic virus delivery improvement

5.3.1 Generation of oHSV-CD68-mCherry

The generation of oHSV-CD68-mCherry followed the same procedure described before (paragraph 5.1.1). oHSV-CD68-mCherry was produced from pZeo-CD68-mCherry plasmid (see Figure 6). The gene cassette with CD68 promoter, mCherry gene and kanamycin resistance gene has a zeocin tails at its ends, useful for homology recombination with the zeocin gene present in the BAC pHSV1(17+)Lox-Luc-$\Delta\gamma$34.5-Zeo-ΔUs12-mir124 (see Figure 7, panel A). The procedure was the same described for the generation of oHSV-mSOCS3-EGFP (paragraph 5.1.1). After viral reconstitution and amplification, the achieved titer via plaque assay, was 6.4 *10^6 PFU/mL.

5.3.2 GL261, LN229, CD14+ monocytes and WEHI infection

To test the cell specific expression of mCherry driven by the CD68 promoter, first of all CD14+ human monocytes were obtained as explained at paragraph 4.2.16.1. Next, CD14+ human monocytes, murine monocytic cells WEHI, as well as GL261 and LN299 cell lines were infected. Specifically, cells were cultured as explained at the paragraph 4.2.7, in two 24 multi-well plate, 100,000 cell/well. For every cell line, four wells were cultured for plate. One of the four wells was not infected and was used as a negative control, while the other three were used as triplicates of the infection. The day after GL261 and LN229 cells,

as well as human monocytes were infected, following the procedure reported at the paragraph 4.2.16. One multi-well was infected with oHSV-hCMV-mCherry and the other was infected with oHSV-CD68-mCherry. WEHI cells grow in suspension, thus they were not cultured as the other three lines. By constrast, they were counted (paragraph 4.2.7.1) the day of the infection, a volume of cell suspension with 100,000 cells for replicate and for each virus was taken and then infected according to the procedures reported at the paragraph 4.2.16.3. After the infection, WEHI cells were seeded in 24 multi-well plates with the other three cell lines. All four cell lines were monitored at different time-points post infection with fluorescence microscopy to analyze the expression of mCherry under different promotors.
Both the recombinant viruses were expected to cause similar cytopathic effect on cells, especially on GL261 and LN229 that grow attached to the plate and can be easily evaluated. Differences in fluorescence emission between the different cell lines were expected. In particular, cells infected with oHSV-hCMV-mCherry virus were expected to show cytopathic effect and red fluorescence independently from the cell type, since hCMV promoter, as strong viral promoted, should drive protein expression in almost every cell type, especially of human origin. By contrast, the red fluorescence associated with CD68 promoter was expected to be present only in CD14+ monocytes, since CD68 promoter is a human monocytes promoter and it should not lead to protein expression in other cells types. The expected results for GL261 cell line were confirmed by fluorescence microscopy. Cells infected with oHSV-hCMV-mCherry showed red fluorescence (Figure 20, image 1). Moreover, infected GL261 showed signs of cytopathic effects when compared with non-infected control cells, with round cells massively detached from the plate (Figure 20, image 2 and 4). When it comes to oHSV-CD68-mCherry infection, GL261 did not show red fluorescence even after days from the infection (Figure 20, image 5). However, GL261 infected with this virus showed cytopathic effects caused by the action of oHSV (Figure 20, image 6). This result indicateds that murine GBM cells were permissive towards oHSV infection but CD68 promoter could not lead to protein expression in this cell line since it is a monocytes-specific promoter.

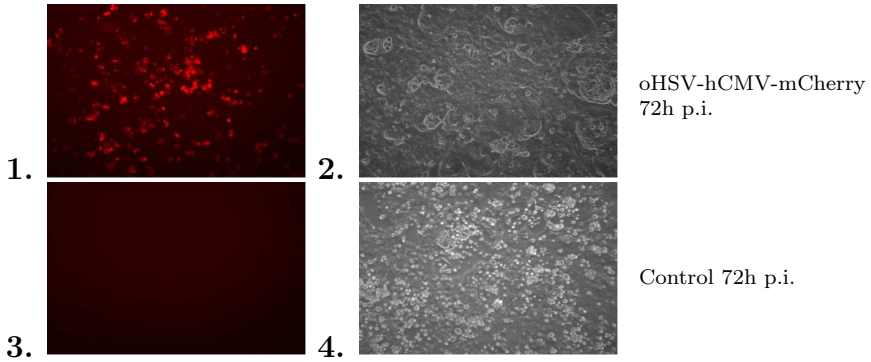

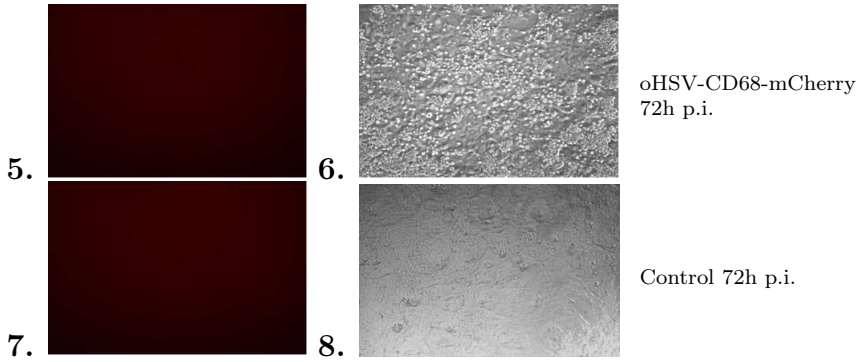

Figure 20. oHSV-hCMV-mCherry and oHSV-CD68-mCherry infects the murine GBM cell lines GL261. *GL261 were infected with oHSV-hCMV-mCherry (1 and 2) or with oHSV-CD68-mCherry (5 and 6) or were left uninfected (3, 4, 7 and 8) as indicated. Seventy-two hours post infection, cells were observed with a fluorescence microscope (Leica DM4000) with red fluorescent filter (left) and in brightfield (right). Representative imagines at a magnification of 10x are displayed.*

Also the expected results for LN229 cell line were confirmed by fluorescence microscopy. Cells infected with oHSV-hCMV-mCherry showed red fluorescence (Figure 21, image 1). In addition, infected LN229 showed cytopathic effects when compared with non-infected control cells (Figure 21, image 2 and 4). When it comes to oHSV-CD68-mCherry infection, LN229 did not show red fluorescence (Figure 21, image 5). However, LN229 infected with this virus showed signs of cytopathic effects caused by the action of oHSV (Figure 21, image 6). This indicated that human GBM cells were permissive towards oHSV infection but CD68 promoter could not lead to protein expression in this cell line since it is a monocytes-specific promoter.

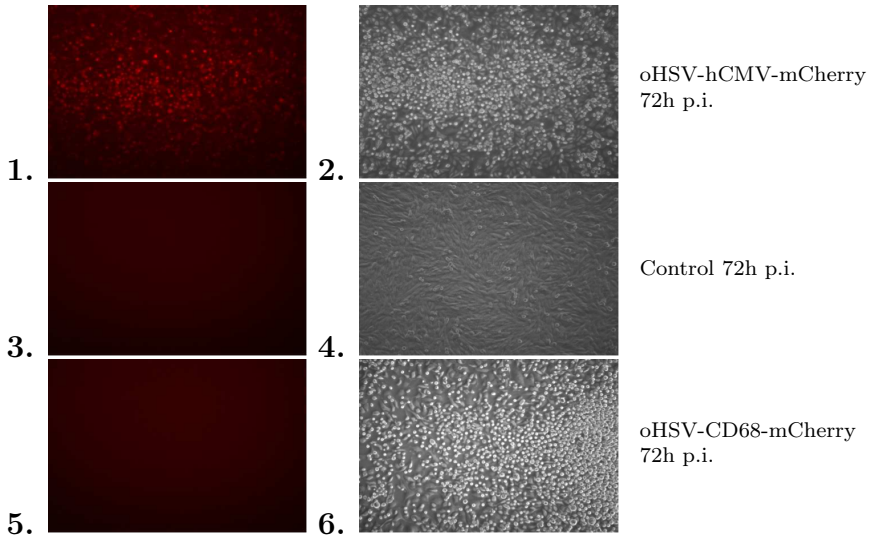

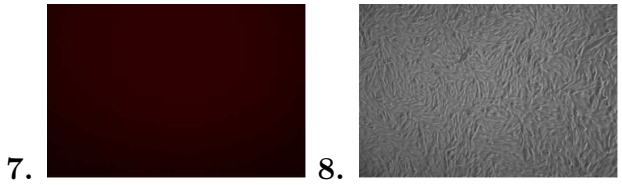

Figure 21. oHSV-hCMV-mCherry and oHSV-CD68-mCherry infects the human GBM cell lines LN229. *LN229 were infected with oHSV-hCMV-mCherry (1 and 2) or with oHSV-CD68-mCherry (5 and 6) or were left uninfected (3, 4, 7 and 8) as indicated. Seventy-two hours post infection, cells were observed with a fluorescence microscope (Leica DM4000) with red fluorescent filter (left) and in brightfield (right). Representative imagines at a magnification of 10x are displayed.*

In the case of human CD14+ monocytes, human monocytes infected with oHSV-hCMV-mCherry showed red fluorescence as expected (Figure 22, image 1) [28]. In this case, however, also upon oHSV-CD68-mCherry infection, cells showed red fluorescence (Figure 22, image 5). This indicated that human monocytes were permissive towards oHSV infection and CD68 promoter could lead to protein expression in these cells since it is a human monocytes-specific promoter.

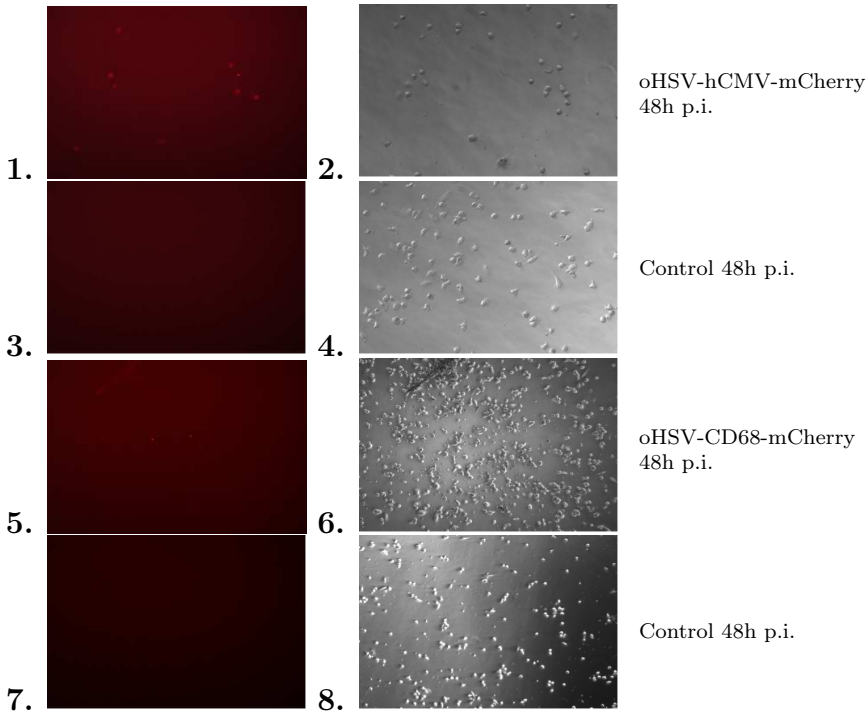

Figure 22. oHSV-hCMV-mCherry and oHSV-CD68-mCherry infects CD14+ human monocytes. *CD14+ human monocytes were infected with oHSV-hCMV-mCherry (1 and 2) or with oHSV-CD68-mCherry (5 and 6) or were left uninfected (3, 4, 7 and 8) as indicated. Forty-eight hours post infection, cells were observed with a fluorescence microscope (Leica DM4000) with red fluorescent filter (left) and in brightfield (right). Representative imagines at a magnification of 10x are displayed.*

Regarding murine monocytes cell line, WEHI infected with oHSV-hCMV-mCherry showed signs of red fluorescence (Figure 23, image A, panel 1). The

fluorescence decreased throughout the days based on the typical trend of infection and protein expression of WEHI cells (Figure 23, image B, panel 1). In the case of oHSV-CD68-mCherry infection, WEHI did not showed red fluorescence neither at 24, nor at 72 h post infection (Figure 23, image A, panel 5, and image B, panel 5). This result suggests that murine monocytic cells were permissive towards oHSV infection but CD68 promoter did not lead to protein expression at least in the time frame of our observation. This finding might be due to the fact that the adopted promoter is a human monocytes-specific promoter that might not be so effective in murine cells. Further experiments are necessary to fully address this point.

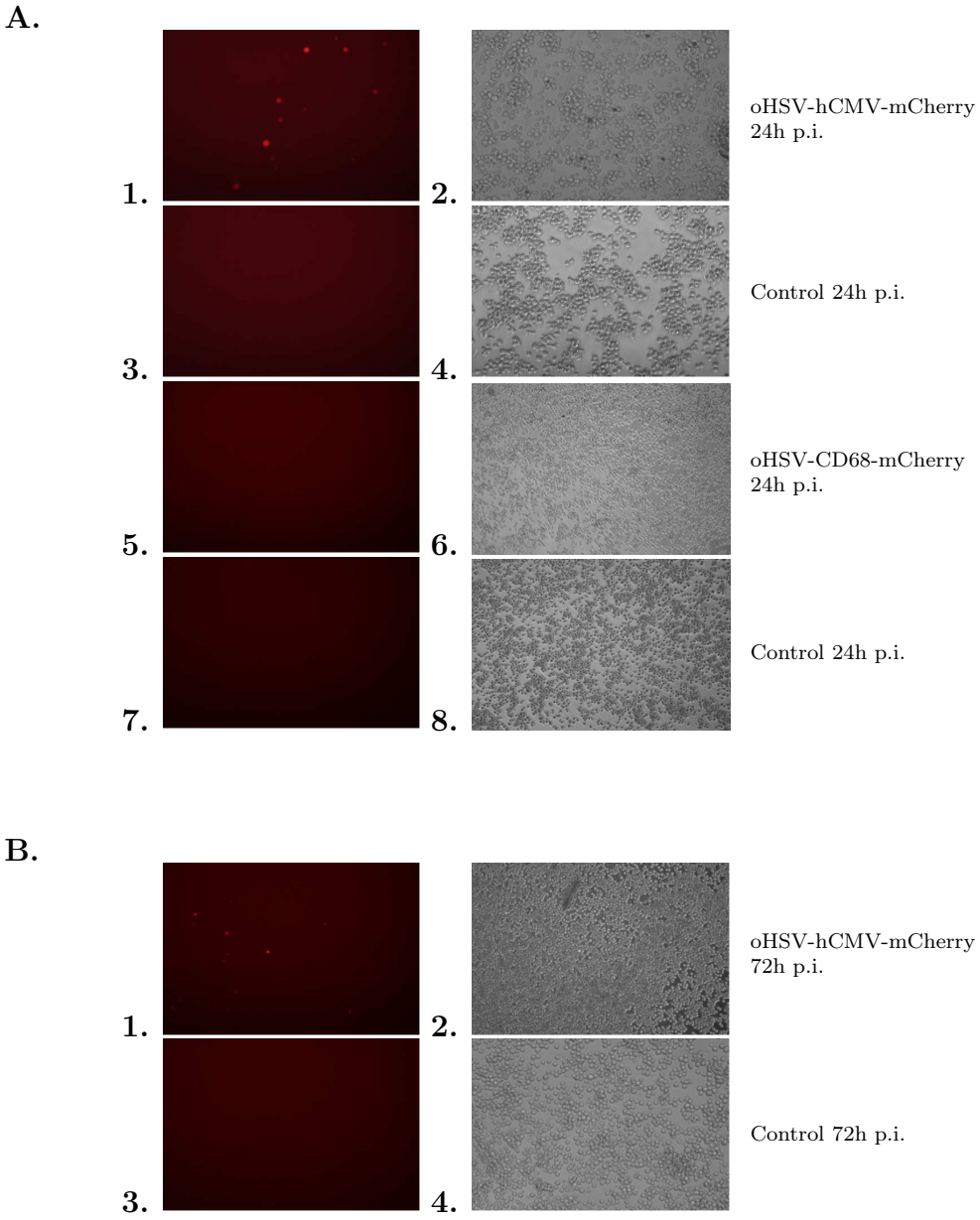

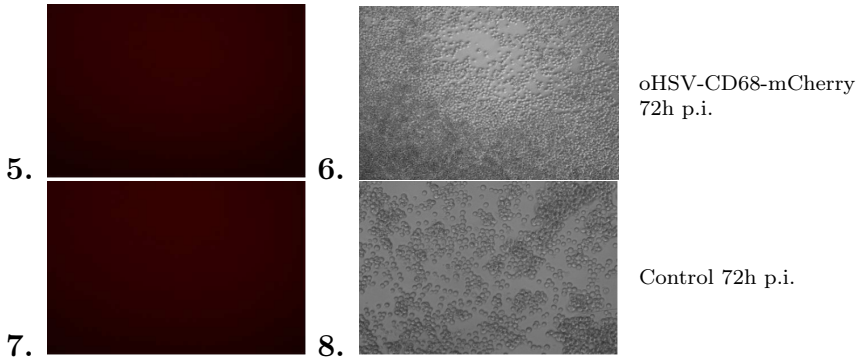

Figure 23. oHSV-hCMV-mCherry and oHSV-CD68-mCherry infects the murine monocytes cell line WEHI. *WEHI were infected with oHSV-hCMV-mCherry (image A, 1 and 2, image B, 1 and 2) or were mock infected (image A, 3 and 4, image B, 3 and 4). WEHI were infected also with oHSV-CD68-mCherry (image A, 5 and 6, image B, 5 and 6) or were mock infected (image A, 7 and 8, image B, 7 and 8). Twenty-four hours (image A) and seventy-two hours (image B) post infection, cells were observed with a fluorescence microscope (Leica DM4000) with red fluorescent filter (left) and in brightfield (right). Representative images at a magnification of 20x (image A, 1 to 4) and 10x (image A, 5 to 8 and image B) are displayed.*

5.3.3 Infected cells supernatants titration

In order to confirm that recombinant viruses were able to replicate in the different cell lines also when mCherry was not expressed, cell supernatants were harvested from the infected at different time points post infection and were used for viral titer evaluation, by plaque assay (paragraph 4.2.10).
As expected, viral replication was visible in GL261 infected with both viruses (Figure 24). It is interesting to notice that while oHSV-hCMV-mCherry titer decreases over time, the one of oHSV-CD68-mCherry increases up to 6 days post infection. This finding suggests that the first recombinant virus reaches a peak in the amount of released particles earlier than the second one. We cannot exclude that this finding resulted from slightly different initial viral inputs, despite the fact that we adopted the same theoretical MOI. However, it has to be mentioned that while hCMV-mCherry was cloned within an intergenic region of HSV-1 (UL55-UL56), CD68-mCherry was inserted within the 5' copy of γ34.5 of the genome, replacing the zeocin resistance cassette. A t-test between the mean PFU/mL of GL261 infected with oHSV-hCMV-mCherry and oHSV-CD68-mCherry was performed for each timepoint to evaluate whether there was a statistically significant difference in the viral replication of the two viruses. The calculated p-values are reported in Figure 25. All of them were below the significance level of 0.05, indicating that there was a statistically significant difference between the viral replication of the two viruses. Further experiments will be carried on to analyze whether the insertion of a promoter/transgene in this region has an impact on viral replication ability. In any case, collected data demonstrate that, as expected mCherry negative GL261 are indeed infected with oHSV-CD68-mCherry.

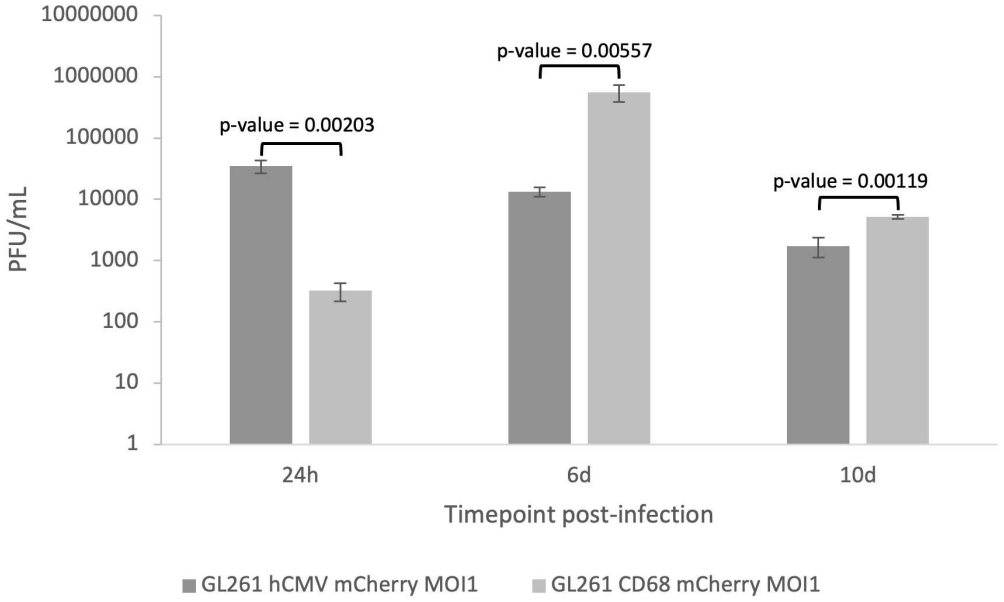

Figure 24. oHSV-hCMV-mCherry and oHSV-CD68-mCherry replication in GL261 cell line. *Supernatants from infected cells were collected twenty-four hours, six days and ten days post-infection and titrated via plaque assay. On the x-axis there are the timepoints in which supernatants were collected, while on the y-axis there is the mean of the titers of the triplicates of the infected cells in PFU/mL expressed in logarithmic scale. The error bars represent the sample standard deviation. The p-values were calculated between the mean PFU/mL of GL261 infected with oHSV-hCMV-mCherry and oHSV-CD68-mCherry for each timepoint. All p-values resulted below the significance level ($\alpha = 0.05$) indicating that the difference in viral replication between the viruses is statistically significant.*

Also the titration of LN229 supernatants confirmed what was previously seen via microscopy analysis (Figure 25). As expected, infected LN229 showed viral replication after the infection with both viruses, despite the presence of fluorescence. In this case, both viruses seem to replicate with a similar kinetic, reaching a peak between 48 and 72 h post infection, although the titer of oHSV-CD68-mCherry at 24 h post infection is significantly lower than the one obtained with oHSV-hCMV-mCherry. A t-test between the mean PFU/mL of LN229 infected with oHSV-hCMV-mCherry and oHSV-CD68-mCherry was performed for each timepoint to evaluate whether there was a statistically significant difference in the viral replication of the two viruses. The calculated p-values are reported in Figure 26. The p-value at 24 h was below the significance level of 0.05, indicating that there was a statistically significant difference between the viral replication of the two viruses. However, the p-values for the other two timepoints were above the significance level, implying that there was not a statistically significant difference between the viral replication of the two viruses. These observations might support the conclusions drawn by the experiments performed with GL261 cells on an impact of the insertion region on viral replication ability. Despite this aspect, the achieved data clearly indicate that LN229 are permissive towards the infection of both viruses even if they do not show red fluorescence.

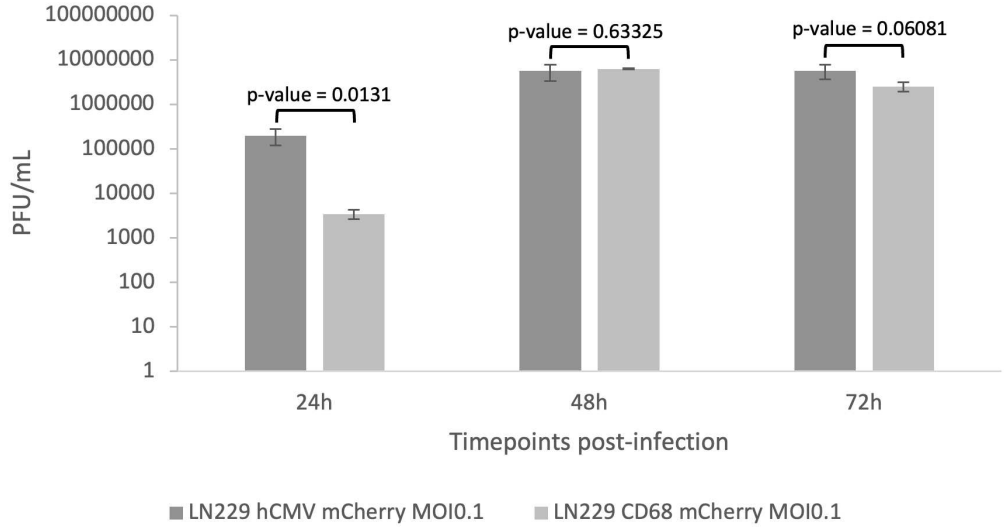

Figure 25. oHSV-hCMV-mCherry and oHSV-CD68-mCherry replication in LN229 cell line. *Supernatants from infected cells were collected twenty-four hours, forty-eight hours and seventy-two hours post-infection and titrated via plaque assay. On the x-axis there are the timepoints in which supernatants were collected, while on the y-axis there is the mean of the titers of the triplicates of the infected cells in PFU/mL expressed in logarithmic scale. The error bars represent the sample standard deviation. The p-values were calculated between the mean PFU/mL of LN229 infected with oHSV-hCMV-mCherry and oHSV-CD68-mCherry for each timepoint. The p-value for 24h resulted below the significance level ($\alpha = 0.05$) indicating that the difference in viral replication between the viruses is statistically significant, while the p-values for the other two timepoints resulted above the significance level, indicating that the difference in viral replication between the viruses is not statistically significant.*

Regarding CD14+ human monocytes, what was previously appreciated with fluorescence microscopy was supported by viral replication evaluation (Figure 26). CD14+ human monocytes proved to be permissive towards oHSV-hCMV-mCherry and oHSV-CD68-mCherry infection and viral replication, as suggested by fluorescence microscopy images. Overall, the amount of infectious particles released in the cell supernatant is low, as already reported [28]. We can exclude that measured particles represent a carry-over of the viral initial input as cells were washed 3 times after viral adsorption and the last washing was controlled for the absence of infectious virions, as previously described [28]. Once again, viral titers obtained with HSV-CD68-mCherry were lower than the ones obtained at the same time points with HSV-hCMV-mCherry. Furthermore, for both viruses, production of infectious particles peaked at 24 h post-infection and a decreased at the following time-points, as it was recently reported [28]. A t-test between the mean PFU/mL of CD14+ human monocytes infected with oHSV-hCMV-mCherry and oHSV-CD68-mCherry was performed for each timepoint to evaluate whether there was a statistically significant difference in the viral replication of the two viruses. The calculated p-values are reported in Figure 27. The p-values at 24 h and 48 h were above the significance level of 0.05, indicating that there was not a statistically significant difference between the viral replication of the two viruses. However,

the p-value for 72 h was below the significance level, suggesting that there was a statistically significant difference between the viral replication of the two viruses. Although additional evaluations are required, these preliminary data confirms that CD14+ human monocytes are permissive towards the infection with both viruses.

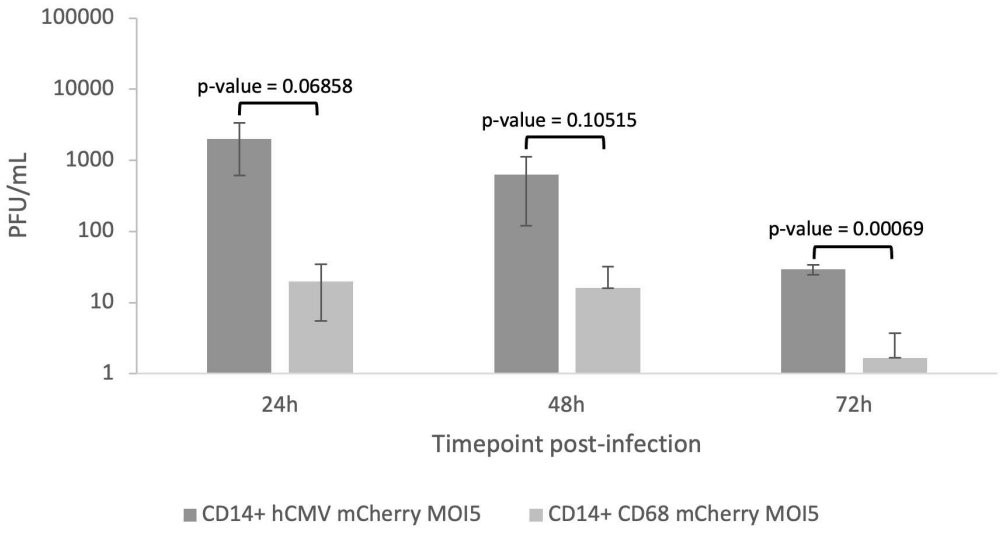

Figure 26. oHSV-hCMV-mCherry and oHSV-CD68-mCherry replication in CD14+ human monocytes. *Supernatants from infected cells were collected twenty-four hours, forty-eight hours and seventy-two hours post-infection and titrated via plaque assay. On the x-axis there are the timepoints in which supernatants were collected, while on the y-axis there is the mean of the titers of the triplicates of the infected cells in PFU/mL expressed in logarithmic scale. The error bars represent the sample standard deviation. The p-values were calculated between the mean PFU/mL of CD14+ human monocytes infected with oHSV-hCMV-mCherry and oHSV-CD68-mCherry for each timepoint. The p-values for 24h and 48h resulted above the significance level ($\alpha = 0.05$) indicating that the difference in viral replication between the viruses is not statistically significant, while the p-value for 72h resulted below the significance level, indicating that the difference in viral replication between the viruses is statistically significant.*

In the case of the murine monocytic cell line, WEHI cells proved to be permissive to the infection (Figure 27), although the number of released particles was again low, as already shown in the case of human monocytic cell lines [28]. A t-test between the mean PFU/mL of WEHI infected with oHSV-hCMV-mCherry and oHSV-CD68-mCherry was performed for each timepoint to evaluate whether there was a statistically significant difference in the viral replication of the two viruses. The calculated p-values are reported in Figure 28. The p-value at 24 h was above the significance level of 0.05, denoting that there was a statistically significant difference between the viral replication of the two viruses. However, the p-values for 48 h and 72 h were above the significance level, implying that there was not a statistically significant difference between the viral replication of the two viruses. Regardless the scarce permissiveness to productive HSV replication, WEHI cells seem to be susceptible to both recombinant viruses, even in the absence of red fluorescence. We will further investigate this point by analyzing the intracellular expression of

immediate early viral proteins, such as ICP4, as previously described [28].

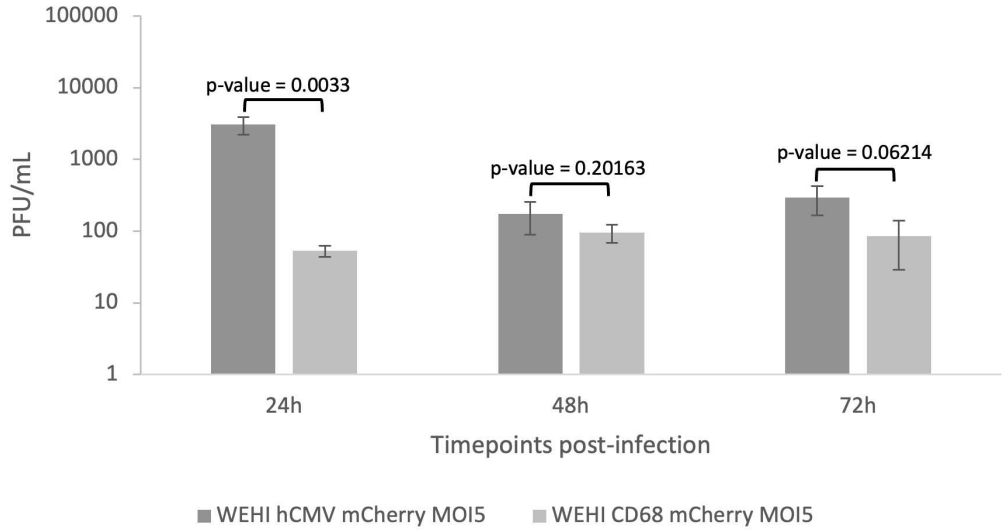

Figure 27. oHSV-hCMV-mCherry and oHSV-CD68-mCherry replication in murine monocytes WEHI cell line. *Supernatants from infected cells were collected twenty-four hours, forty-eight hours and seventy-two hours post-infection and titrated via plaque assay. On the x-axis there are the timepoints in which supernatants were collected, while on the y-axis there is the mean of the titers of the triplicates of the infected cells in PFU/mL expressed in logarithmic scale. The error bars represent the sample standard deviation. The p-values were calculated between the mean PFU/mL of WEHI infected with oHSV-hCMV-mCherry and oHSV-CD68-mCherry for each timepoint. The p-value for 24h resulted below the significance level ($\alpha = 0.05$) indicating that the difference in viral replication between the viruses is statistically significant, while the p-values for 48h and 72h resulted above the significance level, indicating that the difference in viral replication between the viruses is not statistically significant.*

6 Discussion

GBM is one of the deadliest type of tumors and nowadays an effective and specific treatment is not available for most of the cases. GBM therapy relies on surgical resection followed by radio or chemotherapy. However, due to the poor prognosis of GBM and to the high heterogeneity within the tumor mass and between the affected patients, the classical approach is not sufficient to eradicate this disease. The average survival after the diagnosis is 14.5 months [2]. New therapies are being tested and, among these new strategies, oncolytic virotherapy is one of the most promising. Still, there are two main obstacles to overcome: the strong immunosuppressive tumor microenvironment and the difficulties in the delivery of the therapy.
Oncolytic viruses (OVs) are good therapeutic agents to use against the immunosuppressive tumor microenvironment of GBM since they can trigger an immune response towards the tumor site thanks to the release of DAMPs and PAMPs following the cell infection and lysis [17]. Many clinical trials involving OVs are in progress and typically OVs are armed with therapeutic genes to increase their natural anti-tumoral effect.
Yokota et al. [29] had proved that HSV-1 infection can induce SOCS3 expression in target cells and improve viral replication. The study was carried out with various cell lines and the expression of SOCS3 was analyzed by RT-PCR and western blot. It is acknowledged that HSV-1 can block the interferon (IFN) response against viral infections and the IFN cascade of signal can activate JAK/STAT pathway, which is one of the main targets of SOCS3 inhibition. In physiological conditions, STAT3 and SOCS3 acts in a negative loop with each other, where the expression of STAT3 induce the production of SOCS3 that inhibits it. Thus, since HSV-1 can block IFN response and therefore JAK/STAT cascade, SOCS3 can be expressed. ICP34.5, the product of γ34.5 gene of HSV-1, is involved in IFN response escape triggered by HSV-1. Yokota and his research team found out that not in all the cell lines tested in their work there was an induced expression of SOCS3 caused by HSV-1. Moreover, they used the wildtype form of HSV-1, that did not present genomic modifications for attenuation, like the deletion of γ34.5 gene, a typical feature of oHSV-1. Also, in many tumor cells, including GBM cells, JAK/STAT cascade is deregulated as a result of the genomic alterations in the tumor cells. Thus, arming oHSV-1 genome with SOCS3 can be a good strategy since oHSV-1 alone cannot induce SOCS3 expression as stated by Yokota et al. in their work.
Adenovirus vectors armed with SOCS3 gene effects were analyzed in hepatocellular carcinoma [30] and in mouse and human castration-resistant prostate cancer (CRPC) cells [31]. Wei et al. [30] used a combinatory therapy of an adenoviral vector armed with SOCS3 and an adenoviral vector armed with TNF-related apoptosis-inducing ligand (TRAIL) gene to have a synergic effect on hepatocellular carcinoma cells and lead them to apoptosis. They tested the effects of both the adenovirus vectors alone and used together and analyzed the protein expression in infected cells via western blot. They found that both the adenovirus armed with only SOCS3 and the combinatory therapy caused a

reduction of pSTAT3, which is the activated form of STAT3 typically overexpressed in tumors like GBM. A similar result was achieved by Yoneda et al. in their work [31]. Yoneda and his team used two adenoviral vectors, one of them armed with mSOCS3 and the other armed with hSOCS3, to infect mouse and human CRPC cells. They analyzed SOCS3, STAT3 and pSTAT3 expression for the chosen cell lines. They found out that SOCS3 expression level increased after the treatment with the adenovirus vectors and pSTAT3 expression was inhibit. STAT3 levels did not change after the treatment, suggesting that SOCS3 regulates the activation of STAT3 rather than its expression. Moreover, they learned that the adenovirus armed with SOCS3 gene could inhibit cell proliferation and induce apoptosis of JAK/STAT3 overactivating CRPC cells.
Matsumura et al. [32] in their study analyzed the effect of oHSV-1 armed with SOCS3 gene against gastric cancer cells resistant to the action of oHSV-1 T-01, a non-armed third generation oncolytic virus. They armed T-01 with SOCS3 gene and infected MKN1 gastric cancer cells with both the parental and the SOCS3-armed oHSV. SOCS3-armed oHSV proved to be effective in infecting MKN1 cells. In addition, pSTAT3 and SOCS3 expression was analyzed via western blot. In cells infected with oHSV armed with SOCS3 there was a slight increase in the level of SOCS3, while pSTAT3 expression was inhibited in infected cells, supporting the previous results found for the adenoviral vectors armed with SOCS3 gene.
In the current study, oHSV armed with mSOCS3 gene and provided with EGFP reporter protein was used to infect mouse and human GBM cells (GL261 and LN229, respectively). Both cell lines proved to be permissive towards oHSV-mSOCS3-EGFP infection at a fluorescence microscopy analysis and showed signs of cytopathic effect caused by viral infection. GL261 cells were selected for protein extraction to evaluate SOCS3 expression post-infection. Western blot showed the expression of SOCS3 in infected cells compared to control un-infected cells. This result can be the starting point for further analysis using SOCS3-armed oHSV. It must be considered that the expression of therapeutic genes delivered by oncolytic viruses may not be seen via western blot and a more sensitive tool of analysis can be required. Moreover, the transgene expression may not be successful because of the oncolytic effect of the virus that causes cell death before the transgene can be expressed. Finally, as mentioned above, HSV-1 infection per se can induce SOCS3 overexpression, at least in human cells [29]. Thus, additional experiments are requested to better address this point, starting by the adoption of the anti-Flag antibody that would react only with the protein expressed by the recombinant virus. In addition, STAT3 and pSTAT3 level of expression must be analyzed to evaluate the effect of SOCS3 on their expression.
Regarding OVs delivery to the tumor site, there are many difficulties in choosing the correct delivery strategy. Currently, most oHSV adopted in clinics and in the clinical trials are administered locally [19]. Indeed, on one hand HSV-1 displays neurotropism and can cause encephalitis. Although oHSV are neuroattenuated by the deletion of the main neurovirulence factor, γ34.5, and drugs are available in case of side effects, this is a caveat for a systemic deliv-

ery of the recombinant virus. In addition, most of the human population is positive to HSV-1. Thus, oHSV injected in the blood stream could be rapidly neutralized by circulating antibodies as well as captured by different organs, e.g. spleen and liver [26]. However, for the treatment of deeply seeded tumors or of cancer difficult to reach without adopting invasive techniques, as GBM, a systemic delivery would represent the best option [27]. One promising approach is to exploit immune cells as carriers for OVs to the tumor site. Many tumors, including GBM, recruit a plethora of immune cells to the tumor site, typically to create an immunosuppressive microenvironment. Among these immune cells, there are tumor-associated macrophages (TAMs) and their circulating precursors (monocytes) that can be used as cell carriers [27]. Our research group has recently demonstrated that monocytes represent a suitable tool to deliver oHSV to cancer cells in vitro e in vivo [28]. In order to improve the homing of infected monocytes to the tumor bed, we intend to express the CCR5 receptor on the carrier cells surface. CCR5 is a chemokine receptor, important for the migration of myeloid cells to the tumors, including GBM, while the majority of circulating monocytes does not usually express it. However, the CCR5 expression should be limited to monocytes as its expression in cancer cells, once infected with oHSV, would be counter-productive. To this end, the expression of the transgene could be put under the transcriptional control of a OVs can be engineered with monocyte or macrophage-specific promoters that are useful for tissue-specific protein expression.

Tissue-specific promoters have been already used to improve the expression selectivity and reduce off-target protein expression. He et al. in their study generated synthetic promoters for macrophage gene therapy [33]. They developed some macrophage-specific synthetic promoters starting from known monocyte and macrophage specific promoters and they compared the expression of a reporter gene, i.e. EGFP, controlled by the synthetic promoters and CMV promoter. They used lentiviral vectors to drove EGFP gene under the synthetic promoters in hematopoietic stem cells that could ultimately differentiate in macrophage. The aim of their study was to create a high-specificity, high-efficiency promoter, that could lead to high levels of gene expression limited only to macrophage. They used other non-myeloid cells type to evaluate the differential expression of the promoters used. They found out that one of the synthetic promoters was able to limit the expression of EGFP in monocytes/macrophage cells and other cell types originated from myeloid precursors didn't show significant EGFP expression. On the other hand, EGFP under the control of CMV promoter can be detected in various cell types, both myeloid-derived and non-myeloid related. Thus, Ha et al. with this study proved the effectiveness of a tissue-specific promoter to focus gene expression in a limited number of cell types.

Levin et al. in their work compared various monocytes/macrophage-specific promoters in their specificity and effectiveness [34]. They used CD68 full length promoter and CD68-derived promoters (they used part of CD68 promoter in different orientations) associated with EGFP gene to evaluate the expression in various cell types, both macrophage and non-macrophage cells, transduced with lentiviral vectors. Levin and his team learned that CD68 full length pro-

moter and almost every CD68-derived promoter was capable of cause EGFP expression in monocytes and macrophage cells with high efficiency. However, some promoters used were more prone to lead the expression of EGFP in non-macrophage cells, typically lymphocytes. Iqbal et al. took the analysis of the previous study to the next step by using EGFP under CD68 promoter to investigate monocytes trafficking and differentiation in a transgenic mouse [35]. They analyzed the EGFP fluorescence by flow cytometry in various cell types acquired from the mouse. They found out that EGFP expression was present in different subtypes of macrophages, like Kupffer cells, microglia and peritoneal or alveolar macrophage. Also, monocytes showed EGFP expression. Moreover, Iqbal and his team proved that the presence of EGFP gene under CD68 promoter did not interfere with monocytes differentiation into macrophage or with the physiological function of monocytes and macrophages to be recruited in the inflammation sites when needed. In addition, EGFP levels of expression increased after monocytes differentiation into macrophage. Following the aforementioned studies, in this study CD68 promoter was employed to drive the expression of mCherry red fluorescence protein in monocytes and to evaluate the tissue-specificity of CD68 promoter when present in non-monocytes cell types. Human CMV (hCMV) promoter was used as a positive control of infection and protein expression, because of its ability to cause protein expression in almost every cell type. In particular, the promoter/mCherry cassette was introduced within the genome of an oHSV previously developed in the laboratory. Its main feature is represented by the presence of the mir124 target sequence following the gene encoding one of the protein essential for HSV-1 replication. As mi124 is over-expressed in neurons, this virus should be particularly neuro-attenuated as our group demonstrated by adopting murine brain organoids (unpublished observation). As a starting point oHSV-hCMV-mCherry was tested in GL261 and LN299 cells for its ability to kill GBM cells. Once shown that this recombinant virus infects and significantly affects tumor cells viability, it was adopted along with oHSV-CD68-mCherry to infect GBM as well as primary monocytes as well as monocytic cells. CD68 proved to be a monocytes-specific promoter since among all the cell types infected with oHSV-CD68-mCherry, only CD14+ monocytes, both human and murine, as well as mouse monocytic cells resulted positive at the red fluorescence. Importantly, all tested cells, encompassing the one resulted negative to mCherry expression upon infection with oHSV-CD68-mCherry showed signs of cytopathic effect and viral production, as shown by infected-cells supernatants titration via plaque assay. This result indicates that non-monocytes cells did not show red fluorescence but were still permissive towards oHSV infection. This is a promising starting point for the development of a new effective delivery approach. As for future directions, the capability of oHSV-CD68 infected monocytes to migrate towards the inflammation or tumor site could be tested, to evaluate whether monocytes keep the ability to migrate in response to cytokines. In addition, mCherry gene can be substituted with a therapeutic gene, such as CCR5, the gene encoding a chemokine receptor useful to recruit lymphocytes in the tumor site.

7 Conclusion

Oncolytic virotherapy has proved to be a promising new strategy for the treatment of malignities, in which canonical approaches, such as surgical resection and radio or chemotherapy, are not effective, like GBM. The possibility of arming oncolytic viruses with therapeutic genes can be exploited to create a therapy specific to the molecular aberrations present in tumor cells.
As described by the literature, STAT3 is one of the most deregulated genes in GBM and creating a therapy that targets this gene can be the key to improve GBM treatment and survival of affected patients. For this reason, creating an HSV oncolytic virus armed with the gene of one of the main inhibitors of STAT3, i.e. SOCS3, was the starting point in the development of a new GBM therapy. The oncolytic ability of HSV-1 was paired with the inhibitory ability of SOCS3 and oHSV-mSOCS3-EGFP was used to infect mouse and human GBM cells. Both were permissive towards the infection and SOCS3 resulted expressed upon infection in GL261 cells.
oHSV-1 was armed also to analyze the improvement in oncolytic virus delivery. Starting with the idea of using tumor-associated macrophage as carrier cells for the oncolytic virus, monocytes were infected with HSV-1 oncolytic virus armed with a reporter gene under a monocyte-specific promoter. Monocytes proved to be permissive towards oHSV infection and the monocyte-specific promoter limited the expression of the reporter gene only to monocytes. This dual strategy can be the starting point for further analysis to improve GBM oncolytic virotherapy based on oHSV-1.

Bibliographic references

[1] Hans-Georg Wirsching and Michael Weller. "Glioblastoma". en. In: *Malignant Brain Tumors*. Ed. by Jennifer Moliterno Gunel, Joseph M Piepmeier, and Joachim M. Baehring. Cham: Springer International Publishing, 2017, pp. 265–288. ISBN: 978-3-319-49863-8 978-3-319-49864-5. DOI: 10.1007/978-3-319-49864-5_18.

[2] Mary Davis. "Glioblastoma: Overview of Disease and Treatment". en. In: *Clinical Journal of Oncology Nursing* 20.5 (Oct. 2016), S2–S8. ISSN: 1092-1095, 1538-067X. DOI: 10.1188/16.CJON.S1.2-8.

[3] Aaron C. Tan et al. "Management of glioblastoma: State of the art and future directions". en. In: *CA: A Cancer Journal for Clinicians* 70.4 (July 2020), pp. 299–312. ISSN: 0007-9235, 1542-4863. DOI: 10.3322/caac.21613.

[4] Hiroko Ohgaki and Paul Kleihues. "Genetic Pathways to Primary and Secondary Glioblastoma". en. In: *The American Journal of Pathology* 170.5 (May 2007), pp. 1445–1453. ISSN: 00029440. DOI: 10.2353/ajpath.2007.070011.

[5] Hiroko Ohgaki. "Genetic pathways to glioblastomas". en. In: *Neuropathology* 25.1 (Mar. 2005), pp. 1–7. ISSN: 0919-6544, 1440-1789. DOI: 10.1111/j.1440-1789.2004.00600.x.

[6] Sarmad Sheraz Jadoon et al. "Genomic and Epigenomic Features of Glioblastoma Multiforme and its Biomarkers". en. In: *Journal of Oncology* 2022 (Sept. 2022). Ed. by Mingming Deng, pp. 1–16. ISSN: 1687-8469, 1687-8450. DOI: 10.1155/2022/4022960.

[7] Ines Crespo et al. "Molecular and Genomic Alterations in Glioblastoma Multiforme". en. In: *The American Journal of Pathology* 185.7 (July 2015), pp. 1820–1833. ISSN: 00029440. DOI: 10.1016/j.ajpath.2015.02.023.

[8] Nakho Chang et al. "The role of STAT3 in glioblastoma progression through dual influences on tumor cells and the immune microenvironment". en. In: *Molecular and Cellular Endocrinology* 451 (Aug. 2017), pp. 53–65. ISSN: 03037207. DOI: 10.1016/j.mce.2017.01.004.

[9] Karolina Swiatek-Machado and Bozena Kaminska. "STAT Signaling in Glioma Cells". en. In: *Glioma Signaling*. Ed. by Jolanta Barańska. Vol. 1202. Series Title: Advances in Experimental Medicine and Biology. Cham: Springer International Publishing, 2020, pp. 203–222. ISBN: 978-3-030-30650-2 978-3-030-30651-9. DOI: 10.1007/978-3-030-30651-9_10.

[10] Alexander Ou et al. "The Role and Therapeutic Targeting of JAK/STAT Signaling in Glioblastoma". en. In: *Cancers* 13.3 (Jan. 2021), p. 437. ISSN: 2072-6694. DOI: 10.3390/cancers13030437.

[11] Lirui Dai et al. "Emerging roles of suppressor of cytokine signaling 3 in human cancers". en. In: *Biomedicine & Pharmacotherapy* 144 (Dec. 2021), p. 112262. ISSN: 07533322. DOI: 10.1016/j.biopha.2021.112262.

[12] Mira Patel et al. "The Future of Glioblastoma Therapy: Synergism of Standard of Care and Immunotherapy". en. In: *Cancers* 6.4 (Sept. 2014), pp. 1953–1985. ISSN: 2072-6694. DOI: 10.3390/cancers6041953.

[13] Mayra Paolillo, Cinzia Boselli, and Sergio Schinelli. "Glioblastoma under Siege: An Overview of Current Therapeutic Strategies". en. In: *Brain Sciences* 8.1 (Jan. 2018), p. 15. ISSN: 2076-3425. DOI: 10.3390/brainsci8010015.

[14] Samuel W. Cramer and Clark C. Chen. "Photodynamic Therapy for the Treatment of Glioblastoma". en. In: *Frontiers in Surgery* 6 (Jan. 2020), p. 81. ISSN: 2296-875X. DOI: 10.3389/fsurg.2019.00081.

[15] Liang Rong, Ni Li, and Zhenzhen Zhang. "Emerging therapies for glioblastoma: current state and future directions". en. In: *Journal of Experimental & Clinical Cancer Research* 41.1 (Dec. 2022), p. 142. ISSN: 1756-9966. DOI: 10.1186/s13046-022-02349-7.

[16] Jonathan Santos Apolonio et al. "Oncolytic virus therapy in cancer: A current review". en. In: *World Journal of Virology* 10.5 (Sept. 2021), pp. 229–255. ISSN: 2220-3249. DOI: 10.5501/wjv.v10.i5.229.

[17] Miika Martikainen and Magnus Essand. "Virus-Based Immunotherapy of Glioblastoma". en. In: *Cancers* 11.2 (Feb. 2019), p. 186. ISSN: 2072-6694. DOI: 10.3390/cancers11020186.

[18] Paul M. Foreman et al. "Oncolytic Virotherapy for the Treatment of Malignant Glioma". en. In: *Neurotherapeutics* 14.2 (Apr. 2017), pp. 333–344. ISSN: 1933-7213, 1878-7479. DOI: 10.1007/s13311-017-0516-0.

[19] Kevin Harrington et al. "Optimizing oncolytic virotherapy in cancer treatment". en. In: *Nature Reviews Drug Discovery* 18.9 (Sept. 2019), pp. 689–706. ISSN: 1474-1776, 1474-1784. DOI: 10.1038/s41573-019-0029-0.

[20] Russell J. Diefenbach and Cornel Fraefel, eds. *Herpes Simplex Virus: Methods and Protocols*. en. Vol. 1144. Methods in Molecular Biology. New York, NY: Springer New York, 2014. ISBN: 978-1-4939-0427-3 978-1-4939-0428-0. DOI: 10.1007/978-1-4939-0428-0.

[21] Hayle Scanlan et al. "Herpes simplex virus 1 as an oncolytic viral therapy for refractory cancers". en. In: *Frontiers in Oncology* 12 (July 2022), p. 940019. ISSN: 2234-943X. DOI: 10.3389/fonc.2022.940019.

[22] Marilin Koch, Sean Lawler, and E. Chiocca. "HSV-1 Oncolytic Viruses from Bench to Bedside: An Overview of Current Clinical Trials". en. In: *Cancers* 12.12 (Nov. 2020), p. 3514. ISSN: 2072-6694. DOI: 10.3390/cancers12123514.

[23] Laura Menotti and Elisa Avitabile. "Herpes Simplex Virus Oncolytic Immunovirotherapy: The Blossoming Branch of Multimodal Therapy". en. In: *International Journal of Molecular Sciences* 21.21 (Nov. 2020), p. 8310. ISSN: 1422-0067. DOI: 10.3390/ijms21218310.

[24] Chase Kangas, Eric Krawczyk, and Bin He. "Oncolytic HSV: Underpinnings of Tumor Susceptibility". en. In: *Viruses* 13.7 (July 2021), p. 1408. ISSN: 1999-4915. DOI: 10.3390/v13071408.

[25] Lizhi Li et al. “Delivery and Biosafety of Oncolytic Virotherapy”. en. In: *Frontiers in Oncology* 10 (Apr. 2020), p. 475. ISSN: 2234-943X. DOI: 10.3389/fonc.2020.00475.

[26] Guijin Tang et al. “The Dilemma of HSV-1 Oncolytic Virus Delivery: The Method Choice and Hurdles”. en. In: *International Journal of Molecular Sciences* 24.4 (Feb. 2023), p. 3681. ISSN: 1422-0067. DOI: 10.3390/ijms24043681.

[27] Alberto Reale, Arianna Calistri, and Jennifer Altomonte. “Giving Oncolytic Viruses a Free Ride: Carrier Cells for Oncolytic Virotherapy”. en. In: *Pharmaceutics* 13.12 (Dec. 2021), p. 2192. ISSN: 1999-4923. DOI: 10.3390/pharmaceutics13122192.

[28] Alberto Reale et al. “Human Monocytes Are Suitable Carriers for the Delivery of Oncolytic Herpes Simplex Virus Type 1 In Vitro and in a Chicken Embryo Chorioallantoic Membrane Model of Cancer”. en. In: *International Journal of Molecular Sciences* 24.11 (May 2023), p. 9255. ISSN: 1422-0067. DOI: 10.3390/ijms24119255.

[29] Shin-ichi Yokota et al. “Induction of suppressor of cytokine signaling-3 by herpes simplex virus type 1 confers efficient viral replication”. en. In: *Virology* 338.1 (July 2005), pp. 173–181. ISSN: 00426822. DOI: 10.1016/j.virol.2005.04.028.

[30] Rui-Cheng Wei et al. “Augmenting the Antitumor Effect of TRAIL by SOCS3 with Double-Regulated Replicating Oncolytic Adenovirus in Hepatocellular Carcinoma”. en. In: *Human Gene Therapy* 22.9 (Sept. 2011), pp. 1109–1119. ISSN: 1043-0342, 1557-7422. DOI: 10.1089/hum.2010.219.

[31] Tomomi Yoneda et al. “Overexpression of SOCS3 mediated by adenovirus vector in mouse and human castration-resistant prostate cancer cells increases the sensitivity to NK cells in vitro and in vivo”. en. In: *Cancer Gene Therapy* 26.11-12 (Nov. 2019), pp. 388–399. ISSN: 0929-1903, 1476-5500. DOI: 10.1038/s41417-018-0075-5.

[32] Shuichi Matsumura et al. “Oncolytic virotherapy with SOCS3 enhances viral replicative potency and oncolysis for gastric cancer”. en. In: *Oncotarget* 12.4 (Feb. 2021), pp. 344–354. ISSN: 1949-2553. DOI: 10.18632/oncotarget.27873.

[33] Weijing He et al. “Development of a Synthetic Promoter for Macrophage Gene Therapy”. en. In: ().

[34] M C Levin et al. “Evaluation of macrophage-specific promoters using lentiviral delivery in mice”. en. In: *Gene Therapy* 19.11 (Nov. 2012), pp. 1041–1047. ISSN: 0969-7128, 1476-5462. DOI: 10.1038/gt.2011.195.

[35] Asif J. Iqbal et al. “Human CD68 promoter GFP transgenic mice allow analysis of monocyte to macrophage differentiation in vivo”. en. In: *Blood* 124.15 (Oct. 2014), e33–e44. ISSN: 0006-4971, 1528-0020. DOI: 10.1182/blood-2014-04-568691.

Acknowledgements

I would like to show all my gratitude to my primary supervisor, the professor Arianna Calistri for giving me the opportunity to work in her research group for these months. Also, I have to thank her for helping me while writing thesis.

I want to extend my sincere thanks to Dr. Alberto Reale and all the laboratory team for the assistance provided during the internship. In particular, I am deeply grateful to Maria Vittoria which has been one of the fundamental reference points during this internship.

A big thank you goes to my family, who supported me during my university career, and to all my friends, that helped me to overcome the hardships and faced with me the years of university.

Alessia.